

Research in
Earth Physics

Phase Report No. 1
Part I

STRESS-STRAIN BEHAVIOR OF SATURATED CLAY
AND BASIC STRENGTH PRINCIPLES

by

Charles C. Ladd

Cosponsored
Army Materiel Command
Projects Nos. 1-A-0-1101-E-021-30
and 1-T-0-21701-A-046-05

and
Advanced Research Projects Agency
ARPA Order No. 400
Contract No. DA-22-079-eng-330
with
U.S. Army Engineer Waterways Experiment Station

Research Report R64-17

Soil Mechanics Division
Department of Civil Engineering
Massachusetts Institute of Technology

April, 1964

ABSTRACT

This report presents a set of basic principles developed to describe the strength behavior of saturated clay and illustrates stress-strain properties via detailed data on the hypothetical "Simple Clay." The three basic principles are: the relationship between strength and effective stress at failure; the relationship among water content, shear stress, and effective stress during shear; and the relationship among strength, water content at failure, and effective stress at failure as expressed by the Hvorslev parameters. Stress vs. strain, water content vs. log stress, and effective stress path data are presented on the influence of type of triaxial test, over-consolidation ratio, stress path, stress ratio at consolidation, and value of the intermediate principal stress. These principles and data, which represent a simplified picture of the behavior of real clays, can be used as a framework with which to study the properties of actual clays in terms of deviations from this idealized picture, rather than as a set of isolated facts.

PREFACE

"The work described in this report was performed under Contract No. DA-22-079-eng-330 entitled 'Research Studies in the Field of Earth Physics' between the U. S. Army Engineer Waterways Experiment Station and the Massachusetts Institute of Technology. The research is co-sponsored by the U. S. Army Materiel Command under DA Projects 1-A-0-1101-B-021-30, 'Earth Physics (Terrain Analysis),' and 1-T-0-21701-A-046-05, 'Mobility Engineering Support,' and by the Advanced Research Projects Agency, ARPA Order No. 400".

The general objective of the research is the development of a fundamental understanding of the behavior of particulate systems, especially cohesive soils, under varying conditions of stress and environment. Work on the project, initiated in May, 1962, has been carried out in the Soil Mechanics Division (headed by Dr. T. William Lambe) of the Department of Civil Engineering under the supervision of Dr. Charles C. Ladd, Assistant Professor of Civil Engineering. This report represents only one phase of the overall research being conducted under the contract.

Part II of this report will present detailed strength data on normally consolidated Boston Blue Clay. Major topics of investigation, as measured by consolidated-undrained triaxial tests with pore pressure measurements, include:

- (1) Effects of anisotropic consolidation
- (2) Effects of the intermediate principal stress
- (3) Effects of rotation of principal planes

These data are analyzed in terms of deviations from the idealized theoretical framework presented in this report. In particular, common methods for selecting undrained strengths for total stress ($\phi = 0$) stability analyses are examined critically and alternate methods suggested.

In essence, Part I of this report represents the background material required for the presentation and analysis of the experimental data presented in Part II.

TABLE OF CONTENTS

PREFACE

		<u>Page No.</u>
I.	INTRODUCTION	
	A. Purpose of Report	1
	B. Concept of the "Simple Clay"	2
	C. Types of Shear Tests	3
	D. Statement of Strength Principles	7
	E. Variables Considered	7
	F. Consolidation Curves for Simple Clay	8
II.	STRENGTH BEHAVIOR OF NORMALLY CONSOLIDATED SIMPLE CLAY (Compression tests only)	10
	A. CID Tests	10
	1. Stress-Strain Data	10
	2. Mohr Coulomb Strength Criteria and Stress Paths	11
	3. Effect of Different Stress Paths	13
	4. Stress-Strain Data for Different Stress Paths and the Hyperbolic Stress- Strain Relationship	14
	5. Water Content versus Log Stress	16
	6. Review	17
	B. CIU Tests	18
	1. Stress-Strain Data	18
	2. Total and Effective Stress Paths	20
	3. Effective Stress Path and Axial Strain Relationship	23
	4. Water Content versus Log Stress	23
	5. Review	23

	<u>Page No.</u>
C. Unique Relationship Among Water Content, Shear Stress and Effective Stress	24
1. Relationship Between \bar{C}_{IU} and CID Tests	24
2. Effect of Anisotropic Consolidation	26
3. Review	29
D. UU Tests	29
E. Summary and Conclusions	31
1. Statement of Principles	31
2. Equations for Undrained Shear Strength	32
3. Summary of Important Points for Triaxial Compression Tests on Normally Consolidated Simple Clay	33
III. STRENGTH BEHAVIOR OF OVERCONSOLIDATED SIMPLE CLAY (Compression Tests Only)	35
A. CID Tests	35
1. Stress-Strain Data	35
2. Effective Stress Paths and Failure Envelope	36
3. Water Content versus Log Stress	37
B. \bar{C}_{IU} Tests	37
1. Stress-Strain Data	37
2. Effective Stress Paths and Failure Envelope	38
3. Water Content versus Log Stress	40
C. Unique Relationship Among Water Content, Shear Stress and Effective Stress	40
1. Relationship Between \bar{C}_{IU} and CID Tests	40
2. Effect of K_o Consolidation	40
D. Summary of Effect of Overconsolidation on Strength Behavior for Isotropic Consolidation and Rebound	43

	<u>Page No.</u>
1. Strength Data versus Consolidation Pressure and Water Content versus Log Stress	43
2. Stress-Strain Characteristics	44
3. Log OCR versus Strength Parameters	45
IV. HVORSLEV PARAMETERS	46
A. Historical Development	46
B. Significance	48
C. Hvorslev Parameters for Simple Clay	49
V. TRIAXIAL EXTENSION TESTS	52
A. Types of Stress Systems	52
B. Triaxial Extension Tests on Simple Clay	54
1. \overline{CIU} Tests on Normally Consolidated Samples	54
2. CID Tests on Normally Consolidated Samples	57
3. Tests on Overconsolidated Samples	58
VI. SUMMARY	60
A. Background	60
B. Variables Considered	61
C. Strength Principles	62
APPENDIX A - List of References	64
APPENDIX B - Notation	67

LIST OF FIGURES

- I-1 Sample in Triaxial Cell
- 2 Isotropic Consolidation and Rebound Curves for Simple Clay
- II-1 Stress-Strain: CID ($\bar{\sigma}_3 = \bar{\sigma}_c$) Compression Tests on Normally Consolidated Simple Clay
- 2 Mohr Circles at Failure for CID ($\bar{\sigma}_3 = \bar{\sigma}_c$) Compression Tests on Normally Consolidated Simple Clay
- 3 Effective Stress Path and Strength Envelope for CID Test B
- 4 Various Effective Stress Paths for CID Tests on Normally Consolidated Simple Clay
- 5 Stress-Strain: Loading and Unloading CID Compression Tests on Normally Consolidated Simple Clay
- 6 Hyperbolic Stress-Strain Relationship for CID Compression Tests on Normally Consolidated Simple Clay
- 7 Water Content versus Log Stress for CID Compression Tests on Normally Consolidated Simple Clay
- 8 Stress-Strain: \overline{CIU} Compression Tests on Normally Consolidated Simple Clay
- 9 Total and Effective Stress Paths for a \overline{CIU} Test with $\bar{\sigma}_c = 4 \text{ kg/cm}^2$
- 10 Effective Stress Paths and Axial Strains for \overline{CIU} Compression Tests on Normally Consolidated Simple Clay
- 11 Water Content versus Log Stress for \overline{CIU} Compression Tests on Normally Consolidated Simple Clay
- 12 Water Content, Shear Stress and Effective Stress Relationship for \overline{CIU} and CID Compression Tests on Normally Consolidated Simple Clay

- II-13 Effect of K_0 Consolidation on Effective Stress Paths for \overline{CAU} Compression Tests on Normally Consolidated Simple Clay
- 14 Effect of K_0 Consolidation on Water Content versus $\overline{\log}$ Stress for \overline{CU} Compression Tests on Normally Consolidated Simple Clay
- 15 Total and Effective Stress Paths for \overline{UU} Compression Tests on Normally Consolidated Simple Clay with $\overline{\sigma}_c = 4 \text{ kg/cm}^2$
- 16 Ratio of Undrained Strength to Consolidation Pressure
- III-1 Stress-Strain: CID ($\overline{\sigma}_3 = \overline{\sigma}_2$) Compression Tests on Normally Consolidated and Highly Overconsolidated Samples of Simple Clay
- 2 Effect of OCR on Stress-Strain Behavior for Loading and Unloading CID Compression Tests on Simple Clay
- 3 Hyperbolic Stress-Strain Relationships for Loading and Unloading CID Compression Tests on Normally Consolidated and Highly Overconsolidated Samples of Simple Clay
- 4 Effective Stress Paths for Loading and Unloading CID Compression Tests on Overconsolidated Simple Clay with a Maximum Past Pressure of 8 kg/cm^2
- 5 Water Content versus Log Stress for Loading and Unloading CID Compression Tests on Overconsolidated Simple Clay with a Maximum Past Pressure of 8 kg/cm^2
- 6 Stress-Strain: \overline{CIU} Compression Tests on Normally Consolidated and Highly Overconsolidated Samples of Simple Clay
- 7 Effect of OCR on Stress-Strain Behavior for \overline{CIU} Compression Tests on Simple Clay
- 8 Effect of OCR on Hyperbolic Stress-Strain Relationship for \overline{CIU} Compression Tests on Simple Clay
- 9 Effective Stress Paths for \overline{CIU} Compression Tests on Overconsolidated Simple Clay with a Maximum Past Pressure of 8 kg/cm^2

- III-10 Rendulic Plot Showing K_o Consolidation and \overline{CIU} Stress Paths for Overconsolidated Simple Clay
- 11 Comparison of Isotropic and K_o Consolidation and Rebound Curves for Simple Clay
- 12 Strength Data from \overline{CIU} Compression Tests on Normally Consolidated and Overconsolidated Simple Clay
- 13 Strength Data from CID Compression Tests on Normally Consolidated and Overconsolidated Simple Clay
- 14 Water Content versus Log Stress for \overline{CIU} and CID Compression Tests on Normally Consolidated and Overconsolidated Simple Clay
- 15 Hyperbolic Stress-Strain Relationships for \overline{CIU} and CID Compression Tests on Normally Consolidated and Overconsolidated Simple Clay
- 16 Stress Difference versus Pore Pressure and Volume Change for \overline{CIU} and CID Compression Tests on Normally Consolidated and Overconsolidated Simple Clay
- 17 Log OCR versus (s_u at $\overline{\sigma}_c/s_u$ at $\overline{\sigma}_{cm}$), versus $s_u/\overline{\sigma}_c$ and $s_d/\overline{\sigma}_c$, and versus s_d/s_u for Triaxial Compression Tests on Simple Clay
- 18 Log OCR versus ϵ_f , versus ($\overline{\sigma}_1/\overline{\sigma}_3$) at Failure, and versus A_f and Δw_f for Triaxial Compression Tests on Simple Clay
- IV-1 Hvorslev Parameters (Drained Direct Shear Tests)
- 2 Hvorslev Parameters from Triaxial Compression Tests on Simple Clay
- V-1 Types of Stress Systems
- 2 Stress Systems in the Field
- 3 Stress-Strain: \overline{CIU} Compression and Extension Tests on Normally Consolidated Simple Clay

- V-4 Stress Difference versus A Parameter for \bar{C}_{IU} Compression and Extension Tests on Normally Consolidated Simple Clay
- 5 Effective Stress Paths for \bar{C}_{IU} Compression and Extension Tests on Normally Consolidated Simple Clay
- 6 Rendulic Plot Showing Effective Stress Paths for \bar{C}_{IU} Compression and Extension Tests on Normally Consolidated Simple Clay
- 7 Water Content versus Log Stress for \bar{C}_{IU} Compression and Extension Tests on Normally Consolidated Simple Clay

I. INTRODUCTION

A. Purpose of Report

It has been stated many times that the strength of clays is probably the most confusing subject in the area of soil engineering. Not only is it difficult for students to grasp a unifying picture of strength behavior, but many practicing engineers and teachers also tend to be confused at times by the subject. One cause of this confusion is the lack of an organized framework from which a person can start. It is the purpose of this report to present such a framework which will be based on an admittedly simplified picture of the strength behavior of saturated clays. However, once this framework is firmly established, one can then study the behavior of actual clays in terms of deviations from this simplified picture, rather than as a set of isolated facts. By analogy, the behavior of gases, and at times fluids, is studied in relationship to laws derived for ideal gases: under many conditions these laws yield very good approximations to actual behavior but there are also cases wherein the simplified laws are grossly inadequate. The same will be true of the framework presented for the strength of clays, except that its general validity is of course less precise than that of the ideal gas laws.

The principles to be presented were not generally formulated by the author but rather are primarily the result of a selective compilation from existing knowledge. The excellent work on the remolded clays by Dr. Henkel and his associates at Imperial College, as summarized by Henkel (1960)* and Parry (1960), has served as background material for the report. Although reference will be made to some of the other pertinent work, a complete history of the research in this area is beyond the scope of the notes.

B. Concept of the "Simple" Clay

On the basis of measured strength data on a number of clays, an empirical set of strength principles was developed to describe the behavior of saturated clays during shear. For example, the principles of the "unique relationship between strength and water content at failure and between strength and effective stress at failure" for normally consolidated samples were first based on tests on undisturbed clays (Rutledge, 1947; Taylor, 1948). These principles were extended to overconsolidated samples from tests on the remolded Weald and London clays (Henkel, 1960; Parry, 1960). The "unique relationship between water content and effective stress during shear" was derived from data on several remolded clays (Rendulic, 1937; Henkel, 1960; Roscoe and Poorooshasb, 1963) and at least one undisturbed clay (Taylor, 1955).

*Appendix A contains a list of references

Although the above principles were derived as working hypotheses from actual strength data, there is no clay, or at least no available data on a clay, wherein all of the principles are followed exactly. Since a consistent set of data was desired to illustrate strength behavior and principles, the author was forced to create a clay which exactly conformed to the principles. This hypothetical soil is termed the "Simple Clay," in that its behavior is "not complicated or involved."

The properties of the "Simple Clay" are patterned in general after the data obtained on the remolded Weald clay, although practically all of the data were adjusted to varying degrees in order to be completely consistent. However, the resulting properties are believed to be fairly representative of the strength behavior of many remolded and some undisturbed clays (very sensitive clays and clays with cementation are excluded). Comments on the general applicability of the assumed properties to the behavior of actual clays will be made throughout the report. Part II of this report treats some of the deviations in detail.

C. Types of Shear Tests

The report is restricted to triaxial shear testing equipment since it represents a commonly used yet versatile type of apparatus for which the stresses on the three principal planes are always known, drainage can be controlled, and pore

pressures can be conveniently measured.

Suppose that a specimen of saturated clay is placed in a triaxial cell, a confining (cell) pressure σ_c^* applied, and it is then sheared by increasing the axial load P (see Fig. I-1).

Depending upon the drainage conditions during the application of the confining pressure and during subsequent shear, there are three basic types of shear tests:

(1) Consolidated-Drained Test (called a CD test)

(a) The drainage line is opened when the confining pressure is applied. At equilibrium the confining pressure σ_c is equal to the consolidation pressure $\bar{\sigma}_c$, and the pore pressure u is equal to zero. During consolidation, water would move out of the sample if the cell pressure σ_c were larger than the effective stress $\bar{\sigma}_i$ initially acting on the sample. Conversely, the sample would imbibe water if $\bar{\sigma}_i$ had been greater than σ_c .

(b) During shear, in which the axial load P is increased after consolidation has been completed, the drainage line is also kept open. Furthermore, P is increased slowly enough that insignificant excess pore pressures develop during shear. In other words, water is allowed to flow in or out of the sample in order that the pore pressure within the sample remains essentially equal to zero (relative to atmospheric pressure).

* Appendix B presents the list of symbols.

The notation "CD test" therefore means,

C = Consolidated under the confining pressure.

D = Drained, in that full drainage is allowed during shear.

A test which is isotropically consolidated prior to drained shear is denoted by CID, whereas CAD means that the sample had been anisotropically consolidated prior to drained shear.

CD tests are sometimes called Slow tests and S tests.

(2) Consolidated-Undrained Test (called a CU test)

(a) As with the previous test, the specimen is allowed to consolidate under the confining pressure σ_c .

(b) However, just prior to shear the valve in the drainage line is turned off so that the sample can not imbibe or expell water during subsequent shearing. Therefore no drainage occurs during shear, i.e. the shear is undrained. In this case excess pore pressures will develop within the sample.

The notation "CU test" therefore means,

C = Consolidated under the confining pressure.

U = Undrained during subsequent shear. If pore pressures are measured during undrained shear, one then knows the effective stresses $\bar{\sigma}$ acting on the sample; such a test is denoted by a bar over CU, i.e. \overline{CU} test. As before, isotropic and anisotropic consolidation are designated by

CIU and CAU respectively. CU tests are sometimes called Qc tests and R tests.

(3) Unconsolidated-Undrained Test (called a UU test)

(a) In this test, the drainage valve is turned off before the sample is placed in the cell and is kept off during application of the confining pressure. The water content of the sample remains equal to the initial water content w_i and likewise the effective stress remains equal to the initial effective stress $\bar{\sigma}_i$. Consequently the pore pressure in the sample increases by an amount exactly equal* to the confining pressure σ_c , i.e.

$$u = u_i + \sigma_c \text{ where } \bar{\sigma}_i = -u_i$$

(b) As in the CU test, no drainage is allowed during shear. The notation "UU test" therefore means:

U = Unconsolidated with respect to the confining pressure (however the specimen does have an effective stress equal to $\bar{\sigma}_i$).

U = Undrained during subsequent shear. If pore pressures are measured during shear, the test is designated by \overline{UU} .

The most common type of UU test is the simple unconfined compression test wherein the confining pressure is zero and metal top and bottom plattens are used.

UU tests are sometimes called Q tests.

*Since the sample is saturated, Skempton's B parameter is equal to unity.

D. Statement of Strength Principles

What will be called the three basic strength principles are summarized below. Subsequent sections will present stress-strain, stress path, and water content-stress data on the Simple Clay. At appropriate points, the strength principles, and their corollaries, will be explained and applied to the data.

Principle I

For normally consolidated samples, or for overconsolidated samples with the same maximum past pressure $\bar{\sigma}_{cm}$ (considering shear in compression and extension separately), there is an unique relationship between strength [maximum stress difference = $(\sigma_1 - \sigma_3) \text{ max.}$] and effective stress at failure.

Principle II

For normally consolidated samples, or for overconsolidated samples with the same maximum past pressure (considering shear in compression and extension separately), there is an unique relationship among water content, shear stress, and effective stress.

Principle III

For both normally consolidated and overconsolidated samples (considering shear in compression and extension separately), there is an unique relationship among strength, water content at failure, and effective stress at failure as expressed by the Hvorslev parameters.

E. Variables Considered

The variables which will be considered are listed below.

Only triaxial shear tests are treated.

- (1) Type of Shear Test
 - (a) UU test
 - (b) CU test
 - (c) CD test
- (2) Overconsolidation Ratio (O.C.R. = $\bar{\sigma}_{cm} / \bar{\sigma}_c$).
 - (a) Normally consolidated samples with varying $\bar{\sigma}_c$.
 - (b) Overconsolidated samples with varying $\bar{\sigma}_{cm}$ and O.C.R.
- (3) Total Stress Path*
 - (a) Loading: σ_1 increased; σ_3 constant.
 - (b) Unloading: σ_1 constant; σ_3 decreased.
- (4) Value of K_c ($K_c = \bar{\sigma}_{rc} / \bar{\sigma}_{ac}$ = ratio of radial to axial consolidation pressures.)
 - (a) $K_c = 1$ (isotropic consolidation)
 - (b) $K_c \neq 1$ (anisotropic consolidation)
- (5) Value of Intermediate Principle Stress σ_2
 - (a) Triaxial compression: $\sigma_2 = \sigma_3 = \sigma_r$; $\sigma_1 = \sigma_a$
 - (b) Triaxial extension: $\sigma_2 = \sigma_1 = \sigma_r$; $\sigma_3 = \sigma_a$

F. Consolidation Curves for Simple Clay

Consolidation and rebound curves for isotropic stresses are plotted in Fig. I-2 for the Simple Clay. Two facts should be noted.

- (1) Water content versus log consolidation pressure is a straight line for virgin compression. The equation is:

$$w(\%) = 25.4 - 7.65 \log \bar{\sigma}_c \text{ (kg/cm}^2\text{)}$$

*Although an infinite number of stress paths are possible, the two chosen are the most common.

(2) All rebound curves are parallel. The increases in water content versus overconsolidation ratio are:

<u>O.C.R.</u>	<u>$\Delta w(\%)$</u>
1	0
1.5	0.35
2	0.61
4	1.47
8	2.40
12	2.98
24	4.08

The assumptions of a straight line for virgin compression and of parallel rebound curves, which are closely duplicated by many clays, greatly simplify strength behavior.

II. STRENGTH BEHAVIOR OF NORMALLY CONSOLIDATED SIMPLE CLAY (Compression tests only)

A. CID Tests

1. Stress-Strain Data

Samples of clay are normally consolidated to pressures of 4 and 8 kg/cm² (Tests A and B respectively). Drained shear tests are then run in which the axial pressure is increased while holding the radial pressure equal to the consolidation pressure, i. e. $\bar{\sigma}_r = \bar{\sigma}_c = \bar{\sigma}_3$ while $\bar{\sigma}_a = \bar{\sigma}_1$ is increased. The resulting plots of axial strain ϵ versus stress difference $(\sigma_1 - \sigma_3)$, principal stress ratio $\bar{\sigma}_1 / \bar{\sigma}_3$, and change in water content Δw are shown in Fig. II-1.

The data show that:

(1) Failure, i. e. $(\sigma_1 - \sigma_3)$ max., occurs at $\epsilon = 22\%$.

The maximum value of the principal stress ratio, called maximum obliquity, also occurs at the same strain.

(2) At any given strain, the value of $(\sigma_1 - \sigma_3)$ for the test with $\bar{\sigma}_3 = \bar{\sigma}_c = 8 \text{ kg/cm}^2$ is exactly double that for the test with $\bar{\sigma}_3 = \bar{\sigma}_c = 4 \text{ kg/cm}^2$. Hence both tests would yield identical plots of $(\sigma_1 - \sigma_3) / \bar{\sigma}_c$ vs. ϵ .

(3) Both tests have identical plots of ϵ vs. $\bar{\sigma}_1 / \bar{\sigma}_3$ and ϵ vs. Δw .

In summary, when the data are expressed by dimensionless terms ($\bar{\sigma}_1 / \bar{\sigma}_3$ and Δw) and by "normalized"

stresses (wherein the stresses are divided by the consolidation pressure), all CID tests with $\bar{\sigma}_3 = \bar{\sigma}_c$ will yield identical stress-strain plots, independent of the consolidation pressure, as long as all of the samples are normally consolidated. This will be called normalized behavior. We will see that normalized behavior will also hold true for other stress paths and types of shear tests.

2. Mohr Coulomb Strength Criteria and Stress Paths

Tests A and B had the following stresses at failure:

$$\text{Test A: } \bar{\sigma}_{3f} = 4.00 \text{ kg/cm}^2, \bar{\sigma}_{1f} = 9.15 \text{ kg/cm}^2$$

$$\text{Test B: } \bar{\sigma}_{3f} = 8.00 \text{ kg/cm}^2, \bar{\sigma}_{1f} = 18.31 \text{ kg/cm}^2$$

Mohr circles representing these failure stresses are plotted in Fig. II-2. The straight line through the origin and tangent to the Mohr circles at failure is called the Mohr Coulomb envelope*. The slope of this line, denoted by $\bar{\phi}$, is commonly called the friction angle. For the Simple Clay, $\bar{\phi} = 23.0$ degrees.

It is often assumed that clay follows the Mohr Coulomb strength criteria, which state that:

- (1) The Mohr Coulomb envelope represents the limiting condition for any possible combination of τ and $\bar{\sigma}$, i.e. no portion of a Mohr circle can be outside of this

*Mohr Coulomb envelopes do not necessarily go through the origin or form straight lines, as will be seen for overconsolidated samples.

envelope. (as will be discussed later in more detail, the envelope shown in Fig. II-2 will only be valid for normally consolidated samples: overconsolidated samples will have a different envelope).

(2) The point of tangency of a Mohr circle with the envelope represents the stresses on the failure plane at failure (denoted by τ_{ff} and $\bar{\sigma}_{ff}$). The equation relating shear strength and effective stress is therefore given by:

$$\tau_{ff} = \bar{\sigma}_{ff} \tan \bar{\phi} \quad \text{Eq. II-1}$$

The various stresses and angles are illustrated in Fig. II-2.

Although many objections have been raised concerning the general validity of the Mohr Coulomb strength criteria (Hvorslev, 1960, summarizes many of the theoretical and experimental objections), it is still the most convenient and widely used strength theory and moreover it generally is quite accurate.

To simplify matters, the Mohr circle will be replaced by its coordinates at the point of maximum shear stress, which are designated as:

$$q = \frac{(\sigma_1 - \sigma_3)}{2} \quad \text{and} \quad \bar{p} = \frac{(\bar{\sigma}_1 + \bar{\sigma}_3)}{2}$$

$$q_f = \frac{(\sigma_1 - \sigma_3)_f}{2} \quad \text{and} \quad \bar{p}_f = \frac{(\bar{\sigma}_1 + \bar{\sigma}_3)_f}{2}$$

The line through the coordinates q_f and \bar{p}_f will be called the strength envelope, as illustrated in Fig. II-3 for CID Test B. Its slope is called $\bar{\alpha}$ ($\tan \bar{\alpha} = \sin \bar{\phi}$). Fig. II-3 also shows Mohr circles representing two of the infinite numbers of stress conditions which existed prior to failure. The line rising at 45 deg which passes through the top of the three Mohr circles plots all of the values of q and \bar{p} which occurred during the test. It is called an effective stress path and shows graphically the state of stresses throughout the entire test.

3. Effect of Different Stress Paths

The effective stress path shown in Fig. II-3 for CID Test B represents only one of an infinite number of possible stress paths that a drained shear test could follow. Its stress path rises to the right at 45 deg since $\bar{\sigma}_3 = \bar{\sigma}_c$ and $\bar{\sigma}_1$ is increased. The relationship between \bar{p} and q is therefore given by:

$$\bar{p} = 1/2 (\bar{\sigma}_1 + \bar{\sigma}_3) = \bar{\sigma}_c + q$$

Stress paths for two other types of drained shear tests are plotted in Fig. II-4 for $\bar{\sigma}_c = 8 \text{ kg/cm}^2$. In Test C, the axial pressure is kept constant and the radial pressure reduced ($\bar{\sigma}_a = \bar{\sigma}_1 = \bar{\sigma}_c$ and $\bar{\sigma}_r = \bar{\sigma}_3$ is decreased) so that $\bar{p} = \bar{\sigma}_c - q$ and the stress path rises

at 45 deg to the left. In Test D, the axial pressure is increased and the radial pressure decreased by like amounts ($\Delta \bar{\sigma}_a = \Delta \bar{\sigma}_1 = -\Delta \bar{\sigma}_r = -\Delta \bar{\sigma}_3$) so that $\bar{p} = \bar{\sigma}_c$ and the stress path rises vertically.

As shown in Fig. II-4, all three tests will end on the same strength envelope, which has a slope of $\bar{\alpha} = 21.4$ deg. This fact is an example of Principle I (Section ID) which states that there is an unique relationship between strength and effective stress at failure. We have chosen the relationship to be in the form of $q_f = \bar{p}_f \tan \bar{\alpha}$; we could chose other forms such as $\tau_{ff} = \bar{\sigma}_{ff} \tan \bar{\phi}$ or $q_f = \bar{\sigma}_{3f} \tan \bar{\alpha} / (1 - \tan \bar{\alpha})$, all of which simply select different points on the Mohr circle at failure.

Although obvious, it is emphasized that there is no such thing as "the" drained strength of a sample since the strength depends on the stresses which are applied during shear. For example, Tests B, C and D in Fig. II-4 had q_f values equal to 5.15, 2.25 and 3.13 kg/cm² respectively.

4. Stress-Strain Data for Different Stress Paths and the Hyperbolic Stress-Strain Relationship

Fig. II-1 presented stress-strain curves for two CID tests wherein the axial pressure was increased. Just as the strength of drained tests depends on the stress path, so do the stress-strain relationships. This is shown in Fig. II-5 for two types of CID tests, one in which the sample is loaded

during shear ($\bar{\sigma}_3 = \bar{\sigma}_c$) and the second in which the sample is unloaded during shear ($\bar{\sigma}_1 = \bar{\sigma}_c$). These correspond to Tests B and C in Fig. II-4. The normalized stress $(\sigma_1 - \sigma_3) / \bar{\sigma}_c$ is used since the strength behavior is independent of consolidation pressure.

The marked effect of type of stress path on the stress-strain characteristics of drained tests is self-evident. Relative to a loading test, unloading produces the following significant changes:

(1) A greatly decreased strain at failure and a somewhat increased initial stress-strain modulus [$E = (\sigma_1 - \sigma_3) / \epsilon$].

(2) The water content, and hence volume, increases and then decreases during shear with a small net volume increase at failure*, as contrasted to a constantly decreasing volume for the loading test. A test in which $\bar{p} = \bar{\sigma}_c$ would have stress-strain characteristics between those for loading and unloading tests: the volume would increase very slightly and then decrease.

It has been observed that plots of $(\sigma_1 - \sigma_3)$ versus ϵ from triaxial tests on clays generally agree very well with a hyperbolic stress-strain relationship of the form (Kondner, 1963)**:

$$(\sigma_1 - \sigma_3) = \frac{\epsilon}{m' + n' \epsilon} \quad \text{Eq. II-2(a)}$$

If $(\sigma_1 - \sigma_3)$ is divided by $\bar{\sigma}_c$, the equation becomes normalized

*This rather odd volume change behavior follows from Principle II, as will be discussed in detail in Section II C. Actual test data generally show less marked changes in volume, although the trends are correct.

**Hansen (1963) presents other relationships that offer better empirical fits in some instances.

so that:

$$\frac{(\sigma_1 - \sigma_3)}{\bar{\sigma}} = \frac{\epsilon}{m + n\epsilon} \quad \text{Eq. II-2(b)}$$

On a plot of $\epsilon \bar{\sigma}_c / (\sigma_1 - \sigma_3)$ versus ϵ , the line intercepts the $\epsilon \bar{\sigma}_c / (\sigma_1 - \sigma_3)$ axis at a value equal to m and has a slope equal to n . Fig. II-6 presents such plots for the loading and unloading CID tests shown in Fig. II-5 and gives the values of m and n .

The stress-strain equation is only valid for strains equal to or less than the strain at failure [point of $(\sigma_1 - \sigma_3)$ max.].

5. Water Content vs. Log Stress

From the CID test data in Fig. II-4, one obtains the following relationships among q_f , \bar{p}_f , and $\bar{\sigma}_c$ for loading ($\bar{\sigma}_3 = \bar{\sigma}_c$) and unloading ($\bar{\sigma}_1 = \bar{\sigma}_c$) tests:

$$\text{Loading:} \quad q_f = 0.644 \bar{\sigma}_c, \quad \bar{p}_f = 1.644 \bar{\sigma}_c$$

$$\text{Unloading:} \quad q_f = 0.281 \bar{\sigma}_c, \quad \bar{p}_f = 0.719 \bar{\sigma}_c$$

The stress-strain data in Fig. II-5 show that Δw at failure for loading and unloading tests are -2.65% and +0.10% respectively. A plot of water content versus consolidation pressure was given in Fig. I-2. It is thus possible to obtain values of w_f , q_f and \bar{p}_f for loading and unloading CID tests at any consolidation pressure. Values for consolidation pressures of 1, 2 and 4 kg/cm² are tabulated below (stresses in kg/cm²).

σ_c	$w(\%)$	CID Test, $\bar{\sigma}_3 = \bar{\sigma}_c$			CID Test, $\bar{\sigma}_1 = \bar{\sigma}_c$		
		q_f	\bar{p}_f	$w_f(\%)$	q_f	\bar{p}_f	$w_f(\%)$
1	25.40	0.644	1.644	22.75	0.281	0.719	25.50
2	23.10	1.288	3.288	20.45	0.562	1.438	23.20
4	20.80	2.576	6.576	18.15	1.124	2.876	20.90

The data from these tests, plotted in Fig. II-7, yield parallel straight lines for water content vs. $\log q_f$, vs. $\log \bar{p}_f$, and vs. $\log \bar{\sigma}_c$. Moreover, the relationship among water content at failure, strength (q_f), and effective stress at failure (\bar{p}_f) holds for any type of CID test starting at any consolidation pressure, as long as the sample is normally consolidated. In fact, this is an example, for the specific condition of failure, of Principle II which states that there is an unique relationship among water content, shear stress, and effective stress.

The variation in \bar{p} vs. water content is also shown in Fig. II-7 for loading and unloading CID tests starting from a consolidation pressure of 4 kg/cm^2 . This information was obtained from the stress-strain plots in Fig. II-5.

6. Review

The most important concepts presented thus far for CID tests on normally consolidated samples are:

- (1) Strength and stress-strain characteristics depend upon

the stress path, i. e. applied loads, during shear (see Fig. II-5).

(2) There is an unique relationship between strength and effective stress at failure, independent of the stress path. In other words, all tests end up on the same strength envelope which is defined by $q_f = \bar{p}_f \tan \bar{\alpha}$ (see Fig. II-4).

(3) There is an unique relationship among water content at failure, strength, and effective stress at failure, independent of the stress path (see Fig. II-7).

B. CIU Tests

1. Stress-Strain Data

The stress-strain behavior from consolidated-undrained shear tests on normally consolidated Simple Clay can be normalized as was done for the CID tests. In other words, if stresses are divided by consolidation pressure, all CIU tests sheared in the same manner will have identical stress-strain plots independent of consolidation pressure.

Fig. II-8 presents normalized stress-strain curves for CIU tests in which the axial pressure was increased while keeping the radial pressure equal to the consolidation pressure ($\sigma_r = \sigma_3 = \bar{\sigma}_c$), $\sigma_a = \sigma_1$ increased). Skempton's (1954) pore pressure parameter A, plotted at the bottom, is defined by the equation:

$$A = \frac{\Delta u - \Delta \sigma_3}{\Delta \sigma_1 - \Delta \sigma_3} \quad \text{Eq. II-3}$$

Since $\Delta\sigma_3 = 0$ and $\Delta\sigma_1 - \Delta\sigma_3 = (\sigma_1 - \sigma_3)$ for these $\overline{\text{CIU}}$ test data, A will equal $\Delta u / \bar{\sigma}_c$ divided by $(\sigma_1 - \sigma_3) / \bar{\sigma}_c$.

The stress-strain data in Fig. II-8 show the following behavior:

(1) The strain at failure ϵ_f [strain at $(\sigma_1 - \sigma_3)$ max.] equals 12%.*

(2) There is a hyperbolic relationship between $(\sigma_1 - \sigma_3) / \bar{\sigma}_c$ and ϵ ; $m = 1.20$ and $n = 1.625$, which yields a line falling slightly above that for the CID test with $\bar{\sigma}_1 = \bar{\sigma}_c$ shown in Fig. II-6.

(3) Maximum obliquity occurs at $\epsilon_f = 12\%$.**

(4) As with the stress difference, the pore pressure increases rapidly at low strains but slowly at large strains, with a maximum value at failure.

(5) The A parameter starts with a value approximately equal to 1/3 and increases with strain to a value at failure slightly less than one.

(6) The value of $\bar{\sigma}_3$ decreases with increasing strain, since Δu is increasing, but $\bar{\sigma}_1$ increases and then decreases to a value approximately equal to $\bar{\sigma}_c$ at failure.

(7) Although not shown, all of the stress ratios would remain constant at strains greater than ϵ_f . These values are:

*The $\epsilon_f = 12\%$ was obtained from data on remolded Weald clay; many other remolded clays and most undisturbed clays show values of ϵ_f between 5 and 10% for $\overline{\text{CIU}}$ tests on normally consolidated samples.

**Maximum obliquity occurs after failure with most undisturbed normally consolidated clays and many remolded normally consolidated clays.

$$\begin{aligned}
 (\sigma_1 - \sigma_3) / \bar{\sigma}_c &= 0.580 & A &= 0.945 \\
 \Delta u / \bar{\sigma}_c &= 0.548 & \bar{\sigma}_1 / \bar{\sigma}_c &= 1.032 \\
 \bar{\sigma}_1 / \bar{\sigma}_3 &= 2.287 & \bar{\sigma}_3 / \bar{\sigma}_c &= 0.452
 \end{aligned}$$

The undrained shear strength from triaxial tests is commonly defined as

$$s_u = \frac{(\sigma_1 - \sigma_3) \max.}{2}$$

and is thus equal to q_f . A widely used ratio, when dealing with normally consolidated clay, is that of $s_u / \bar{\sigma}_c$. For the Simple Clay, $s_u / \bar{\sigma}_c = 0.290$.*

2. Total and Effective Stress Paths

Total (q, p) and effective (q, \bar{p}) stress paths for a \overline{CIU} test with $\sigma_3 = \bar{\sigma}_c = 4 \text{ kg/cm}^2$ are plotted in Fig. II-9 based on the data in Fig. II-8. The total stress path rises at 45 deg to the right since it is defined by the equation $p = \sigma_3 + q = \bar{\sigma}_c + q$. The effective stress path is displaced to the left by a value equal to the pore pressure, i. e. $\bar{p} = p - u$. The stress conditions existing at an axial strain of 3% (Fig. II-8) are taken as an example (stresses in kg/cm^2).

$$(\sigma_1 - \sigma_3) / \bar{\sigma}_c = 0.50, (\sigma_1 - \sigma_3) = 2.00, q = 1.00$$

$$\Delta u / \bar{\sigma}_c = 0.360, \Delta u = 1.44$$

$$p = 4.00 + 1.00 = 5.00, \bar{p} = 5.00 - 1.44 = 3.56$$

*CIU triaxial tests on normally consolidated undisturbed clays generally yield values of $s_u / \bar{\sigma}_c$ equal to 0.3 ± 0.1 . The $s_u / \bar{\sigma}_c$ ratio is more commonly called the " c_u / p " ratio.

The Mohr circles in terms of total and effective stresses are also plotted. Similar points on the two circles are displaced by a stress equal to the pore pressure. For example, $\sigma_1 = 6.00 \text{ kg/cm}^2$ and $\bar{\sigma}_1 = 6.00 - 1.44 = 4.56 \text{ kg/cm}^2$.

The effective stress path for this $\overline{\text{CIU}}$ test ends up at failure on a strength envelope with a slope $\bar{\alpha} = 21.4^\circ$. This is the same envelope which defined failure for the CID tests (see Fig. II-4), i. e. undrained and drained triaxial compression tests have the same relationship between strength and effective stress at failure given by the equation $q_f = \bar{p}_f \tan 21.4^\circ$. This is another example of the meaning of Principle I.

Thus far we have discussed the behavior of an undrained test wherein $\sigma_1 = \sigma_a$ was increased at constant $\sigma_3 = \sigma_r = \bar{\sigma}_c = 4 \text{ kg/cm}^2$. What would happen for a different set of applied stresses, such as a constant $\sigma_1 = \sigma_a = \bar{\sigma}_c = 4 \text{ kg/cm}^2$ with a decreasing $\sigma_3 = \sigma_r$? The answer is that the behavior in terms of effective stresses and axial strains would be exactly the same but different pore pressures would be developed during shear. Fig. II-9 shows the total stress path, which rises at 45 deg to the left, for an undrained test with decreasing σ_3 . For the same value of $q = 1.00 \text{ kg/cm}^2$ considered previously, $p = \bar{\sigma}_c - q = 4.00 - 1.00 = 3.00 \text{ kg/cm}^2$. The corresponding pore pressure is therefore $u = p - \bar{p} = 3.00 - 3.56 = -0.56 \text{ kg/cm}^2$ since this test will have the same effective stress path as the previous test.

What is the A parameter for the above stress conditions?

We find that: $u = \Delta u = -0.56 \text{ kg/cm}^2$, $\Delta\sigma_3 = -2.00 \text{ kg/cm}^2$ and $\Delta\sigma_1 = 0$.

Therefore:

$$A = \frac{\Delta u - \Delta\sigma_3}{\Delta\sigma_1 - \Delta\sigma_3} = \frac{-0.56 - (-2.00)}{0 - (-2.00)} = \frac{1.44}{2.00} = 0.72$$

Referring to Fig. II-8 for $(\sigma_1 - \sigma_3) / \bar{\sigma}_c = 0.50$ and $\epsilon = 3\%$, one notes that the A parameter has remained the same even though the total stress path was different.

A very important concept regarding the undrained shear behavior of a consolidated sample becomes evident: the shear strength s_u , the effective stress path and the strength envelope and the stress $[(\sigma_1 - \sigma_3), \bar{\sigma}_1, \bar{\sigma}_3, \bar{\sigma}_1 / \bar{\sigma}_3$ and A but not $\Delta u]$ versus strain characteristics are independent* of the total stress path followed by a sample during undrained shear. Furthermore, the difference in pore pressure during shear for different stress paths is solely a function of the difference in $\Delta\sigma_3$ (see Eq. II-3 defining A).

The following statements also follow from this concept:

- (1) s_u is uniquely related to $\bar{\sigma}_c$, i.e. for a given consolidation pressure there is only one undrained shear strength.
- (2) s_u is uniquely related to w_f , i.e. a given water content at failure has only one corresponding shear strength.

*Remember that Section II is restricted to compression tests for which $\sigma_3 = \sigma_2 = \sigma_r$.

3. Effective Stress Path and Axial Strain Relationship

Effective stress paths for $\overline{\text{CIU}}$ tests with $\overline{\sigma}_c = 2, 4, 6$ and 8 kg/cm^2 are plotted in Fig. II-10. Since these tests show normalized behavior, all of the stress paths are geometrically similar. The radial lines superimposed on the plot are contours of equal axial strain which occur during undrained shear. Since the stress paths are normalized, the equal strain lines pass through the origin.

4. Water Content versus Log Stress

The $\overline{\text{CIU}}$ stress-strain data showed that at failure $s_u = q_f = 0.290 \overline{\sigma}_c$ and $\overline{p}_f = 0.742 \overline{\sigma}_c$. Using the w vs. $\log \overline{\sigma}_c$ consolidation data from Fig. I-2 and the fact that the water content does not change during an undrained shear test, the relationship plotted in Fig. II-11 results for $\overline{\text{CIU}}$ compression tests. A comparison of these curves with those derived from the CID tests (Fig. II-7) shows that they are identical. This follows from Principle II.

5. Review

Important concepts to remember regarding $\overline{\text{CIU}}$ tests on normally consolidated samples are:

(1) The ratio of undrained shear strength s_u to consolidation pressure $\overline{\sigma}_c$ is a constant. For the Simple Clay, $s_u / \overline{\sigma}_c = 0.290$.

(2) The stress-strain behavior is normalized in that it is independent of $\overline{\sigma}_c$ (see Fig. II-8).

(3) The undrained shear behavior in terms of strains and effective stresses is independent of the total stress path followed by samples during shear. Only the pore pressure is different (Fig. II-9).

(4) Undrained tests have the same strength envelope as drained tests, as stated in Principle I.

(5) Undrained tests have the same relationship at failure among water content, strength, and effective stress as drained tests, as stated in Principle II.

C. Unique Relationship Among Water Content, Shear Stress and Effective Stress

1. Relationship Between $\bar{C}IU$ and CID Tests

Effective stress paths for $\bar{C}IU$ tests at several consolidation pressures were drawn in Fig. II-10. Since these are undrained shear tests, the effective stress paths are also lines of constant water content. These paths, with the corresponding water contents, are plotted in Fig. II-12 for consolidation pressures of 4, 6 and 8 kg/cm². As will be shown, and as stated in Principle II, these lines represent an unique relationship among water content, shear stress (q), and effective stress (\bar{p}). * Unique means that the same relationship holds whether a stress condition was arrived at by

*The shear stress and effective stress could be represented by other stresses, such as $(\sigma_1 - \sigma_3)$ and $1/3 (\bar{\sigma}_1 + \bar{\sigma}_2 + \bar{\sigma}_3)$.

undrained shear or by drained shear or by anisotropic consolidation.* This uniqueness will be illustrated for loading and unloading CID tests in Fig. II-12.

A loading $\overline{\text{CID}}$ test with $\overline{\sigma}_3 = \overline{\sigma}_c = 4 \text{ kg/cm}^2$ intersects the effective stress path of a $\overline{\text{CIU}}$ test with $\overline{\sigma}_c = 6 \text{ kg/cm}^2$ at Point (1) for which $q = 1.45 \text{ kg/cm}^2$ and $\overline{p} = 5.45 \text{ kg/cm}^2$. Refer back to the stress-strain data for CID tests in Fig. II-5: at $(\sigma_1 - \sigma_3) / \overline{\sigma}_c = 2(1.45)/4 = 0.725$, $\epsilon = 3.8\%$ and $\Delta w = -1.35\%$. The water content at this stress condition in the CID test is therefore $w = 20.80 - 1.35 = 19.45\%$, which equals that of the $\overline{\text{CIU}}$ test with the stress path through this point. At Point (2) the value of Δw in the CID test should be $18.50 - 20.80 = -2.30\%$; referring again to Fig. II-5, the corresponding data are: $\epsilon = 10.9\%$ and $(\sigma_1 - \sigma_3) / \overline{\sigma}_c = 1.105$ or $q = 2.21 \text{ kg/cm}^2$ and $\overline{p} = 6.21 \text{ kg/cm}^2$, which agree with the location of Point (2).

The water contents for an unloading CID test also agree with those derived from $\overline{\text{CIU}}$ tests, as illustrated in Fig. II-12 for a CID test with $\overline{\sigma}_1 = \overline{\sigma}_c = 6.5 \text{ kg/cm}^2$. At Points (3), and (4), the CID test yields $w = 19.20 + 0.25 = 19.45\%$ at axial strains of about 0.15% and 2.7% respectively.

Although the effective stress paths from $\overline{\text{CIU}}$ tests represent unique values of water content, the equal strain

*The distinction between drained shear tests and consolidation tests lies in the fact that K changes during shear tests but remains constant during consolidation tests (for normally consolidated clays).

contours shown in Fig. II-10 hold only for \overline{CIU} tests.*

The assumed uniqueness among w , q and \bar{p} described above and extended to anisotropically consolidated samples in the next section has been verified approximately for only one remolded clay* (a kaolinite, see Roscoe and Poorooshab, 1963). Tests at M.I.T. on other remolded clays and on natural clays have shown several deviations from an unique relationship, some of which were quite significant. For example, \overline{CAU} tests (see next section) do not in reality follow an extension of \overline{CIU} tests as hypothesized.

2. Effect of Anisotropic Consolidation

The previous section showed that a loading CID test with $\bar{\sigma}_3 = \bar{\sigma}_c = 4 \text{ kg/cm}^2$ yielded the same water content at Point (1) in Fig. II-12 as a \overline{CIU} test with $\bar{\sigma}_c = 6 \text{ kg/cm}^2$. Suppose that the drainage valve in this CID test were shut-off when the test reached Point (1) so that the remaining portion of the shear was undrained. In other words, a \overline{CAU} test is run on a sample anisotropically consolidated to Point (1) for which $w = 19.45\%$, $q_c = 1.45 \text{ kg/cm}^2$, $\bar{p}_c = 5.45 \text{ kg/cm}^2$, $\bar{\sigma}_{3c} = 4.00 \text{ kg/cm}^2$ and $\bar{\sigma}_{1c} = 6.90 \text{ kg/cm}^2$. What would be the effective stress path during the undrained shear? From Principle II, the \overline{CAU} test must follow the

*A theory has been developed (Roscoe and Poorooshab, 1963) to compute volumetric and axial strains for a loading CID test from the results of \overline{CIU} tests and from consolidation tests with varying values of $K_c = (\bar{\sigma}_{rc} / \bar{\sigma}_{ac})$.

**Whereas the first series of tests on remolded Weald clay (Henkel, 1960 Geotechnique) showed an unique relationship, subsequent tests (Henkel and Sowa, 1963) showed significant discrepancies.

effective stress path of the $\overline{\text{CIU}}$ test through Point (1) since both tests have the same water content. Consequently, the $\overline{\text{CAU}}$ test would have the following properties at failure:

$$\begin{aligned} s_u = q_f &= 1.74 \text{ kg/cm}^2 \\ \bar{p}_f &= 4.45 \text{ kg/cm}^2 \\ \Delta u_f = u_f &= 1.29 \text{ kg/cm}^2 \\ A_f &= 1.29/0.58 = 2.224 \\ s_u / \bar{\sigma}_{1c} &= 1.74/6.90 = 0.252 \end{aligned}$$

If samples were consolidated to other stress conditions which lay on the effective stress path for the $\overline{\text{CIU}}$ test with $\bar{\sigma}_c = 6 \text{ kg/cm}^2$, $\overline{\text{CAU}}$ tests on these samples would all have the same value of s_u , \bar{p}_f , and w_f , but the values of u_f , A_f and $s_u / \bar{\sigma}_{1c}$ would be different.

The value of $K_c = \bar{\sigma}_{rc} / \bar{\sigma}_{ac}$ for anisotropic consolidation under stresses which yield no change in the radial (lateral) dimension of the sample is denoted by K_o . Thus consolidation in the standard oedometer ring is K_o consolidation. Most horizontal deposits of clay are also in a K_o condition (if structures are not placed on them or excavations made).

It has been determined experimentally that $K_o = 1 - \sin \bar{\phi}$ as a very good approximation for normally consolidated clays (Bishop, 1958; Simons, 1958 and data at M.I.T.). Thus K_o for the Simple Clay is:

$$K_o = 1 - \sin 23.0^\circ = 0.608$$

The line representing K_o consolidation is drawn on the $q - \bar{p}$ plot shown in Fig. II-13. It is evident that $q_c / \bar{p}_c = (1 - K_o) / (1 + K_o) = 0.244$ along this line. Effective stress paths for several \overline{CAU} tests starting from K_o consolidation are also shown in the figure (the paths are those corresponding to \overline{CIU} tests with $\bar{\sigma}_c = 4, 6$ and 8 kg/cm^2).

\overline{CAU} tests with K_o consolidation have the following properties, which can be determined from Fig. II-13 or from Fig. II-8 [a \overline{CIU} test crosses the K_o line at $\epsilon \approx 2.1\%$ for which $(\sigma_1 - \sigma_3) / \bar{\sigma}_c = 0.454$, $\Delta u / \bar{\sigma}_c = 0.295$ and $\bar{\sigma}_1 / \bar{\sigma}_c = 1.159$].

$$\begin{aligned} s_u / \bar{\sigma}_c &= 0.250 \\ A_f &= 2.01* \\ \Delta u / \bar{\sigma}_{1c} &= 0.218 \text{ (for } \Delta \sigma_3 = 0) \\ \tan \bar{\alpha} &= 0.3915 \text{ (as before)} \end{aligned}$$

Hence K_o consolidation reduces the ratio of $s_u / \bar{\sigma}_{1c}$ from 0.290 to 0.250 while increasing A_f from 0.945 to 2.01.

Fig. II-13 shows that the \overline{CAU} test which follows the effective stress path corresponding to a \overline{CIU} test with $\bar{\sigma}_c = 4 \text{ kg/cm}^2$ has a value of $\bar{\sigma}_{1c} = 4.64 \text{ kg/cm}^2$. Both samples have, of course, the same water content. Hence $\bar{\sigma}_{1c} (K = K_o) / \bar{\sigma}_c (K = 1) = 4.64 / 4.00 = 1.159$. The same ratio of $\bar{\sigma}_{1c} / \bar{\sigma}_c$ also holds for other consolidation pressures along the K_o line. This means that the line of water content vs. $\log \bar{\sigma}_{1c}$ for K_o consolidation is parallel and to the right of the line

*Remember that $A_f = \frac{\Delta u - \Delta \sigma_3}{\Delta \sigma_1 - \Delta \sigma_3}$ where $\Delta \sigma_1 - \Delta \sigma_3 = 2(q_f - q_c)$.

representing isotropic consolidation, as is shown in Fig. II-14. However, \overline{CIU} and \overline{CAU} tests have the same relationship among water, strength and effective stress at failure. As stated in Principle II, this same relationship also holds for all types of CD tests.

3. Review

It has been shown that for the failure condition, all types of CD tests (loading and unloading CID and CAD tests) and all types of CU and (\overline{CIU} tests and \overline{CAU} tests with varying values of K_c) on normally consolidated Simple Clay have the same strength envelope, given by $q_f = \bar{p}_f \tan 21.4^\circ$, and the same lines of w_f vs. $\log q_f$ and w_f vs. $\log \bar{p}_f$. This section stressed the fact that for all conditions (consolidation, shear prior to failure and at failure) there is an unique relationship among water content, shear stress, and effective stress. This relationship is best shown by the effective stress paths from \overline{CIU} tests which are also lines of constant water content (see Fig. II-12). The resulting $w - q - \bar{p}$ plot also holds for consolidation at any value of K_c , for all types of CD tests, and for all types of \overline{CU} tests. (Again remember that we are only treating triaxial compression tests.)

D. UU Tests

An Unconsolidated-Undrained test was described as an undrained shear test on a sample which had not been consolidated under the pre-shear chamber pressure σ_c . Hence the water content of the sample is unchanged throughout testing.

Imagine that four UU tests, A through D with $\sigma_c = 0$ (an unconfined compression test), 2, 4 and 6 kg/cm², are run on samples of Simple Clay which had previously been consolidated to $\bar{\sigma}_c = 4$ kg/cm². During shear, the axial pressure is increased at constant chamber pressure. The total stress paths during shear are plotted in Fig. II-15. All four tests show the same value of $q_f^* = s_u = 1.16$ kg/cm² and of course have the same water content $w_f = w_c = 20.80\%$. Moreover, the four tests have identical effective stress paths during shear and the same stress-strain behavior, except for pore pressures. These are different by magnitudes equal to the differences in chamber pressure, as the data tabulated in Fig. II-15 show.

The above concepts are valid for any total stress path during a UU compression test, i. e. p can increase, decrease or remain constant. In fact, all of the concepts which hold for \overline{CIU} tests also hold for UU tests. One might look at a UU test as a \overline{CIU} test with unknown consolidation pressure. However, if the \overline{CIU} behavior of a clay is known, the effective stress and stress-strain behavior which occurs in any UU test can be deduced from the strength principles which have been discussed since the same $w - q - \bar{p}$ relationship holds for both types of tests.

*An envelope through the points of q_f and p_f has a slope $\alpha = 0$ and hence $\phi = 0$. This is the basis for the so-called " $\phi = 0$ " method of stability analysis since the clay behaves as a "frictionless" (i. e. purely "cohesive") material with respect to the applied total stresses during undrained shear.

E. Summary and Conclusions

1. Statement of Principles

For triaxial compression tests (i.e. $\sigma_2 = \sigma_3 = \sigma_r$) on normally consolidated Simple Clay:

(a) There is an unique relationship between strength and effective stress at failure which can be expressed by the equation:

$$q_f = \bar{p}_f \tan \bar{\alpha} .$$

This relationship holds for all types of CD tests (CID and CAD; increasing σ_1 or decreasing $\bar{\sigma}_3$), all types of CU tests (\overline{CIU} or \overline{CAU} ; increasing σ_1 or decreasing σ_3), and all types of UU tests (increasing σ_1 or decreasing σ_3).

(b) There is an unique relationship among water content, shear stress, and effective stress throughout all conditions of consolidation and shear. This relationship is best shown by a $w - q - \bar{p}$ plot (such as Fig. II-12) derived from \overline{CIU} tests. However, these $w - q - \bar{p}$ lines also hold for all types of CD tests, all types of CU tests, all types of UU tests, and all types of consolidation tests (i.e. for any value of $K_c = \bar{\sigma}_{rc} / \bar{\sigma}_{ac}$).

One very important qualification must be specified regarding the $w - q - \bar{p}$ relationship: it is only valid for tests wherein the shear stress q remains constant or increases; it is not valid for tests wherein the shear stress on a sample is decreased. For example, if the shear stress on a sample is

reduced after it has been sheared in a $\overline{\text{CIU}}$ test, the resulting effective stress path will not follow the stress paths shown in Fig. II-12. In this case different stress paths occur for the same water content and the $w - q - \bar{p}$ relationship is no longer unique.

2. Equations for Undrained Shear Strength

The ratio of undrained shear strength to consolidation pressure is commonly used in practice. For isotropic consolidation, the equation for $s_u / \bar{\sigma}_c$ can be derived as follows:

At failure,

$$s_u = \frac{(\sigma_1 - \sigma_3)_f}{2} = \bar{p}_f \tan \bar{\alpha} = \frac{(\bar{\sigma}_1 + \bar{\sigma}_3)_f}{2} \tan \bar{\alpha}$$

and

$$\begin{aligned} \bar{\sigma}_{3f} &= \bar{\sigma}_c + \Delta\sigma_{3f} - \Delta u_f = \bar{\sigma}_c - A_f(\sigma_1 - \sigma_3)_f \\ \bar{\sigma}_{1f} &= \bar{\sigma}_1 + \Delta\sigma_{1f} - \Delta u_f = \bar{\sigma}_c + (\sigma_1 - \sigma_3)_f + \Delta\sigma_{3f} - \Delta u_f \\ &= \bar{\sigma}_c + (1 - A_f)(\sigma_1 - \sigma_3)_f \end{aligned}$$

$$\frac{(\bar{\sigma}_1 + \bar{\sigma}_3)_f}{2} = \bar{\sigma}_c - \frac{(\sigma_1 - \sigma_3)_f}{2} (2A_f - 1)$$

which results in,

$$\frac{s_u}{\bar{\sigma}_c} = \frac{\tan \bar{\alpha}}{1 + (2A_f - 1) \tan \bar{\alpha}} \quad \text{Eq. II-4a}$$

$$\frac{s_u}{\bar{\sigma}_c} = \frac{\sin \bar{\phi}}{1 + (2A_f - 1) \sin \bar{\phi}} \quad \text{Eq. II-4b}$$

For anisotropic consolidation, the appropriate equations are:

$$\frac{s_u}{\bar{\sigma}_{1c}} = \frac{[K_c + (1 - K_c) A_f] \tan \bar{\alpha}}{1 + (2A_f - 1) \tan \bar{\alpha}} \quad \text{Eq. II-5a}$$

$$\frac{s_u}{\bar{\sigma}_{1c}} = \frac{[K_c + (1 - K_c) A_f] \sin \bar{\phi}}{1 + (2A_f - 1) \sin \bar{\phi}} \quad \text{Eq. II-5b}$$

For normally consolidated horizontal clay deposits

$K_c = K_o = 1 - \sin \bar{\phi}$, so that we have the following equation:*

$$\frac{s_u}{\bar{\sigma}_{1c}} = \frac{[1 - \sin \bar{\phi} + A_f \sin \bar{\phi}] \sin \bar{\phi}}{1 + (2A_f - 1) \sin \bar{\phi}}$$

The variations in $s_u / \bar{\sigma}_{1c}$ for isotropic and K_o consolidation as a function of friction angle and pore pressure parameter A_f are plotted in Fig. II-16.

3. Summary of Important Points for Triaxial Compression Tests on Normally Consolidated Simple Clay

- (a) All tests have a common effective stress envelope.
- (b) Drained strengths depend on the applied stress path during shear.
- (c) Undrained strengths do not depend on the applied (total) stress path during shear, although excess pore pressures do depend upon the total stress path.

* $s_u / \bar{\sigma}_{1c}$ is often denoted in the literature by "c/p" where $c = s_u$ and $p = \bar{\sigma}_{1c}$ = vertical effective overburden pressure.

(d) The undrained strength for a given value of $\bar{\sigma}_{1c}$ depends upon the value of $\bar{\sigma}_{3c}$, i.e. $s_u / \bar{\sigma}_{1c}$ varies with K_c .

(e) For a given water content at failure, there is only one shear strength and effective stress, but for a given water content at consolidation, there can be many values of shear stress and effective stress.

(f) From a single \overline{CIU} test and a knowledge of the consolidation curve, one can determine the effective stress and volume change behavior for any other type of shear test (e.g. \overline{CAU} , CID, CAD and UU) and any consolidation pressure under any total stress path. However, the axial strains can not be evaluated.

III. STRENGTH BEHAVIOR OF OVERCONSOLIDATED SIMPLE CLAY (Compression Tests Only)

A. CID Tests

1. Stress-Strain-Data

Two samples of Simple Clay are isotropically consolidated to 8 kg/cm^2 , one is rebounded back to $\bar{\sigma}_c = 0.667 \text{ kg/cm}^2$. The resulting values of OCR are 1 and 12. Stress-strain curves for CID tests with $\bar{\sigma}_3 = \bar{\sigma}_c$ on these samples are presented in Fig. III-1. The highly overconsolidated sample has a much lower strain at failure, an increased maximum obliquity, and a net positive volume change (note that the volume decreases and then increases).* At strains beyond failure the overconsolidated sample continues to imbibe water even though the stress difference is decreasing. In contrast, the normally consolidated sample will strain at constant stress difference and water content at strains beyond failure.

Normalized stress-strain data for loading and unloading CID tests for OCR values of 1 and 12 are presented in Fig. III-2. Note that unloading of highly overconsolidated samples produces a very low strain at failure and a constantly increasing water content throughout shear.

*This is typical of CID loading tests on highly overconsolidated clays and on dense sands.

As for normally consolidated samples, CID tests on over-consolidated samples are assumed to yield a hyperbolic stress-strain relationship. The relationships for OCR values of 1 and 12 are plotted in Fig. III-3. The plots of $\epsilon(\bar{\sigma}_c)/(\sigma_1 - \sigma_3)$ vs. ϵ for the overconsolidated samples fall below but roughly parallel to the plots for comparable CID tests on normally consolidated samples.

2. Effective Stress Paths and Failure Envelope

Effective stress paths are presented in Fig. III-4 for loading and unloading CID tests on several samples of Simple Clay with $\bar{\sigma}_{cm} = 8 \text{ kg/cm}^2$. All tests which end up with an effective stress \bar{p}_f of less than 5.75 kg/cm^2 lie on a common envelope defined by the equation.*

$$q_f = \bar{a} + \bar{p}_f \tan \bar{\alpha} = 0.05 + \bar{p}_f \tan 20.95^\circ.$$

Hence the envelope for overconsolidated samples shows a "cohesion intercept" but a lower slope (by about 0.5 deg) relative to that for normally consolidated samples. The magnitude of the cohesion intercept will be proportional to the maximum past pressure, i.e. for $\bar{\sigma}_{cm} = 4 \text{ kg/cm}^2$, $\bar{a} = 0.025 \text{ kg/cm}^2$.

The common effective stress envelope in Fig. III-4 represents the unique relationship between strength and effective stress at failure referred to in Principle I for overconsolidated samples having the same maximum past pressure ($\bar{\sigma}_{cm} = 8 \text{ kg/cm}^2$ in this case).

*Although a straight line relationship has been assumed, envelopes on overconsolidated samples usually show a concave downward curve for values of \bar{p}_f considerably below $\bar{\sigma}_{cm}$ (say $\bar{p}_f \leq .05 \bar{\sigma}_{cm}$).

3. Water Content versus Log Stress

The results of loading and unloading CID tests with $\bar{\sigma}_{cm} = 8 \text{ kg/cm}^2$ and OCR values of 2, 4, 8, 12 and 24 are plotted in Fig. III-5 in the form of water content versus $\log \bar{\sigma}_c$, $\log \bar{p}_f$ and $\log q_f$. The lines for normally consolidated specimens are shown for comparison. The figure also presents the variation in \bar{p} and w during drained shear with $\bar{\sigma}_3 = \bar{\sigma}_c$ and $\bar{\sigma}_1 = \bar{\sigma}_c$ for samples with an OCR = 12. Note that the directions of these paths are considerable different from those on normally consolidated samples (see Fig. II-7).

B. CIU Tests

1. Stress-Strain Data

Stress-strain curves are presented in Fig. III-6 for CIU tests on samples with maximum past pressures of 8 kg/cm^2 and consolidation pressures of 8 and 0.667 kg/cm^2 (OCR = 1 and 12 respectively). The effects of OCR on the stress-strain behavior in dimensionless terms are shown in Fig. III-7. An OCR = 2 corresponds to slightly overconsolidated samples and OCR = 12 corresponds to highly overconsolidated samples. These data show that as the samples become more overconsolidated:

- (a) The strain at failure increases
- (b) The undrained strength for a given maximum past pressure decreases but the ratio $s_u / \bar{\sigma}_c$ undergoes a

marked increase. Likewise the value of $(\sigma_1 - \sigma_3) / \bar{\sigma}_c$ at a given strain is greatly increased.

(c) The excess pore pressures are greatly decreased and become negative after some straining for highly overconsolidated samples.

(d) Instead of increasing with strain, the A parameter decreases with strain for OCR values exceeding about two to four.

(e) The obliquity at a given strain increases, particularly at low strains.

The effects of OCR on the hyperbolic stress-strain relationships for \overline{CIU} tests are plotted in Fig. III-8. As the overconsolidation ratio increases, the slope of the $\epsilon(\bar{\sigma}_c) / (\sigma_1 - \sigma_3)$ vs. ϵ line decreases, indicating increased rigidity of the samples (i. e. $(\sigma_1 - \sigma_3) / \bar{\sigma}_c$ at a given strain increases).

2. Effective Stress Paths and Failure Envelope

Effective stress paths for three samples with a maximum past pressure of 8 kg/cm^2 are shown in Fig. III-9. The characteristic shapes change radically with increasing overconsolidation. For $\text{OCR} = 1$, the average effective stress \bar{p} remains approximately constant and then shows a large decrease as the shear stress increases. The value of \bar{p} undergoes a moderate increase and then a slight decrease for the slightly overconsolidated sample whereas the highly overconsolidated sample ($\text{OCR} = 12$) yields a constantly increasing value of \bar{p} .

According to Principle I, the \overline{CIU} tests on overconsolidated samples end up on the same effective stress envelope at failure as that obtained with the CID tests. Although the data on the Simple Clay were constructed to show this to be true, and although this is also a good approximation for many actual overconsolidated clays, some comments are called for. In comparing envelopes from \overline{CU} and CD tests several problems arise. One is which failure criteria to employ for the \overline{CU} tests, maximum stress difference (used for this report) or maximum principal stress ratio (which will yield the higher envelope)? Another is the effect of rate of volume change on shear stresses (so-called dilatancy or energy correction) in the CD tests. Still another is the different rates of strain commonly used for undrained and drained tests. And finally with some clays, loading and unloading CID tests yield different envelopes. In conclusion, one generally finds the best agreement between uncorrected CD tests and \overline{CU} tests at maximum obliquity for both normally consolidated and overconsolidated samples. (See Bjerrum and Simons, 1960, for a general discussion on comparisons between \overline{CU} and CD envelopes and Rowe, 1963, for a discussion of the correct* expression for the dilatancy correction.)

*For CID, $\overline{\sigma}_3 = \overline{\sigma}_c$, tests, the component of $(\sigma_1 - \sigma_3)$ caused by the volume change is equal to $\overline{\sigma}_1 (dv/d\epsilon)/(1 + dv/d\epsilon)$ where v = volumetric strain and ϵ = axial strain.

3. Water Content versus Log Stress

The relationship among water content, $\log \bar{\sigma}_c$, $\log \bar{p}_f$ and $\log q_f$ for the \overline{CIU} tests with a maximum past pressure of 8 kg/cm^2 is the same as that for the CID tests, which was presented in Fig. III-5.

C. Unique Relationship Among Water Content, Shear Stress and Effective Stress

1. Relationship Between \overline{CIU} and CID Tests

Principle II states that the effective stress paths from \overline{CIU} tests on overconsolidated samples represent an unique $w - q - \bar{p}$ relationship for samples with the same maximum past pressure.* This relationship was plotted in Fig. III-9. Thus a CID test with a stress path which crossed one of the effective stress paths from a \overline{CIU} test should have a water content at that point equal to that of the \overline{CIU} test.

2. Effect of K_o Consolidation

We have seen (Section IIC2) that normally consolidated Simple Clay consolidated one-dimensionally with no lateral deformation yielded a value of $K_o = (\bar{\sigma}_{rc} / \bar{\sigma}_{ac})$ equal to $1 - \sin \bar{\phi}$ or 0.608. The relation between axial and radial pressure for one-dimensional compression of a sample of

*There are insufficient data on a variety of soils to ascertain the general validity of Principle II as applied to overconsolidated samples. Data on the Weald clay by Henkel and Sowa (1963) show that there is qualitative rather than quantitative agreement. However, this principle is still used in practice. For example, Lowe and Karafiath (1960) apply it to determine the undrained strength of anisotropically consolidated compacted clay from the results of \overline{CIU} tests.

Simple Clay normally consolidated up to an axial pressure of 8 kg/cm^2 is plotted in Fig. III-10. Plots of axial versus radial pressure will be called Rendulic plots.* It is seen that along the line which extends from the origin to Point A, $\bar{\sigma}_r = 0.608 \bar{\sigma}_a$ since this represents K_0 stresses for normally consolidated samples. Isotropically consolidated samples will fall on the $K = 1$ line since $\bar{\sigma}_a = \bar{\sigma}_r$.

When a sample is rebounded one-dimensionally, i.e. the radial dimension is still kept constant, the relation between axial and radial pressure and hence K_0 changes. Fig. III-10 shows the change in K_0 as a sample of Simple Clay** is rebounded from a maximum past pressure of 8 kg/cm^2 . It is seen that K_0 increases with overconsolidation ratio and for OCR values exceeding four ($\bar{\sigma}_{ac} < 2$), the radial pressure is actually greater than the axial pressure, i.e. $K_0 > 1$. When the radial pressure is greater than the axial pressure, $\bar{\sigma}_1 = \bar{\sigma}_2 = \bar{\sigma}_r$ and $\bar{\sigma}_3 = \bar{\sigma}_a$. Thus the direction of the principal planes has changed. This fact can not be conveniently shown on a $q - \bar{p}$ plot, which explains why the Rendulic plot was introduced.

*This type of plot is actually a modification of the plot originally used by Rendulic (1937) and later by Henkel (1960 a and b) in that they used $\sqrt{2} \bar{\sigma}_r$ for the abscissa. For the investigation of strength theories, the $\sqrt{2} \bar{\sigma}_r$ abscissa is more proper. However, when one is simply presenting data, it is far more convenient to leave out the $\sqrt{2}$.

** The K_0 rebound curve shown closely approximates that reported by Henkel and Sowa (1963) for the Weald clay.

The stress paths for the three $\overline{\text{CIU}}$ tests on overconsolidated Simple Clay presented in Fig. III-9 are replotted in terms of $\overline{\sigma}_a$ and $\overline{\sigma}_r$ in Fig. III-10 (in all cases $\overline{\sigma}_a = \overline{\sigma}_1$ and $\overline{\sigma}_r = \overline{\sigma}_2 = \overline{\sigma}_3$; the use of the Rendulic plot will be expanded upon when treating extension tests in Section V). These stress paths are lines of constant water content and hence represent the unique $w - \overline{\sigma}_a - \overline{\sigma}_r$ relationship just as the $q - \overline{p}$ stress paths represented the unique $w - q - \overline{p}$ relationship.

Let us look at Points B and C wherein the K_o rebound curve intersects a $\overline{\text{CIU}}$ stress path ($\overline{\sigma}_c = 4 \text{ kg/cm}^2$, $\text{OCR} = 2$, $w = 19.11\%$) and the isotropic rebound curve ($\overline{\sigma}_c = 2 \text{ kg/cm}^2$, $w = 19.97\%$), respectively. At Point B, the $\overline{\text{CIU}}$ test and the K_o rebound curve have the same stresses ($\overline{\sigma}_r = 3.68 \text{ kg/cm}^2$ and $\overline{\sigma}_a = 5.28 \text{ kg/cm}^2$) and according to Principle II should have the same water content of 19.11%. At Point C, the corresponding water content would be 19.97%. Fig. II-14 has already shown that the water content at Point A is equal to 19.00%. Using these three data points as a guideline, a comparison between water contents for isotropic and K_o consolidation and rebound was derived. The resulting water content vs. log consolidation pressure curves are plotted in Fig. III-11. Since K_o varies during rebound, the K_o rebound curve is not parallel to the isotropic rebound curve. Referring

to Fig. III-11, the K_o curve lies above the isotropic curve for $\bar{\sigma}_c \geq 2 \text{ kg/cm}^2$ since $K_o \leq 1$; conversely, the K_o curve lies below the isotropic curve for $\bar{\sigma}_c \leq 2 \text{ kg/cm}^2$ since $K_o \geq 1$ for this range. Remember that the stress $\bar{\sigma}_{ac}$ is plotted for the K_o curve and that the radial pressure $\bar{\sigma}_{rc} = \bar{\sigma}_{1c}$ is larger than $\bar{\sigma}_{ac}$ when $K_o \geq 1$. If $\bar{\sigma}_{1c}$ is plotted rather than $\bar{\sigma}_{ac}$, the K_o rebound curve would always fall to the right of the isotropic rebound curve.

D. Summary of Effect of Overconsolidation on Strength Behavior for Isotropic Consolidation and Rebound

1. Strength Data versus Consolidation Pressure and Water Content versus Log Stress

Effective stress paths, strength versus consolidation pressure, and A_f or water content change versus consolidation pressure are presented in Fig. III-12 and 13 for \overline{CIU} and CID tests respectively. The relationship among water content, log consolidation pressure, and log stresses at failure for both \overline{CIU} and CID tests is shown in Fig. III-14.

Important trends to note include:

- (1) Undrained strengths s_u are greatly affected by overconsolidation, whereas drained strengths s_d are primarily affected by the applied loading path.
- (2) Pore pressures in undrained tests and volume changes in drained tests are both very much affected by overconsolidation.

- (3) The effective stress envelope is little affected by overconsolidation.
- (4) The relationship among water content, consolidation pressure, strength and effective stress at failure is greatly affected by overconsolidation.

2. Stress-Strain Characteristics

The stress difference-axial strain curves for undrained and drained tests are greatly affected by overconsolidation as shown by the changes in the hyperbolic stress-strain relationship plots in Fig. III-15.

The effects of overconsolidation ratio on pore pressures in \overline{CIU} tests and volume changes in CID tests as a function of the applied shear stress are shown in Fig. III-16. The pore pressures developed during undrained shear are particularly interesting. If the Simple Clay were a linear-elastic isotropic material with $B = 1$, $\Delta u / \bar{\sigma}_c$ would equal exactly $(1/3) (\sigma_1 - \sigma_3) / \bar{\sigma}_c$ for a test wherein $\Delta \sigma_3 = 0$, which corresponds to $A = 1/3$. One notes that although A starts out with a value near one third, it deviates appreciably from this value at higher shear stresses. Normally consolidated samples develop much higher pore pressures and very overconsolidated samples develop much lower pore pressures. It is also obvious that the value of A depends to a large degree on the magnitude of applied shear stress*.

*Juarez-Badillo (1968) has developed a quasi-theoretical curve fitting method for calculating pore pressure as a function of stress level, overconsolidation ratio, and value of σ_2 .

3. Log OCR versus Strength Parameters

The variation in strength behavior as defined by several parameters as a function of log OCR is presented in Fig. III-17 and 18.

Fig. III-17a shows the reduction in undrained strength with rebound from the maximum past pressure. For OCR = 2 and 12, the reduction amounts to 19.7 and 66.6% respectively.

Fig. III-17b shows the change in $s_u / \bar{\sigma}_c$ and $s_d / \bar{\sigma}_c$ with OCR. The latter ratio is little affected.

Fig. III-17c shows that the relationship between undrained and drained strength depends on the applied stress path as much as on the OCR.

Fig. III-18a shows that the strain at failure increases with increasing OCR for undrained tests; the reverse is true for drained tests.

Fig. III-18b shows that the principal stress ratio (obliquity) at failure increases moderately with increasing OCR.

Fig. III-18c shows the variation in A_f for CIU tests and Δw_f for CID tests.

IV. HVORSLEV PARAMETERS

A. Historical Development (see Hvorslev, 1960, for a more detailed treatment)

The strength of normally consolidated and overconsolidated samples has thus far been treated separately. For example, there were different strength envelopes and different relationships between water content at failure and strength. There is however a theory, developed by Dr. Juul Hvorslev, relating the strength of normally consolidated and overconsolidated samples. During 1933-1936 Hvorslev was engaged in research for his doctor's thesis at the Technical University of Vienna, Austria, under the general direction of Professor K. Terzaghi. The test program included consolidated-drained direct shear tests on normally consolidated and overconsolidated samples of two saturated remolded clays.

Terzaghi suggested that the data be plotted in the form presented in Fig. IV-1a. Let us look at the plots of water content at failure w_f versus effective normal stress at failure $\bar{\sigma}_{ff}$ and shear strength τ_{ff} versus $\bar{\sigma}_{ff}$ (analogous to w_f vs. \bar{p}_f and q_f vs. \bar{p}_f respectively). Select two points with the same value of $w_f = w_f(A)$ shown by Points A' and A'' and project these points onto the $\tau_{ff} - \bar{\sigma}_{ff}$ plot. Point A' falls on the strength envelope for normally consolidated samples having a maximum past pressure of $\bar{\sigma}_{cm}$. The straight line through these two points has an intercept $\bar{c}_e(A)$ equal to A'''

and a slope of $\bar{\phi}_e$. The equation for the line is therefore:

$$\tau_{ff} = \bar{c}_e + \bar{\sigma}_{ff} \tan \bar{\phi}_e \quad \text{Eq. IV-1}$$

where \bar{c}_e = Hvorslev cohesion

$\bar{\phi}_e$ = Hvorslev friction angle.

Moreover, the line through A', A'' and A''' gives the relationship between strength and effective stress for all samples having the same water content at failure equal to $w_f(A)$.

Now select two samples having $w_f = w_f(B)$ with corresponding Points B', B'' and B'''. The envelope through these points will have a different Hvorslev cohesion $\bar{c}_e(B) = B'''$ but the same slope $\bar{\phi}_e$. In other words, the Hvorslev cohesion is a function of water content at failure whereas the Hvorslev friction angle is independent of water content. The variation in \bar{c}_e with w_f is plotted on the top portion of Fig. IV-1a. The consolidation curve for normally consolidated samples is also shown. If \bar{c}_e at a given water content is plotted against the $\bar{\sigma}_c$ required to achieve the same water content at consolidation for normally consolidated samples, called Hvorslev's equivalent consolidation pressure $\bar{\sigma}_e$, a straight line with a slope of \mathbf{K} results, as shown in Fig. IV-1b. Thus a general expression for strength as a function of water content and effective stress at failure can be written as follows:

$$\tau_{ff} = \mathbf{K} \bar{\sigma}_e + \bar{\sigma}_{ff} \tan \bar{\phi}_e \quad \text{Eq. IV-2}$$

where $\mathbf{K} = \bar{c}_e / \bar{\sigma}_e$

$\bar{\sigma}_e$ = Hvorslev's equivalent consolidation pressure =
 $\bar{\sigma}_c$ acting on a normally consolidated sample
having the same water content.

Now divide Eq. IV-2 by $\bar{\sigma}_e$:

$$\frac{\tau_{ff}}{\bar{\sigma}_e} = \mathbf{K} + \frac{\bar{\sigma}_{ff}}{\bar{\sigma}_e} \tan \bar{\phi}_e \quad \text{Eq. IV-3}$$

A plot of this equation is shown in Fig. IV-1c. This type of plot was used by Hvorslev in his research to determine the parameters \mathbf{K} and $\bar{\phi}_e$. The results of each test were plotted and the best straight line fitted through the data points. In other words, the values of τ_{ff} , $\bar{\sigma}_{ff}$, and w_f were measured in a particular test. The value of $\bar{\sigma}_e$ was then obtained from the magnitude of $\bar{\sigma}_c$ required to get the same water content for a normally consolidated sample [for example, $\bar{\sigma}_e = A$ at $w_f(A)$]. The ratios of $\tau_{ff} / \bar{\sigma}_e$ and $\bar{\sigma}_{ff} / \bar{\sigma}_e$ were then computed and plotted.

B. Significance

The equation $\tau_{ff} = \bar{c}_e + \bar{\sigma}_{ff} \tan \bar{\phi}_e$ for the Hvorslev envelope through tests having the same water content at failure has two components. One component of strength, the Hvorslev cohesion \bar{c}_e , depends only on water content; the other component of strength, $\bar{\sigma}_{ff} \tan \bar{\phi}_e$, is proportional to the effective stress. Some researchers

believe that these two components also represent the true manner by which strength is generated. That is, \bar{c}_e represents a "true cohesion" due to cohesive bonds between soil particles and $\bar{\phi}_e$ presents a "true friction" due to frictional resistance between soil particles. There is, however, much controversy concerning the physical significance of the Hvorslev parameters. At the present state of knowledge it is perhaps best to look upon these parameters as a convenient method of unifying test results on normally consolidated and overconsolidated samples without attaching too much significance to any physical interpretation. In other words, these parameters simply divide strength into water content dependent and effective stress dependent components. The Hvorslev parameters have also been used to correct the results of $\bar{C}\bar{U}$ tests for excessive volume changes due to sample disturbance (see Ladd and Lambe, 1963).

If the Hvorslev parameters did represent the physical manner by which strength was generated and if the Mohr-Coulomb strength criteria were correct (see Section IIA2 and Fig. II-2), the actual failure plane would form an angle $\theta = 45 + \bar{\phi}_e/2$ to the plane of the major principal stress.*

C. Hvorslev Parameters for Simple Clay

While Hvorslev's Eq. IV-2 is in a convenient form for direct shear tests, since τ_{ff} and $\bar{\sigma}_{ff}$ presumedly correspond to the measured

*Although Gibson (1953) found a good correlation between the angles of observed failure planes and $\theta = 45 + \bar{\phi}_e/2$, recent work by Rowe (1962, 1963) has shown that the angle of the failure plane bears no relationship to the physical manner of strength generation for granular soils.

values of shear stress and normal effective stress respectively, it is difficult to use when evaluating the results of triaxial tests. Bishop and Henkel (1962) transformed Eq. IV-2 so that the stress difference is expressed in terms of the minor principal stress:

$$\frac{(\sigma_1 - \sigma_3)_f}{2} = q_f = H \bar{\sigma}_e + \bar{\sigma}_{3f} \tan \bar{\theta}_e \quad \text{Eq. IV-4}$$

Hence:

$$\frac{q_f}{\bar{\sigma}_e} = H + \frac{\bar{\sigma}_{3f}}{\bar{\sigma}_e} \tan \bar{\theta}_e \quad \text{Eq. IV-5}$$

The relationship between the parameters H and $\bar{\theta}_e$ and the original Hvorslev parameters K and $\bar{\phi}_e$ is shown in Fig. IV-2. This figure also shows the type of plot used to obtain the parameters from triaxial tests. Data points from triaxial compression tests on the Simple Clay have been plotted for $\bar{C}IU$, CID ($\bar{\sigma}_3 = \bar{\sigma}_c$) and CID ($\bar{\sigma}_1 = \bar{\sigma}_c$) tests at overconsolidation ratios of 1, 2, 4, 8, 12 and 24. The following table illustrates how two of these points were obtained from ~~CID~~^{CUC} tests (stresses in kg/cm²).

OCR	$\bar{\sigma}_c$	q_f	\bar{p}_f	$\bar{\sigma}_{3f}$	w_f	$\bar{\sigma}_e$	$q_f / \bar{\sigma}_e$	$\bar{\sigma}_{3f} / \bar{\sigma}_e$
1	8.00	2.320	5.935	3.615	18.50	8.00	0.290	0.452
24	0.333	0.486	1.139	0.653	22.58	2.35	0.207	0.278

It turns out that all tests (drained and undrained) on normally consolidated samples have essentially the same coordinates ($q_f/\bar{\sigma}_e = 0.290$ and $\bar{\sigma}_{3f}/\bar{\sigma}_e = 0.451 \pm .001$) and that the coordinate points move progressively toward the origin as the OCR increases.

The Hvorslev parameters and equations for the Simple Clay are:

Triaxial Tests

$$H = 0.075 \text{ and } \bar{\theta}_e = 25.43^\circ$$

$$q_f = 0.075 \bar{\sigma}_e + 0.4755 \bar{\sigma}_{3f}$$

On "Failure" Plane

$$K = 0.0536 \text{ and } \bar{\phi}_e = 18.85^\circ$$

$$\tau_{ff} = 0.0536 \bar{\sigma}_e + 0.341 \bar{\sigma}_{ff}$$

The following example illustrates the use of the Hvorslev parameters. A CID compression test with $\bar{\sigma}_3 = \bar{\sigma}_c$ on a sample of Simple Clay yielded $q_f = 0.350 \text{ kg/cm}^2$ and $w_f = 23.8\%$. What was the consolidation pressure? For $w_f = 23.8\%$, $\bar{\sigma}_e = 1.62 \text{ kg/cm}^2$ (Fig. III-14 or any other figure showing $w - \log \bar{\sigma}_c$ for normally consolidated samples.) Therefore:

$$0.350 = 0.075 (1.62) + 0.4755 (\bar{\sigma}_{3f})$$

and $\bar{\sigma}_{3f} = 0.480 \text{ kg/cm}^2$, which also equals the consolidation pressure.

V. TRIAXIAL EXTENSION TESTS

A. Types of Stress Systems

Figure V-1a shows a cube of soil acted upon by the three principal stresses σ_x , σ_y , σ_z . The x, y, and z planes are planes on which the shear stress is zero. The three types of stress systems of particular interest are presented in Fig. V-1b, c, and d.

These are:

- (1) Triaxial compression, in which $\sigma_1 > \sigma_2 = \sigma_3$
- (2) Triaxial extension, in which $\sigma_1 = \sigma_2 > \sigma_3$;
- (3) Plane strain, in which $\sigma_1 > \sigma_2 > \sigma_3$; plane strain is defined by the fact that linear and shear strains occur only in the $\sigma_1\sigma_3$ plane, that is the linear strain in the σ_2 direction and the shear strains in the $\sigma_1\sigma_2$ and σ_2 and σ_3 planes are zero. Preliminary tests at Imperial College (Henkel, 1960a) suggest that σ_2 has a value about equal to $1/2 (\sigma_1 + \sigma_3)$ for clays at failure.

The first two states of stress can be obtained with the triaxial apparatus by having the larger stress acting in the axial and radial directions respectively. The standard direct shear device approximates, although rather crudely, a state of plane strain.

Examples of the above stress systems as they could occur in the field are shown in Fig. V-2.

At this point one might ask about the practical significance of having different stress systems. In other words, what effect does σ_2 have on the stress-strain-strength behavior of soils. Although a detailed discussion of this topic is beyond the scope of this report

(see Hvorslev 1960, p. 242-256 for a good review of the topic and a list of references), a few comments are called for. The Mohr-Coulomb strength theory assumes that the effective stress envelope is independent of the value of σ_2 . Very limited data suggest that this assumption is quite valid for normally consolidated clays but with heavily overconsolidated clays the envelope increases somewhat as $\bar{\sigma}_2$ increases from $\bar{\sigma}_3$ to $\bar{\sigma}_1$, i.e. higher envelopes as one progresses from triaxial compression to plane strain to triaxial extension.* Consequently the actual value of $\bar{\sigma}_2$ may not be very important for analyses involving drained strengths (except for dense sands).

Such is not the case, however, with analyses involving undrained strengths. As discussed in the next section, the undrained strength of normally consolidated Simple Clay is lower in \overline{CIU} triaxial extension than in \overline{CIU} triaxial compression even though the friction angle $\bar{\phi}$ is unchanged. In other words, higher pore pressures and hence an increased value of A_f result when σ_2 equals σ_1 . A revised pore pressure equation has been suggested by Henkel (1960a) to account for this effect:

$$\Delta u = \frac{\Delta \sigma_1 + \Delta \sigma_2 + \Delta \sigma_3}{3} + a \sqrt{(\Delta \sigma_1 - \Delta \sigma_2)^2 + (\Delta \sigma_2 - \Delta \sigma_3)^2 + (\Delta \sigma_3 - \Delta \sigma_1)^2} \quad \text{Eq. V-1}$$

*Experimental data on sands by several researchers employing drained tests have shown conflicting results. In the author's opinion, which may be an oversimplification, the friction angle $\bar{\phi}$ increases as σ_2 increases, the effect being small for loose sands and quite large for very dense sands.

For $\overline{\text{CIU}}$ triaxial compression tests with $\Delta\sigma_2 = \Delta\sigma_3 = 0$ (i.e. the axial pressure is increased), the equation reduces to

$$A_c = \frac{\Delta u}{(\sigma_1 - \sigma_3)} = 1/3 + \sqrt{2} a_c \quad \text{Eq. V-2}$$

and for $\overline{\text{CIU}}$ triaxial extension tests with $\Delta\sigma_3 = 0$ (i.e. the radial pressure is increased), one obtains

$$A_e = \frac{\Delta u}{(\sigma_1 - \sigma_3)} = 2/3 + \sqrt{2} a_e \quad \text{Eq. V-3}$$

If the parameter "a" is independent of σ_2^* , the A parameter for extension tests would then be equal to that for compression tests plus 1/3 for the same value of $(\sigma_1 - \sigma_3)$.

Test data on typical normally consolidated clays show the value of $s_u / \bar{\sigma}_c$ for $\overline{\text{CIU}}$ extension tests to be 10 to 25% below that for $\overline{\text{CIU}}$ compression tests.

B. Triaxial Extension Tests on Simple Clay

1. $\overline{\text{CIU}}$ Tests on Normally Consolidated Samples

Stress-strain curves for $\overline{\text{CIU}}$ compression and extension tests on normally consolidated Simple Clay are compared in Fig. V-3. In the compression test the axial pressure is increased at a constant radial pressure and the axial strain is a compression (axial shortening); in the extension test the radial pressure is increased at a constant axial pressure and the axial strain is an extension (axial elongation.)

*For N.C. Weald clay, $\sqrt{2} a_e$ was $0.10 \pm .05$ higher than $\sqrt{2} a_c$ whereas for OCR values between 2 and 8, $\sqrt{2} a_e$ was $0.2 \pm .1$ lower than $\sqrt{2} a_c$ over a wide range of $(\sigma_1 - \sigma_3) / (\sigma_1 - \sigma_3)_f$ values.

At equal axial strains, extension tests show the following changes relative to compression tests:

(1) $(\sigma_1 - \sigma_3) / \bar{\sigma}_c$ is slightly larger at low strains but lower at larger strains*;

(2) The magnitudes of $\bar{\sigma}_1 / \bar{\sigma}_c$ and $\bar{\sigma}_3 / \bar{\sigma}_c$ are always decreased;

(3) $\Delta u / \bar{\sigma}_c$, $\bar{\sigma}_1 / \bar{\sigma}_3$ and A all show large increases.

The differences in stress-strain characteristics between extension and compression tests are more pronounced if both are compared in terms of strains in the direction of the major principal stress, ϵ_1 . In the extension tests, $\epsilon_1 = \epsilon_2$ acts in the radial direction and $\epsilon_3 = \epsilon$ (axial strain). Since the volume remains constant, ϵ_1 will therefore be equal to minus one half of the axial strain and the magnitudes of strain shown in Fig. V-3 for the extension tests would be cut in half.

At failure, the extension tests show a lower value of $s_u / \bar{\sigma}_c$ (0.246 vs. 0.290), an increased A_f (1.255 vs. 0.945) and the same friction angle $\bar{\phi}$, since $(\bar{\sigma}_1 / \bar{\sigma}_3)_f$ remains unchanged.

The relationship between stress difference and the pore pressure parameter A is plotted in Fig. V-4 for the extension and compression tests. The difference in the A

*The hyperbolic stress-strain parameters are: $m = 0.68$ and $n = 1.92$.

parameters, $A_e - A_c$, starts with a value of one third and increases with increasing stress difference (at failure, $A_e - A_c$ equals $1.255 - 0.945 = 0.310$ but the stress difference in the two tests is not equal).

The effective stress paths, in terms of q and \bar{p} divided by consolidation pressure $\bar{\sigma}_c$ are compared in Fig. V-5. The extension test lies to the left of the compression test since higher pore pressures are developed in the former test. These stress paths represent the relationship between water content, shear stress, and effective stress as stated in Principle II. Obviously this relationship is different for compression and extension tests and hence the two stress systems must be considered separately. Since compression and extension represent the limiting values of $\bar{\sigma}_2$, the $w - q - \bar{p}$ relationships for intermediate values of $\bar{\sigma}_2$ would presumably lie between the two stress paths shown in Fig. V-5.

The conventional $q - \bar{p}$ plot can not distinguish between triaxial compression and extension so that the Rendulic plot with axial and radial pressures is better suited for presenting the results of such tests. Normalized stress paths in terms of axial and radial pressures are presented in Fig. V-6. This type of plot, but with values of $\bar{\sigma}_a$ and $\bar{\sigma}_r$ from \overline{CIU} compression and extension tests at different consolidation pressures, could be used to present the $w - \bar{\sigma}_a - \bar{\sigma}_r$ relationships stated in Principle II.

The relationship between water content, shear strength q_f , effective stress at failure \bar{p}_f and consolidation pressure for \overline{CIU} compression and extension tests is plotted in Fig. V-7.

2. CID Tests on Normally Consolidated Samples

Section II, which treated compression tests on normally consolidated Simple Clay, showed that drained and undrained tests had the same effective stress envelope and the same $w - q - \bar{p}$ relationship. Hence the volume changes which occur during drained tests could be calculated from \overline{CIU} stress paths, as was shown in Fig. II-12. In a like manner, volume changes during CID extension tests can be computed from the stress paths obtained with \overline{CIU} extension tests.

Stress-strain curves for CID extension tests are different from those for compression tests just as the undrained test results were different. The hyperbolic stress-strain parameters and axial strain at failure for loading ($\bar{\sigma}_r$ increased, $\Delta\bar{\sigma}_a = 0$) and unloading ($\bar{\sigma}_a$ decreased, $\Delta\bar{\sigma}_r = 0$) CID extension tests are given below:

	<u>CID Extension Tests</u>		
	<u>m</u>	<u>n</u>	<u>ϵ_f (%)</u>
Loading	2.20	0.600	12.5
Unloading	1.50	1.580	7.5

Remember however that drained strengths in compression and extension are the same for identical stress paths in terms of $\bar{\sigma}_1$ and $\bar{\sigma}_3$. For example, $s_d/\bar{\sigma}_c$ equals 0.644 for loading tests ($\bar{\sigma}_1$ increased, $\bar{\sigma}_3 = \bar{\sigma}_c$) in both cases.

3. Tests on Overconsolidated Samples*

Although the effective stress envelopes for extension and compression tests on normally consolidated Simple Clay are identical, extension tests yield a higher envelope for overconsolidated samples. For a maximum past pressure of 8 kg/cm^2 , the corresponding envelopes are:

Compression Tests

$$q_f = 0.05 + 0.383 \bar{p}_f \quad (\bar{p}_f \leq 6 \text{ kg/cm}^2)$$

Extension Tests

$$q_f = 0.10 + 0.372 \bar{p}_f \quad (\bar{p}_f \leq 5 \text{ kg/cm}^2)$$

The results of $\overline{\text{CIU}}$ extension tests on overconsolidated samples show the same $(s_u \text{ at } \bar{\sigma}_c)/(s_u \text{ at } \bar{\sigma}_{cm})$ versus OCR relationship as obtained from the compression tests (see Fig. III-17a).

The above data can be used to establish the w_f vs. $\log q_f$, $\log \bar{p}_f$ and $\log \bar{\sigma}_c$ relationships for extension tests on overconsolidated samples. This information can then be used to compute water content changes at failure in drained tests. An alternate

*The behavior is patterned after tests on the remolded Weald clay.

approach for obtaining w_f for drained tests is to use the Hvorslev parameters, which can be computed from the \overline{CIU} extension test data. One obtains:

$$H = 0.110 \text{ and } \tan \bar{\theta}_e = 0.356$$

$$\text{or } \mathbf{K} = 0.085 \text{ and } \tan \bar{\phi}_e = 0.272$$

(Note that the Hvorslev cohesion increases and the Hvorslev friction decreases.) Hence $q_f = 0.11 \bar{\sigma}_e + 0.356 \bar{\sigma}_{3f}$; since q_f and $\bar{\sigma}_{3f}$ are known for any drained test (since the effective stress envelope is known), the value of $\bar{\sigma}_e$ and hence the water content at failure can be computed.

VI. SUMMARY

A. Background

On the basis of measured strength data on a number of clays, a set of principles, for the most part empirical, was developed with the purpose of describing the behavior of saturated clays during shear. Some of these principles accurately describe the strength behavior of many remolded and natural clays; other principles work well only with a limited number of clays, and finally there are clays, such as the quick clays, for which most of the principles find little application. In conclusion, although these principles are widely used as an aid in solving many practical problems, they generally represent an oversimplified picture of the true behavior. One can, however, study the actual strength behavior of clays in terms of deviations from this idealized framework rather than in terms of a host of isolated facts. Herein lies the major benefit which can be obtained from a thorough knowledge of the basic strength principles.

A hypothetical clay, called the "Simple Clay," is used to present the strength principles and to illustrate the stress-strain behavior of "typical" saturated clay. Many properties of the Simple Clay are patterned after measured data on the remolded Weald clay, some properties represent the average behavior of other clays, and still other properties were made up due to lack of data. The Simple Clay exhibits "normalized" behavior in that all tests of a like nature with the same overconsolidation ratio have identical stress-strain characteristics when the stresses are divided by consolidation pressure.

B. Variables Considered

The five major variables in addition to strain which were studied via triaxial shear tests are listed below:

1. Type of Triaxial Test
 - a) CD: Consolidated-Drained
 - b) CU: Consolidated-Undrained
 - c) UU: Unconsolidated-Undrained
2. Overconsolidation Ratio
 - a) Normally consolidated ($OCR = 1$)
 - (1) $\bar{\sigma}_c$ varied
 - b) Overconsolidated ($OCR > 1$)
 - (1) $\bar{\sigma}_c$ varied at constant $\bar{\sigma}_{cm}$
 - (2) $\bar{\sigma}_{cm}$ varied
3. Stress Path
 - a) Loading: σ_1 increased, $\Delta\sigma_3 = 0$
 - b) Unloading: σ_3 decreased, $\Delta\sigma_1 = 0$
 - c) Constant stress: $p = \text{constant}$, $\Delta\sigma_1 = -\Delta\sigma_3$
4. Stress Ratio at Consolidation
 - a) Isotropic: $K = 1$
 - b) Anisotropic: $K \neq 1$
 - (1) K_0 for $OCR \geq 1$
 - (2) Other values of K
5. Value of Intermediate Principal Stress σ_2
 - a) Triaxial compression: $\sigma_2 = \sigma_3$
 - b) Triaxial extension: $\sigma_2 = \sigma_1$

C. Strength Principles

1. Principle 1

a) Statement:

There is an unique relationship between strength and effective stress at failure; for example, $q_f = f(\bar{p}_f)$ as in Fig. III-12.

b) Relationship is dependent upon:

(1) Value of $\bar{\sigma}_{cm}$ if $OCR > 1$

(2) Value of σ_2 if $OCR > 1$

c) Relationship is independent of:

(1) Type of triaxial test

(2) Value of $\bar{\sigma}_c$ if $OCR = 1$

(3) Stress path (within certain broad limits for CD tests).

(4) Value of K at consolidation

(5) Value of σ_2 if $OCR = 1$

2. Principle II

a) Statement:

There is an unique relationship among water content, shear stress and effective stress; for example, effective stress paths from \overline{CIU} tests, which are lines of constant water content, represent the unique relationship among w , q and \bar{p} , as in Fig. II-12.

- b) Relationship is dependent upon:
 - (1) Value of $\bar{\sigma}_{cm}$ if $OCR > 1$
 - (2) Value of σ_2
- c) Relationship is independent of:
 - (1) Type of triaxial test
 - (2) Stress path (within certain broad limits for CD tests)
 - (3) Value of K at consolidation

3. Principle III

- a) Statement:

There is an unique relationship among water content at failure, shear strength, and effective stress at failure as expressed by the Hvorslev parameters; for example, $q_f = f(w_f) + f(\bar{\sigma}_{3f})$ as in Fig. IV-2.

- b) Relationship is dependent upon:
 - (1) Value of σ_2
- c) Relationship is independent of:
 - (1) Type of triaxial test
 - (2) OCR and $\bar{\sigma}_{cm}$
 - (3) Stress path (no limitations)
 - (4) Value of K at consolidation

APPENDIX A

Notation: RCSSCS = Research Conference on Shear Strength of Cohesive Soils

ICSMFE = International Conference of Soil Mechanics and Foundation Engineering

JSMFE = Journal Soil Mechanics and Foundation Engineering

ASTM-NRS Symp. = ASTM-NRC Symposium on Laboratory Shear Testing of Soils

1. Bishop, A. W. (1958) "Test Requirements for Measuring the Coefficient of Earth Pressure at Rest", Brussels Conf. on Earth Pressure Problems. Proceedings, Vol. 1, p. 2-14.
2. Bishop, A. W. and Henkel, D. J. (1962) The Measurement of Soil Properties in the Triaxial Test, Ed. Arnold, London, 2nd Edition, 228 pp.
3. Bjerrum, L. and Simons, N. E. (1960) "Comparison of Shear Strength Characteristics of Normally Consolidated Clays", ASCE RCSSCS, Boulder, Colo., p. 711-726.
4. Gibson, R. E. (1953) "Experimental Determination of the True Cohesion and True Angle of Internal Friction in Clays," 3rd ICSMFE, Vol. 1, p. 126-130.
5. Hansen, J. B. (1963) Discussion to Kondner (1963), ASCE, JSMFE, Vol. 89, No. SM 4, p. 241-242.
6. Henkel, D. J. (1960a) "The Shear Strength of Saturated Remolded Clays", ASCE, RCSSCS, Boulder, Colo., p. 533-554.
7. Henkel, D. J. (1960b) "The Relationship Between the Effective Stresses and Water Content in Saturated Clays", Geotechnique, Vol. X, p. 41.
8. Henkel, D. J. and Sowa, V. A. (1963) "The Influence of Stress History on the Stress Paths Followed in Undrained Triaxial Tests", ASTM-NRC Sym., Ottawa, Canada (Advance Copy).
9. Hvorslev, M. J. (1960) "Physical Components of the Shear Strength of Saturated Clays", ASCE RCSSCS, p. 169-273.

10. Juarez-Badillo, E. (1963) "Pore Pressure Functions in Saturated Soils", ASTM-NRC Sym., Ottawa, Canada (Advance Copy).
11. Kondner, R. L. (1963) "Hyperbolic Stress-Strain Response; Cohesive Soils", ASCE JSMFE, Vol. 89, No. SM 1, p. 115-144.
12. Ladd, C. C. and Lambe, T. W. (1963) "The Strength of 'Undisturbed' Clay Determined from Undrained Tests", ASTM-NRC Sym., Ottawa, Canada (Advance Copy).
13. Lowe, J. and Karafiath, L. (1960) "Effect of Anisotropic Consolidation on the Undrained Shear Strength of Compacted Clays", ASCE RCSSCS, Boulder, Colo., p. 837-858.
14. Parry, R. H. G. (1960) "Triaxial Compression and Extension Tests on Remolded Saturated Clays", Geotechnique, Vol. 10, p. 166-180.
15. Rendulic, L. (1937) "Ein Grundgesetz der Tonmechanik und sein experimenteller Beweis", Bauingenieur, Vol. 18, p. 459-467 (translated into English by J. Varallyay, Dept. of Civil Engineering, M.I.T.).
16. Roscoe, K. H. and Poorooshasb, H. B. (1963) "A Theoretical and Experimental Study of Strains in Triaxial Compression Tests on Normally Consolidated Clays", Geotechnique, Vol. XII, No. 1, p. 12-38.
17. Rowe, P. W. (1962) "The Stress-Dilatancy Relation for Static Equilibrium of an Assembly of Particles in Contact", Proceedings Royal Soc., London, Series A, Vol. 269, p. 500-527.
18. Rowe, P. W. (1963) "Stress-Dilatancy, Earth Pressures, and Slopes", ASCE, JSMFE, Vol. 89, No. SM 3, p. 37-62.
19. Rutledge, P. C. (1947) "Review of Cooperative Triaxial Research Program of the Corps of Engineers", Progress Report on Soil Mechanics Fact Finding Survey, Waterways Experiment Station, Vicksburg, Miss., p. 1-178.
20. Simons, N. E. (1958) "Laboratory Determination of the Coefficient of Earth Pressure at Rest", Brussels Conf. on Earth Pressure Problems, Contribution to the Discussion. (Also N.G.I. Publ. No. 33, 1958).

21. Skempton, A. W. (1954) "The Pore-Pressure Coefficients A and B", *Geotechnique*, Vol. 4, p. 143-147.
22. Taylor, D. W. (1948), Fundamentals of Soil Mechanics, John Wiley and Sons, New York, 700 pp.
23. Taylor, D. W. (1955) "Review of Research on Shearing Strength of Clay at M.I.T. 1948-1953," Report to Waterways Experiment Station, Vicksburg, Miss.

APPENDIX B

NOTATION

Note: Suffix f indicates a failure condition

Prefix Δ indicates a change

A bar over a stress indicates an effective stress

1. Stresses

u	pore (water) pressure
u_i	initial pore pressure
σ	total normal stress
$\bar{\sigma}$	effective normal stress
$\bar{\sigma}_i$	initial effective stress
σ_c	chamber pressure
$\bar{\sigma}_c$	consolidation pressure
$\bar{\sigma}_{cm}$	maximum past pressure
$\sigma_a, \bar{\sigma}_a$	total and effective axial pressures
$\sigma_r, \bar{\sigma}_r$	total and effective radial pressures
$\sigma_1, \bar{\sigma}_1$	total and effective major principal stress
$\sigma_2, \bar{\sigma}_2$	total and effective intermediate principal stress
$\sigma_3, \bar{\sigma}_3$	Total and effective minor principal stress
$\bar{\sigma}_{ac}, \bar{\sigma}_{rc}$	$\bar{\sigma}_a, \bar{\sigma}_r$ at consolidation
$\bar{\sigma}_{af}, \bar{\sigma}_{rf}$	$\bar{\sigma}_a, \bar{\sigma}_r$ at failure
$\bar{\sigma}_{1c}, \bar{\sigma}_{2c}, \bar{\sigma}_{3c}$	$\bar{\sigma}_1, \bar{\sigma}_2, \bar{\sigma}_3$ at consolidation
$\bar{\sigma}_{1f}, \bar{\sigma}_{2f}, \bar{\sigma}_{3f}$	$\bar{\sigma}_1, \bar{\sigma}_2, \bar{\sigma}_3$ at failure
$\bar{\sigma}_e$	Hvorslev's equivalent consolidation pressure
τ	shear stress
τ_{ff}	shear stress on failure plane at failure

$\bar{\sigma}_{ff}$		effective stress on failure plane at failure
q	=	$(\sigma_1 - \sigma_3)/2$
q_c		q at consolidation
q_f		q at failure
p	=	$(\sigma_1 + \sigma_3)/2$
\bar{p}		$(\bar{\sigma}_1 + \bar{\sigma}_3)/2$
\bar{p}_c		\bar{p} at consolidation
\bar{p}_f		\bar{p} at failure
s_u		value of q_f for undrained shear
s_d		value of q_f for drained shear

2. Stress Ratios

A		Skempton's A parameter = $(\Delta u - \Delta \sigma_3)/(\Delta \sigma_1 - \Delta \sigma_3)$
A_c		A for compression tests
A_e		A for extension tests
B		Skempton's B parameter = $\Delta u/\Delta \sigma_c$
K	=	$\bar{\sigma}_r/\bar{\sigma}_a$
K_c		K at consolidation
K_o		value of K_c for no lateral strain
K_f		K at failure
OCR		Overconsolidation Ratio = $\bar{\sigma}_{cm}/\bar{\sigma}_c$

3. Strength and Stress-Strain Parameters

\bar{c}		cohesion intercept of a τ_{ff} vs. $\bar{\sigma}_{ff}$ envelope
$\bar{\phi}$		friction angle of a τ_{ff} vs. $\bar{\sigma}_{ff}$ envelope

\bar{a}	intercept of a q_f vs. \bar{p}_f envelope
$\bar{\alpha}$	slope of a q_f vs. \bar{p}_f envelope
\bar{c}_e	Hvorslev cohesion using τ_{ff} and $\bar{\sigma}_{ff}$
$\bar{\phi}_e$	Hvorslev friction angle using τ_{ff} and $\bar{\sigma}_{ff}$
$\bar{\sigma}_e$	Hvorslev equivalent consolidation pressure
\mathbf{K}	$= \bar{c}_e / \bar{\sigma}_e$
$\bar{\theta}_e$	modified version of $\bar{\phi}_e$ using q_f and $\bar{\sigma}_{3f}$
H	modified version of \mathbf{K} using q_f and $\bar{\sigma}_{3f}$
m, n	hyperbolic stress-strain parameters
E	stress-strain modulus = $\Delta(\sigma_1 - \sigma_3) / \epsilon$

4. Miscellaneous

e	void ratio
G_s	specific gravity of soil solids
S	degree of saturation
w	water content
w_i	initial water content
w_f	water content at failure
Δw	change in water content
ϵ	axial strain
$\epsilon_1, \epsilon_2, \epsilon_3$	linear strains in the direction of the 3 principal stresses

5. Types of Shear Tests

CD	Consolidated-Drained
CU	Consolidated-Undrained
\overline{CU}	CU test with pore pressure measurements

UU Unconsolidated-Undrained

\overline{UU} UU test with pore pressure measurements

6. Types of Triaxial Tests

CID CD test with isotropic consolidation

CAD CD test with anisotropic consolidation

CIU, \overline{CIU} CU, \overline{CU} test with isotropic consolidation

CAU, \overline{CAU} CU, \overline{CU} test with anisotropic consolidation

Sample in Triaxial Cell

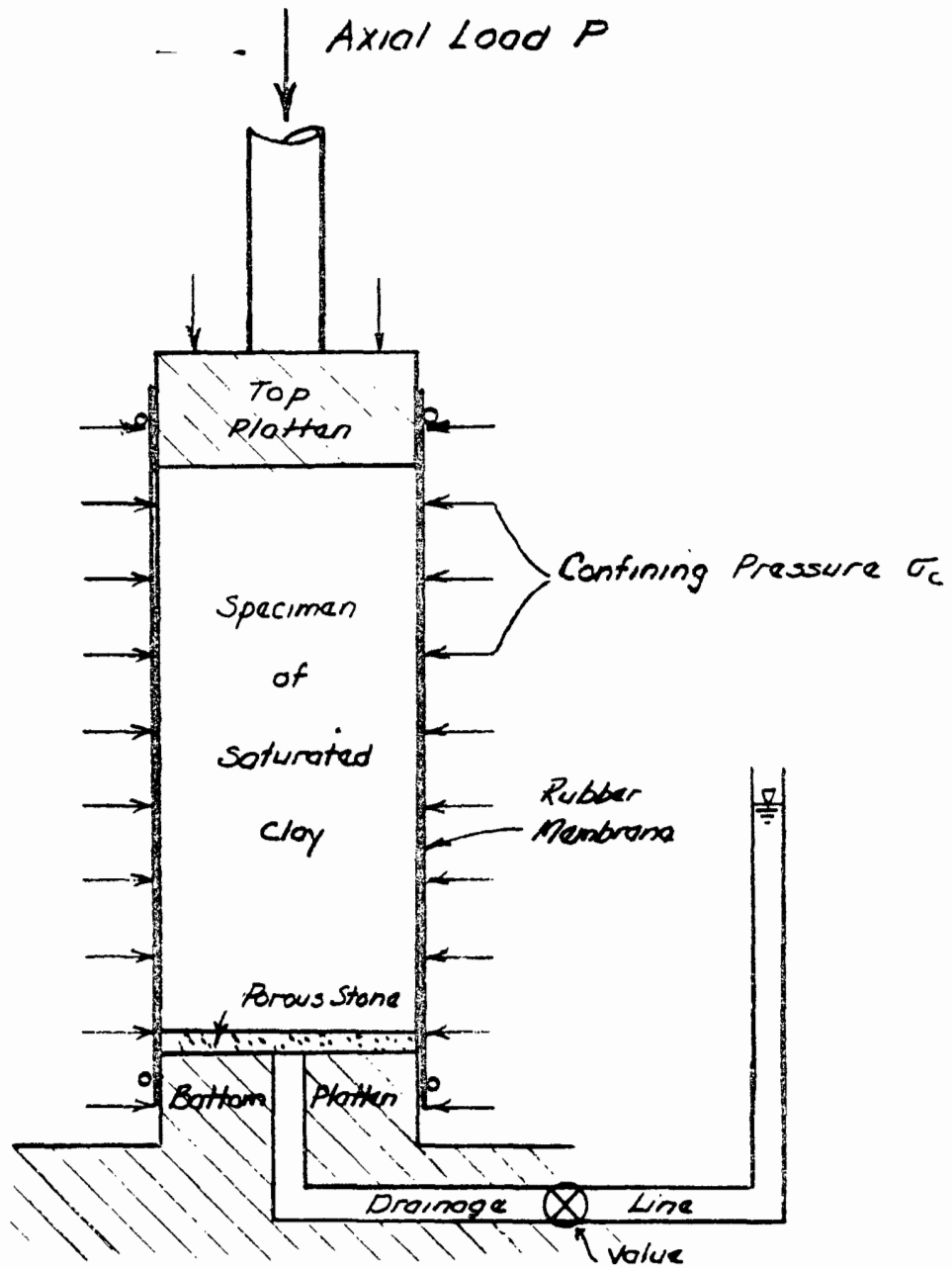


Figure I-1

CEL 8/28/63

ISOTROPIC CONSOLIDATION AND
 REBOUND CURVES FOR SIMPLE CLAY

$G_s = 2.74$

$w = 25.4 - 7.65 \log \bar{\sigma}_c$

Note: Rebound curves are parallel
 i.e., same Δw for some $\Delta \log \bar{\sigma}_c = \bar{\sigma}_{cm} / \bar{\sigma}_c$
 For example: $\Delta w = +2.40\%$ at $\Delta \log \bar{\sigma}_c = 0.30$

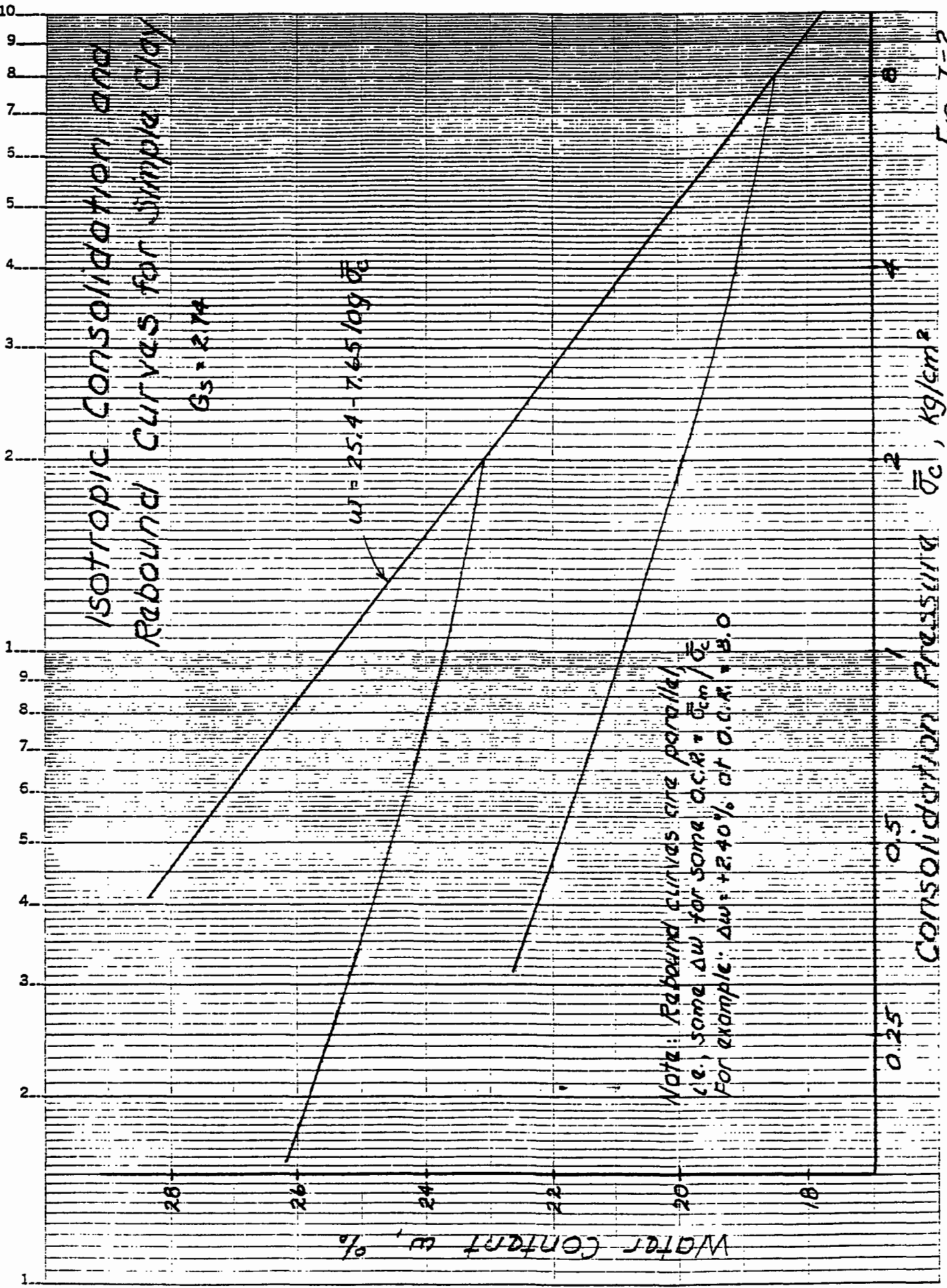


FIG. I-2

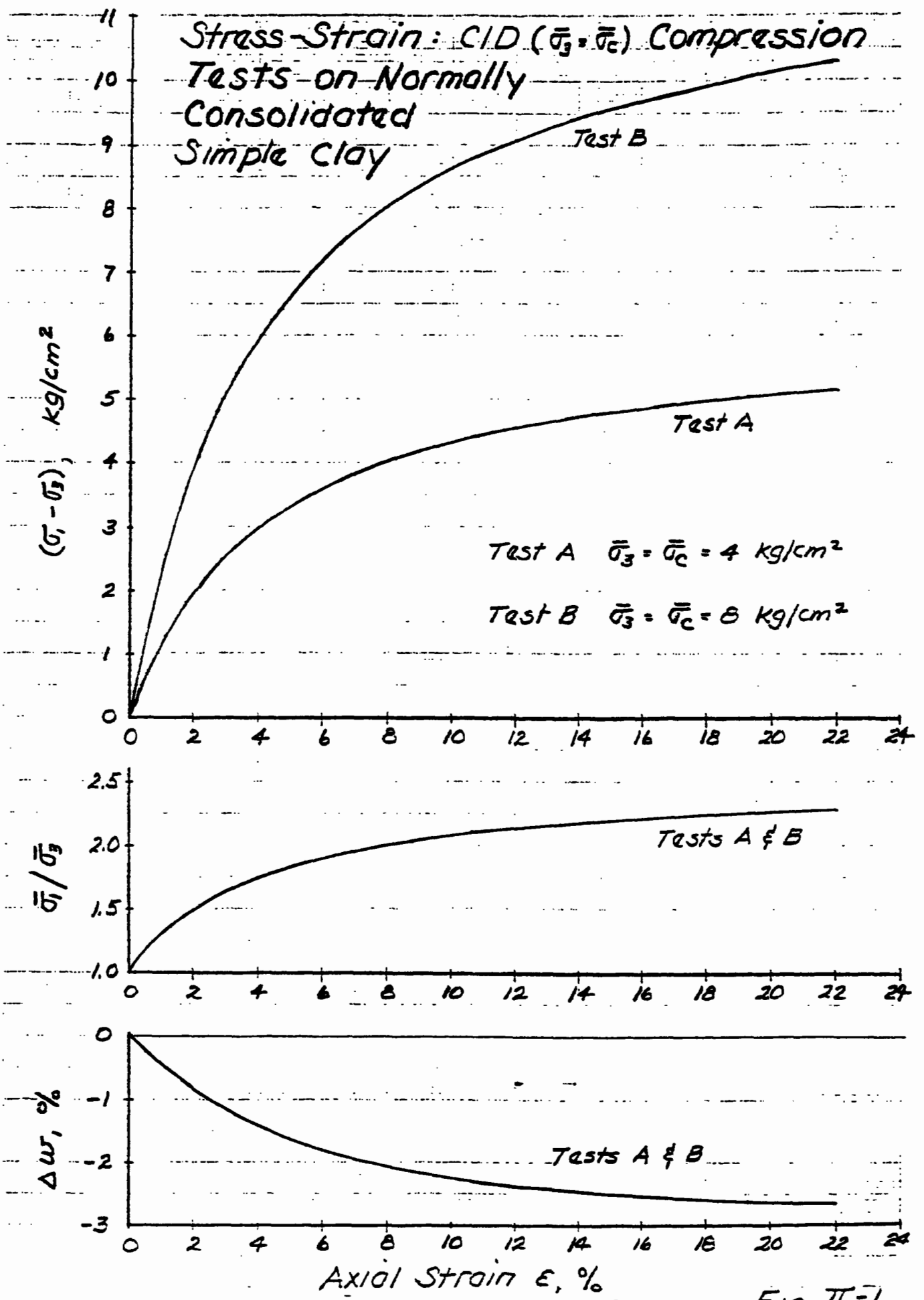


Fig. II-1

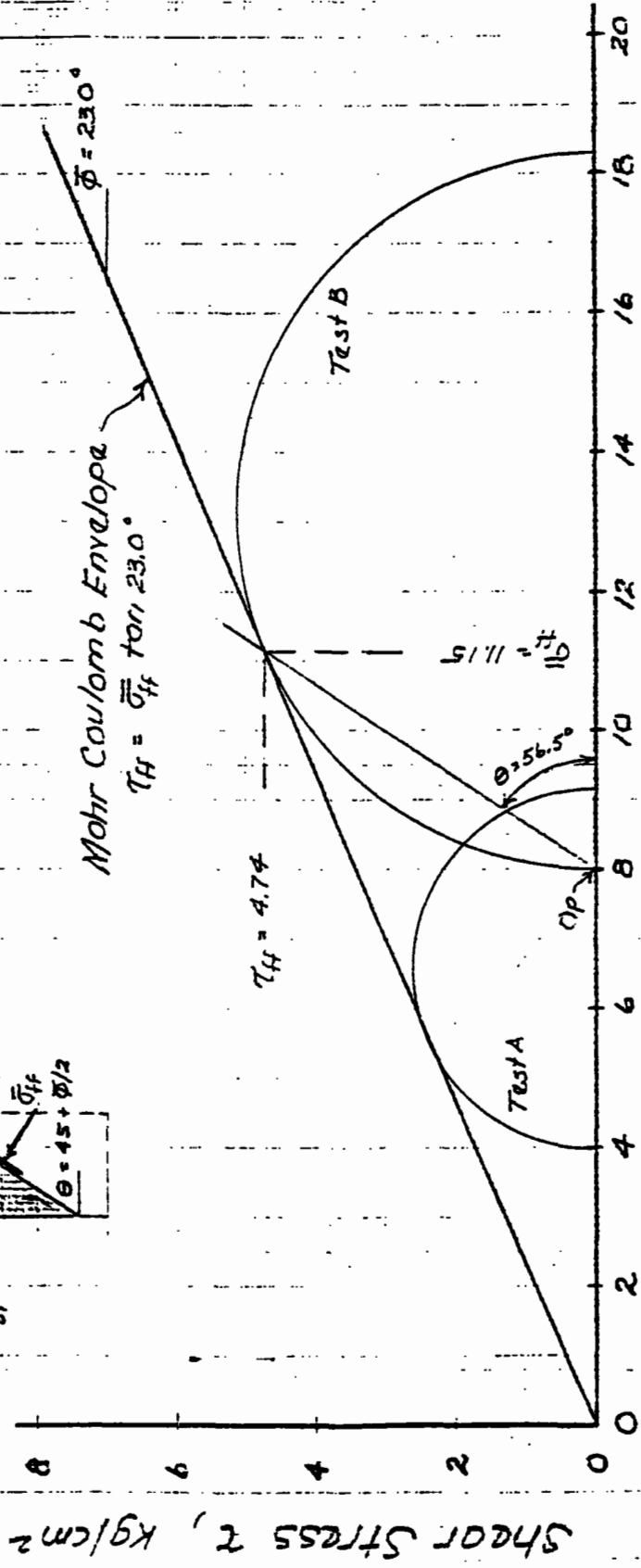
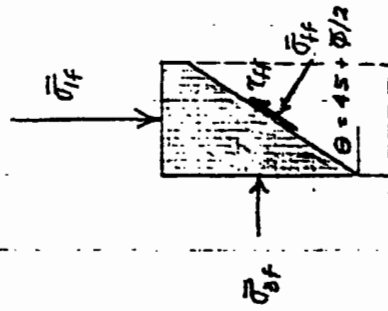
Mohr Circles at Failure for CID ($\bar{\sigma}_3 = \bar{\sigma}_c$) Compression Tests on Normally Consolidated Simple Clay

Relationship among stresses and angles

$$\bar{\sigma}_{3f} / \bar{\sigma}_{3f} = (1 + \sin \phi) / (1 - \sin \phi)$$

$$\tau_{ff} = \frac{1}{2} (\sigma_1 - \sigma_3)_f \cos \phi$$

$$\bar{\sigma}_{1f} = \bar{\sigma}_{3f} (1 + \sin \phi) = \bar{\sigma}_{1f} (1 - \sin \phi)$$



Normal Effective Stress $\bar{\sigma}$, kg/cm^2

FIG. II-2

Effective Stress Path and Strength Envelope for CID Test B

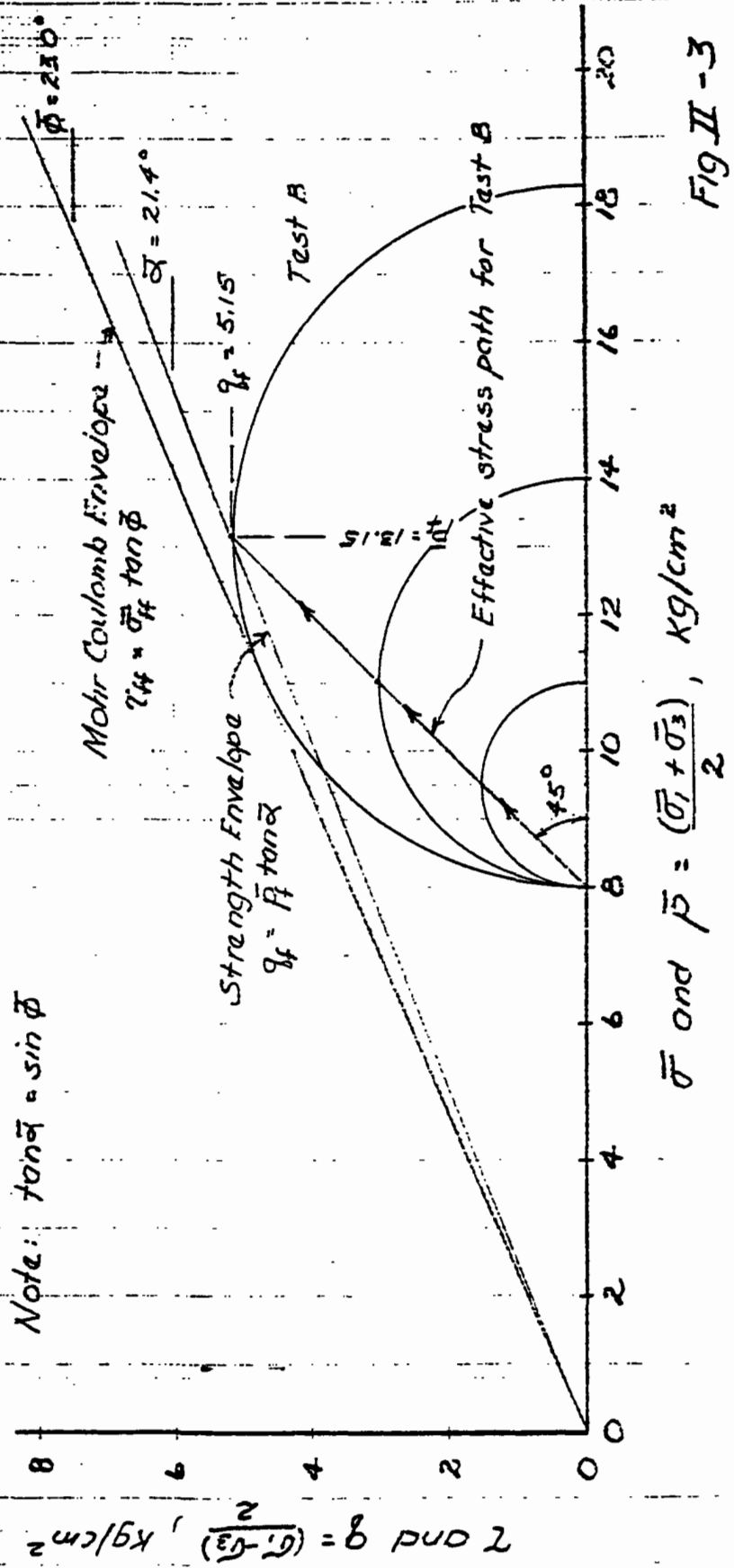


FIG II - 3

C.C.L. 9/25/63

Various Effective Stress Paths for CID Tests on Normally Consolidated Simple Clay

Test	Type of Test	\bar{p}	q_f kg/cm ²	$q_f/\bar{\sigma}_c$
B	$\bar{\sigma}_3 = \bar{\sigma}_c$	$\bar{p} = \bar{\sigma}_c + q$	5.15	0.644
C	$\bar{\sigma}_1 = \bar{\sigma}_c$	$\bar{p} = \bar{\sigma}_c - q$	2.25	0.281
D	$\Delta\bar{\sigma}_1 = -\Delta\bar{\sigma}_3$	$\bar{p} = \bar{\sigma}_c$	3.13	0.3915

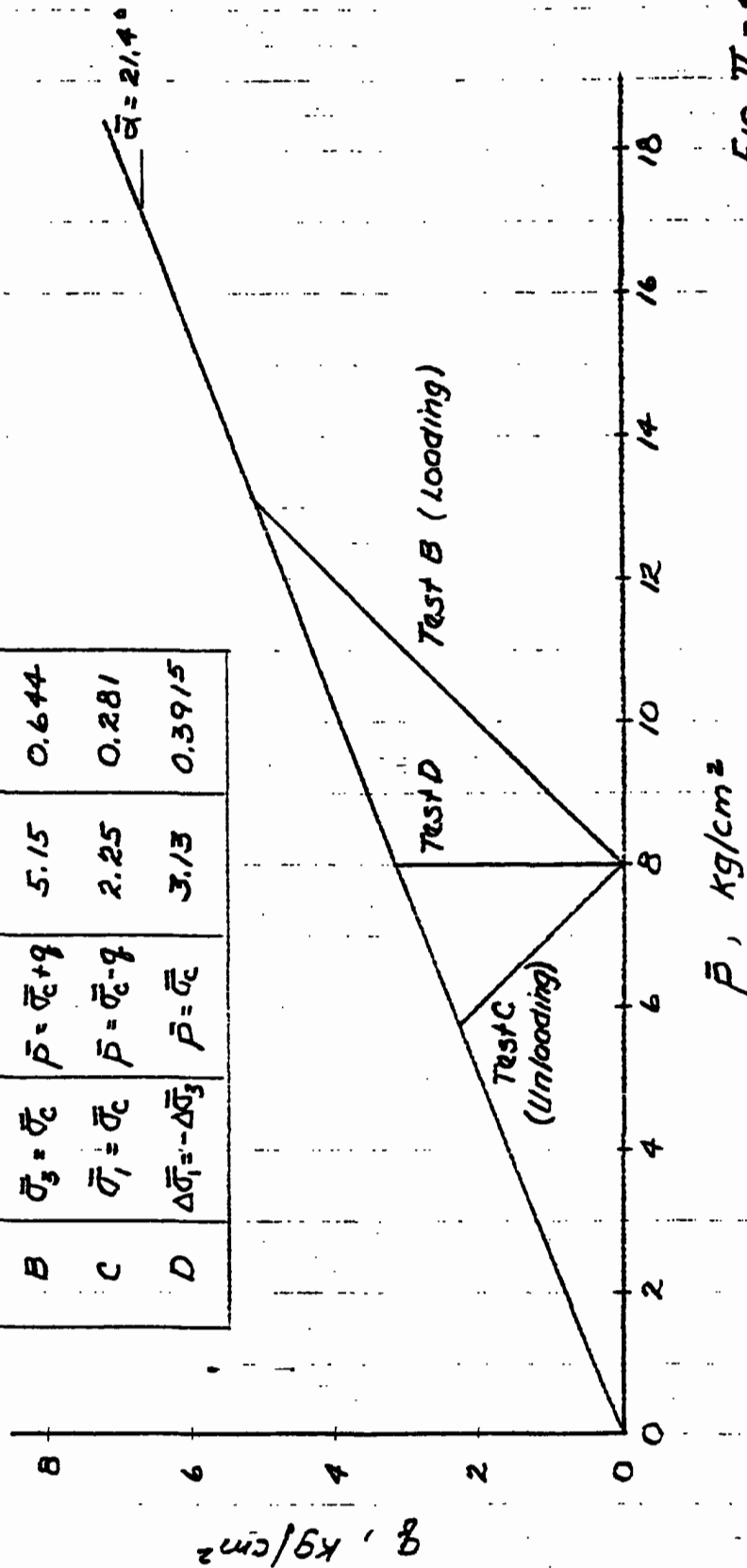


FIG II - 4

Stress-Strain: Loading and Unloading

C/D Compression Tests on Normally Consolidated Simple Clay

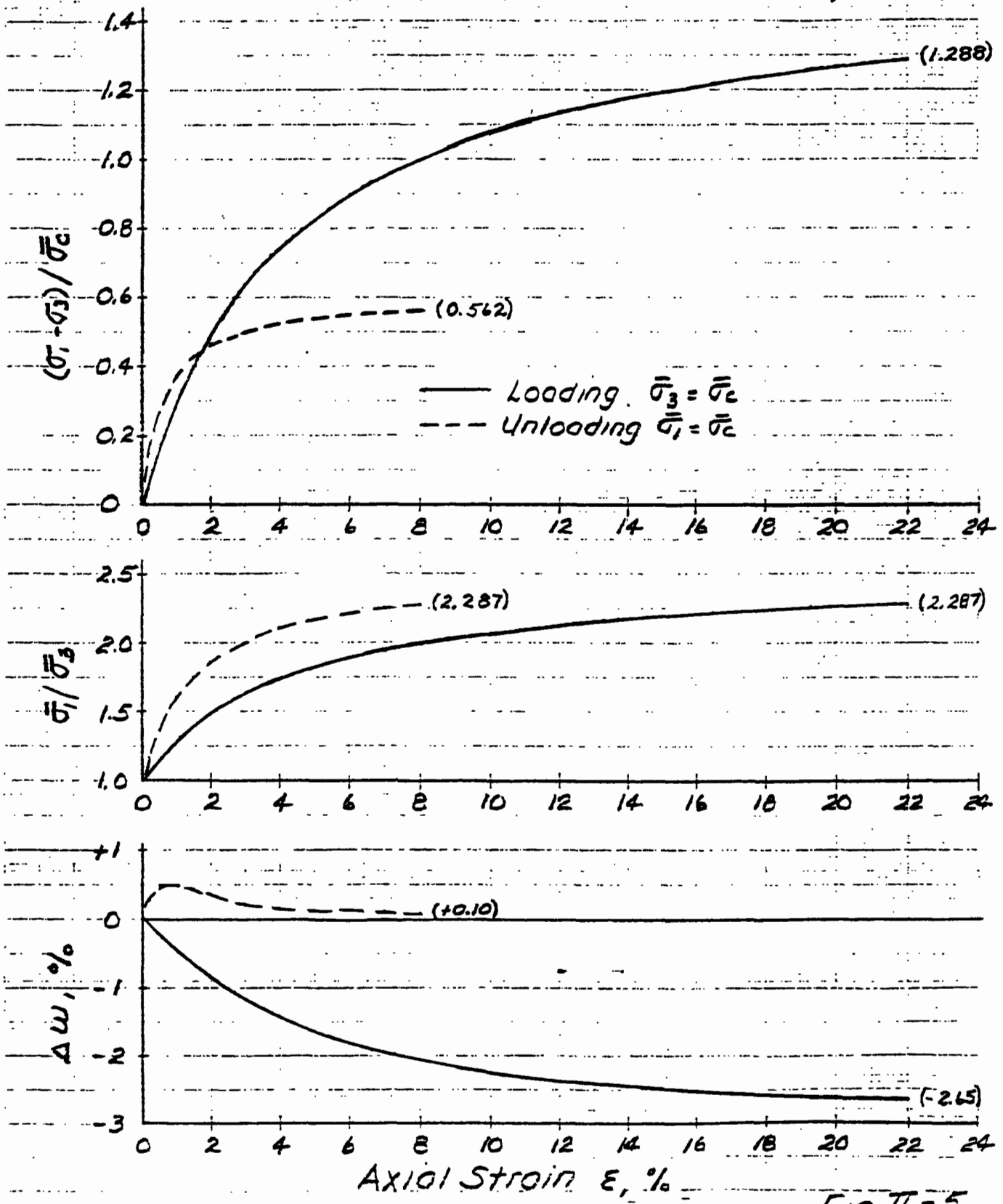


Fig II-5

Hyperbolic Stress-Strain Relationship for CID Compression Tests on Normally Consolidated Simple Clay

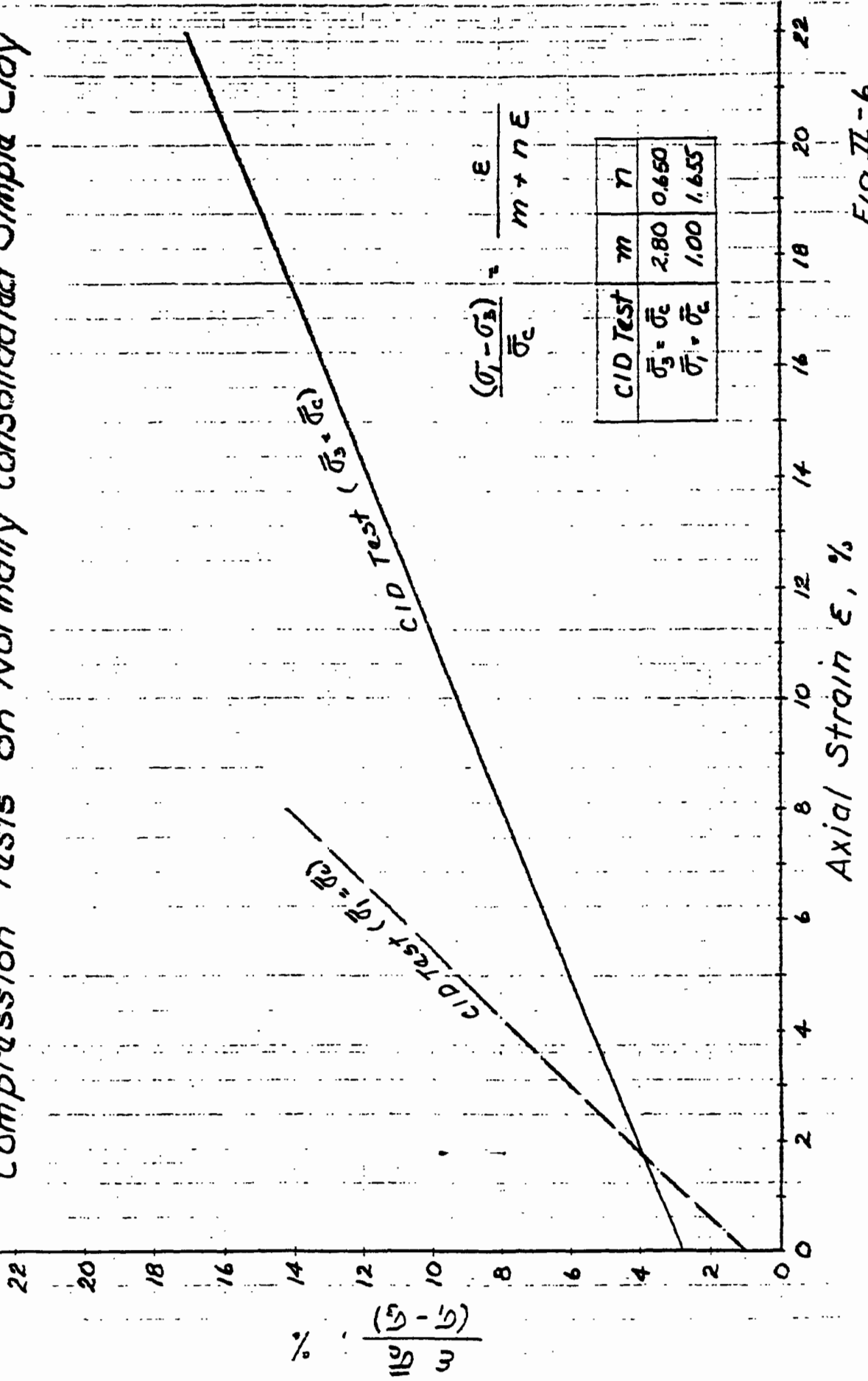
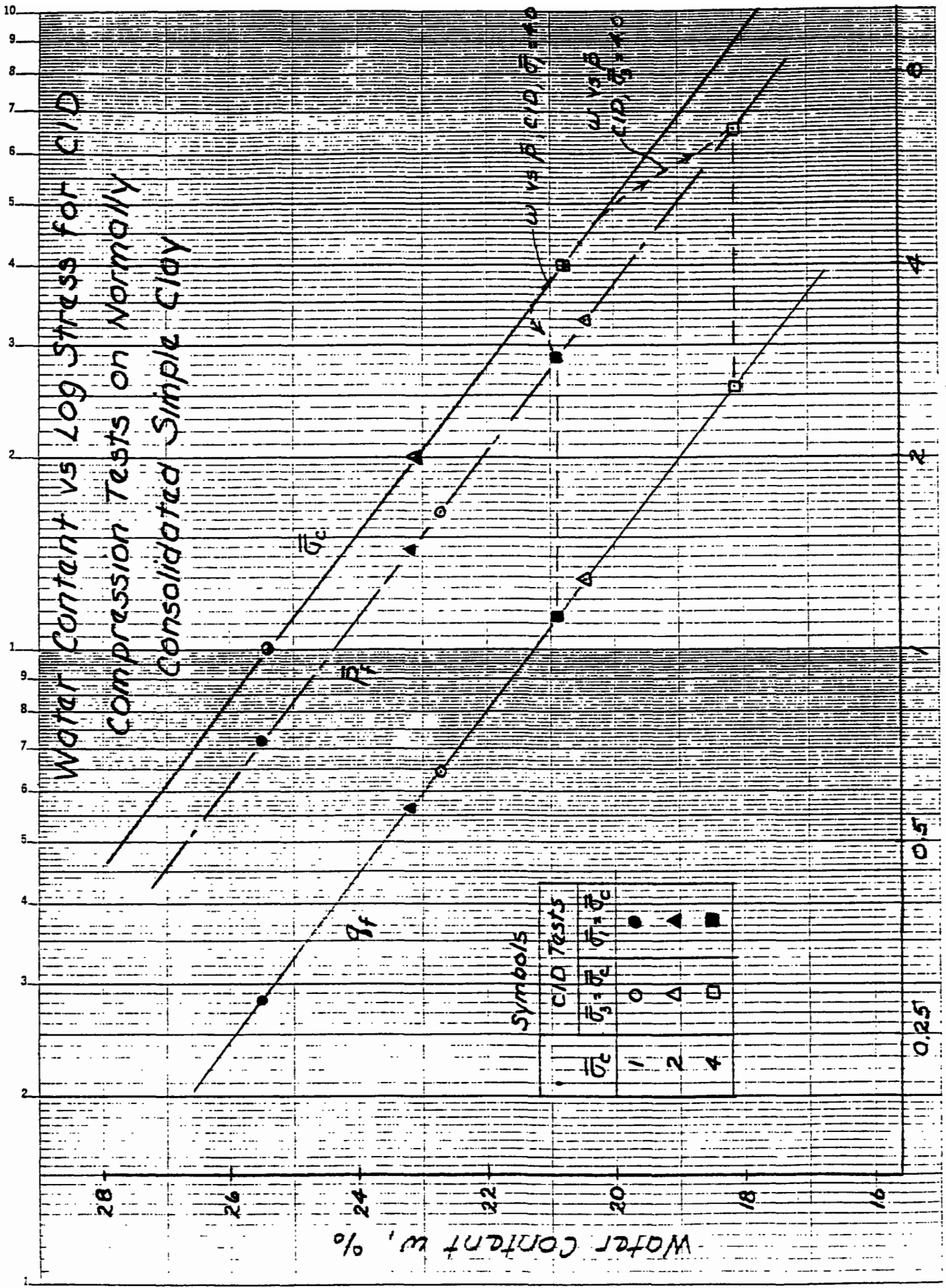


FIG II-6



Stress - Strain : CIU Compression Tests ON N.C. Simple Clay

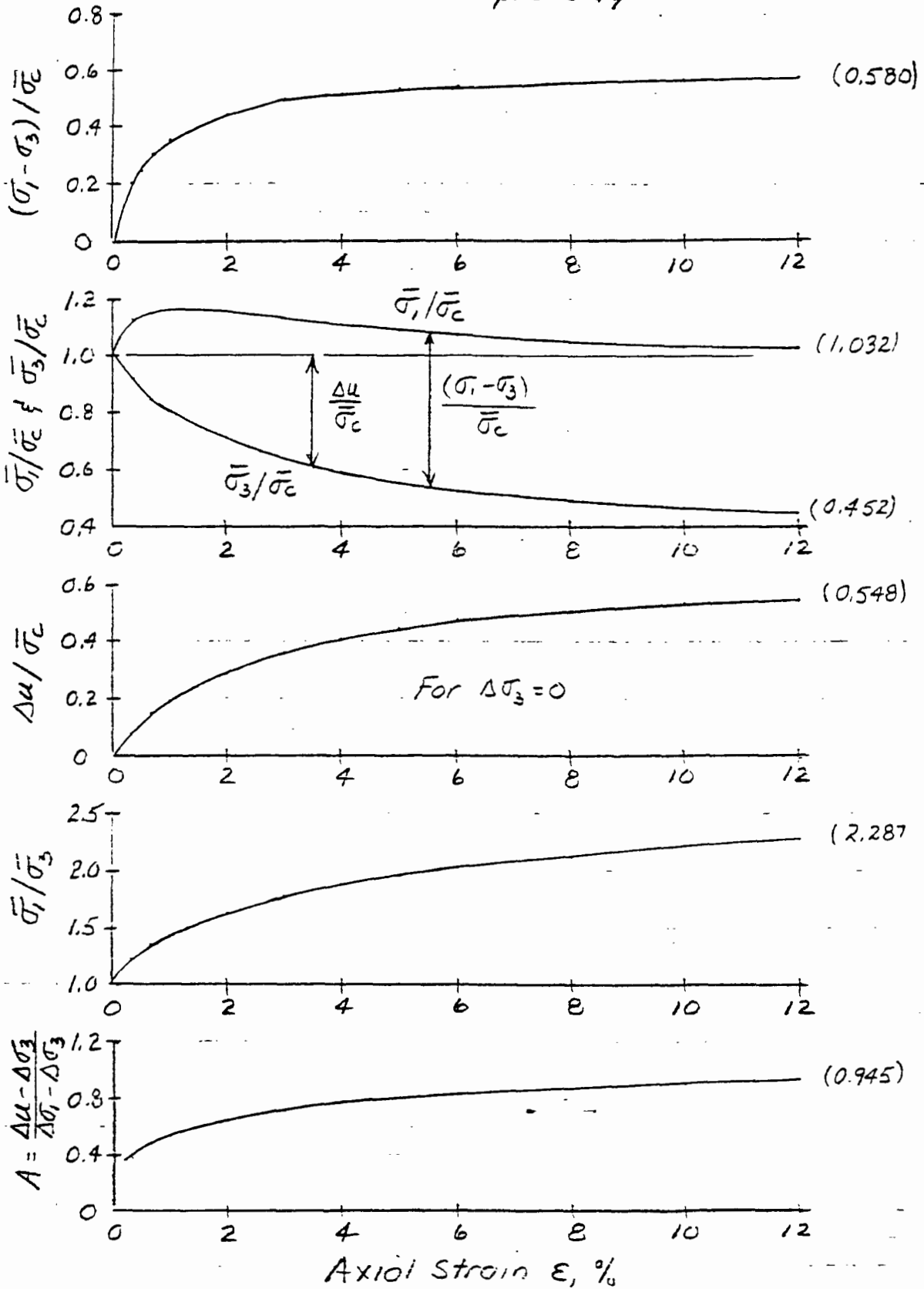


Fig II-3

Total and Effective Stress Paths for a

CTU Test with $\bar{\sigma}_c = 4 \text{ kg/cm}^2$

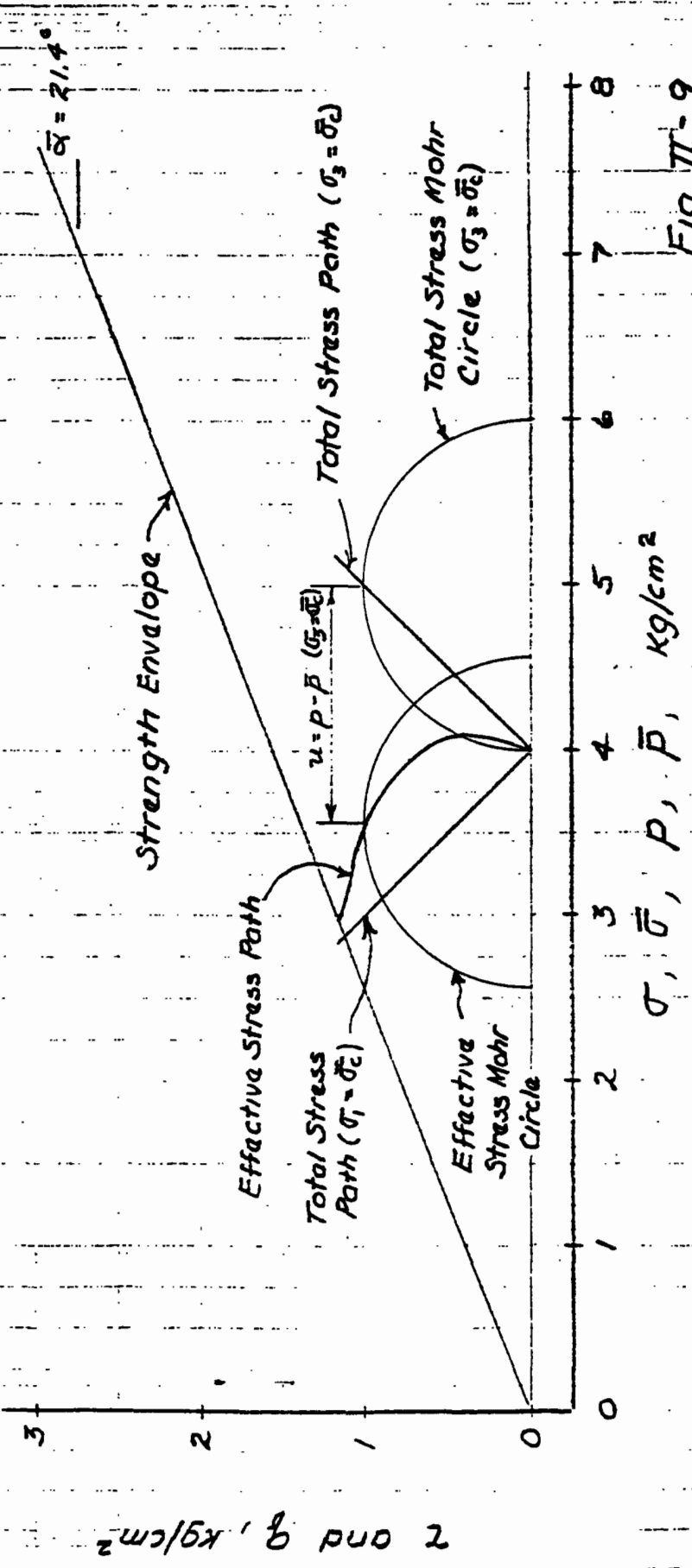


Fig. III-9

Effective Stress Paths and Axial Strains for CU Compression Tests on Normally Consolidated Simple Clay

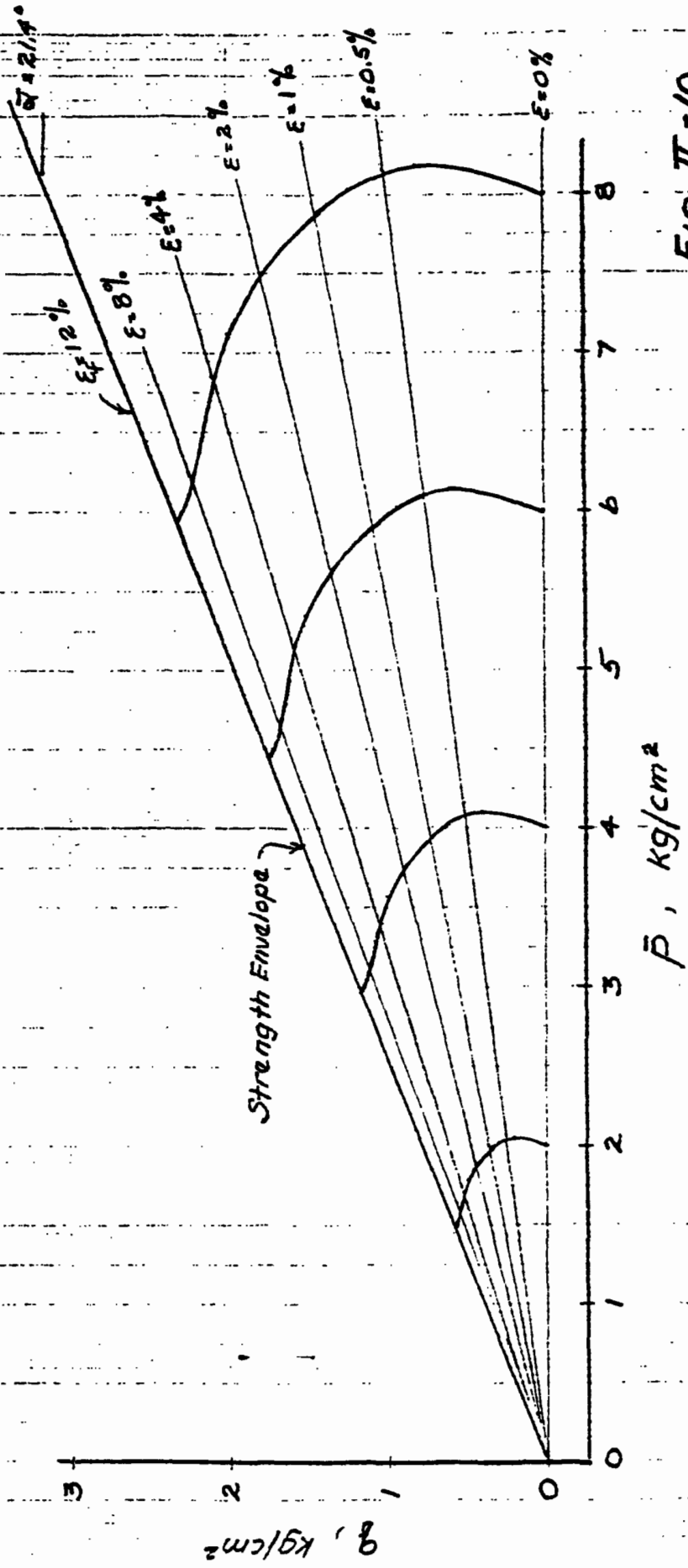


FIG. II-10

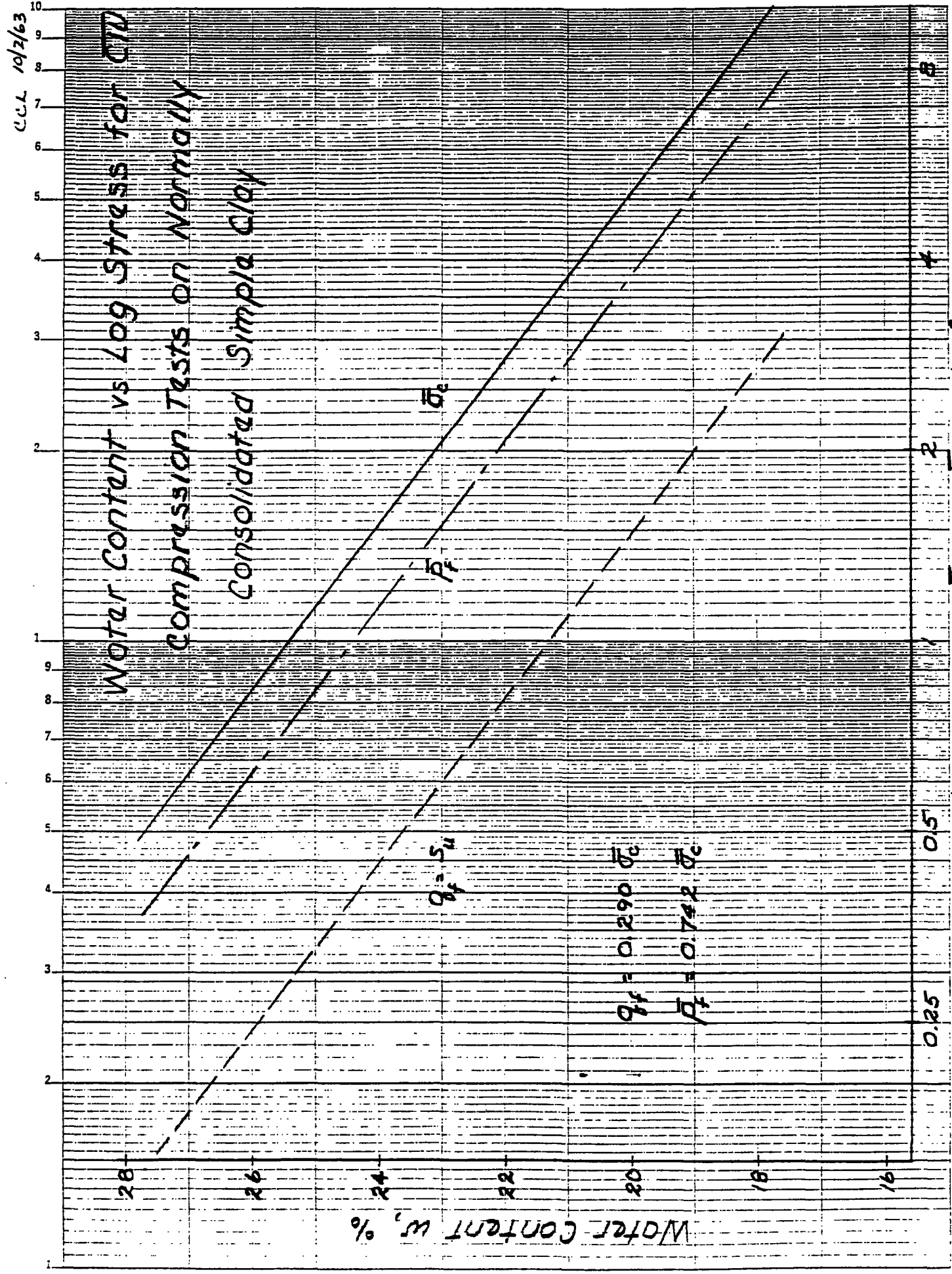


Fig. II-11

Water Content, Shear Stress, and Effective Stress
 Relationship for $\bar{c}\bar{t}\bar{u}$ and CID Compression
 Tests on Normally Consolidated Simple Clay

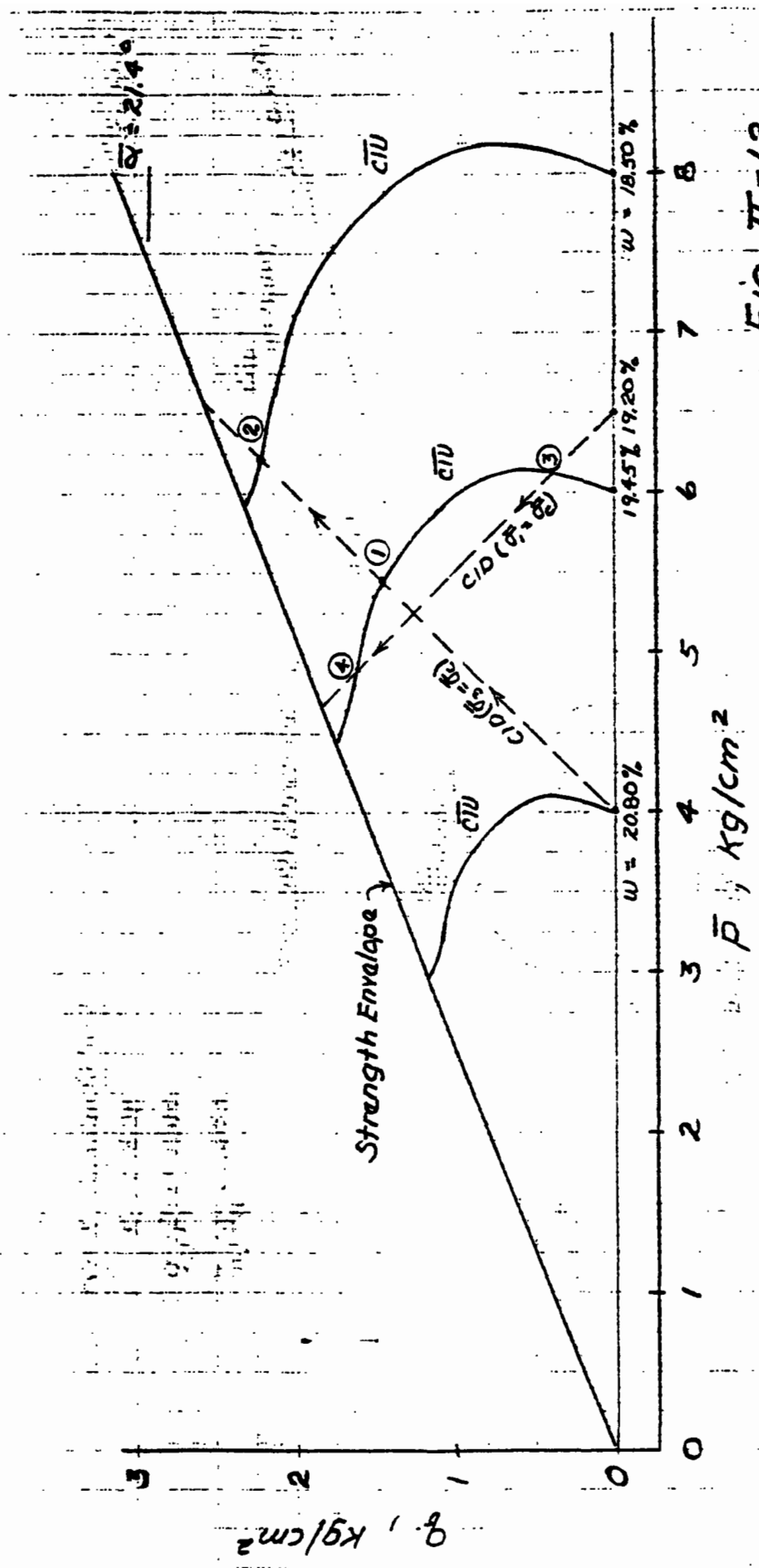
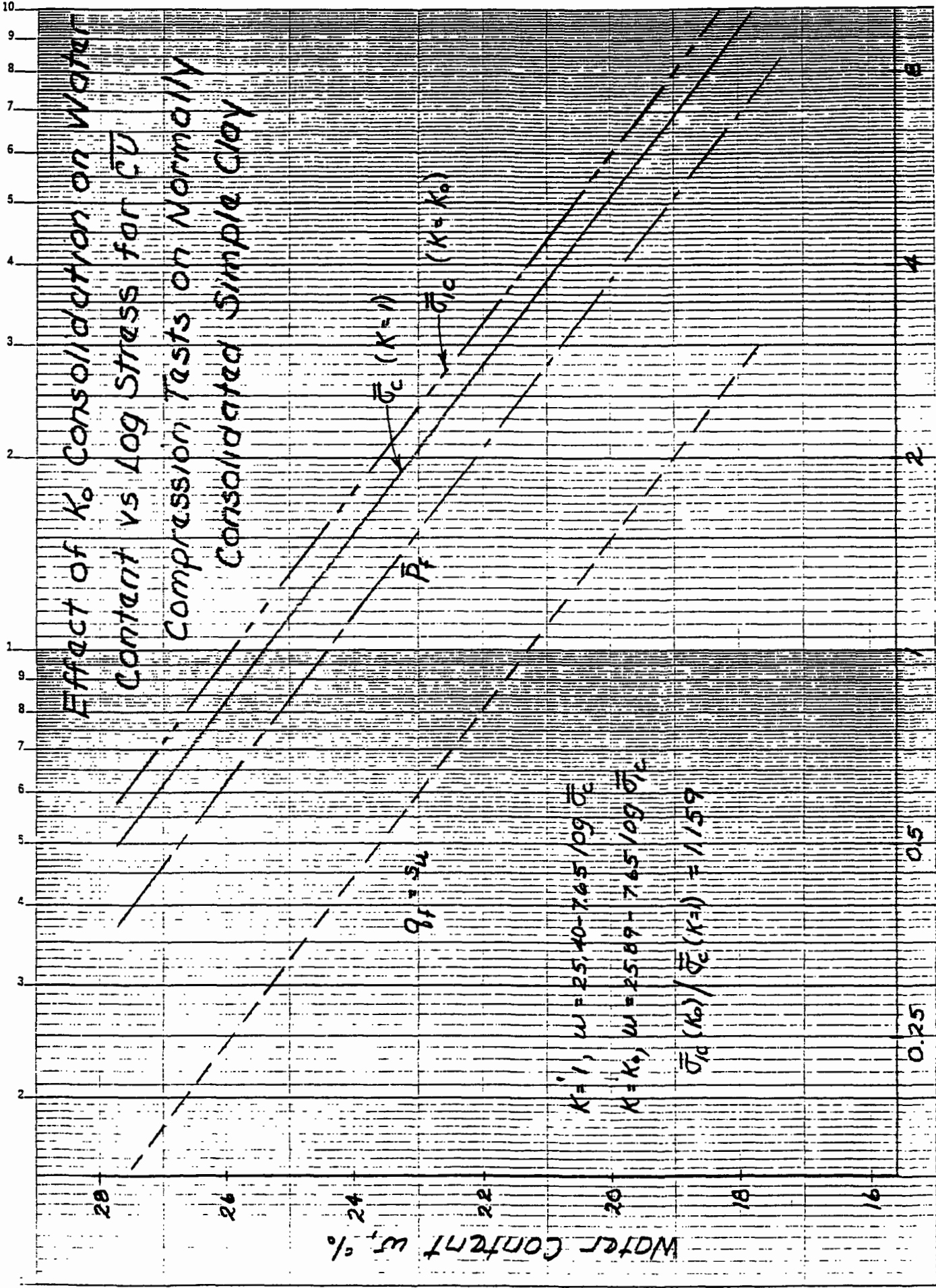


Fig. II-12

CCL 14/5/63

Effect of K_0 Consolidation on Water Content vs Log Stress for \bar{c}_v Consolidated Simple Clay



Stresses $q_f, \bar{P}_f, \bar{\sigma}_c$ and $\bar{\sigma}_{1c}, \text{kg/cm}^2$ FIG II-14

CEL 10/6/63

Total and Effective Stress Paths for UU Compression Tests on Normally Consolidated Simple Clay

with $\bar{\sigma}_c = 4 \text{ kg/cm}^2$

Test	σ_c	Prestress		At Failure	
		u	\bar{p}	u	\bar{p}
A	0	-4	4	-1.805	2.965
B	2	-2	"	10.195	"
C	4	0	"	12.195	"
D	6	+2	"	14.195	"

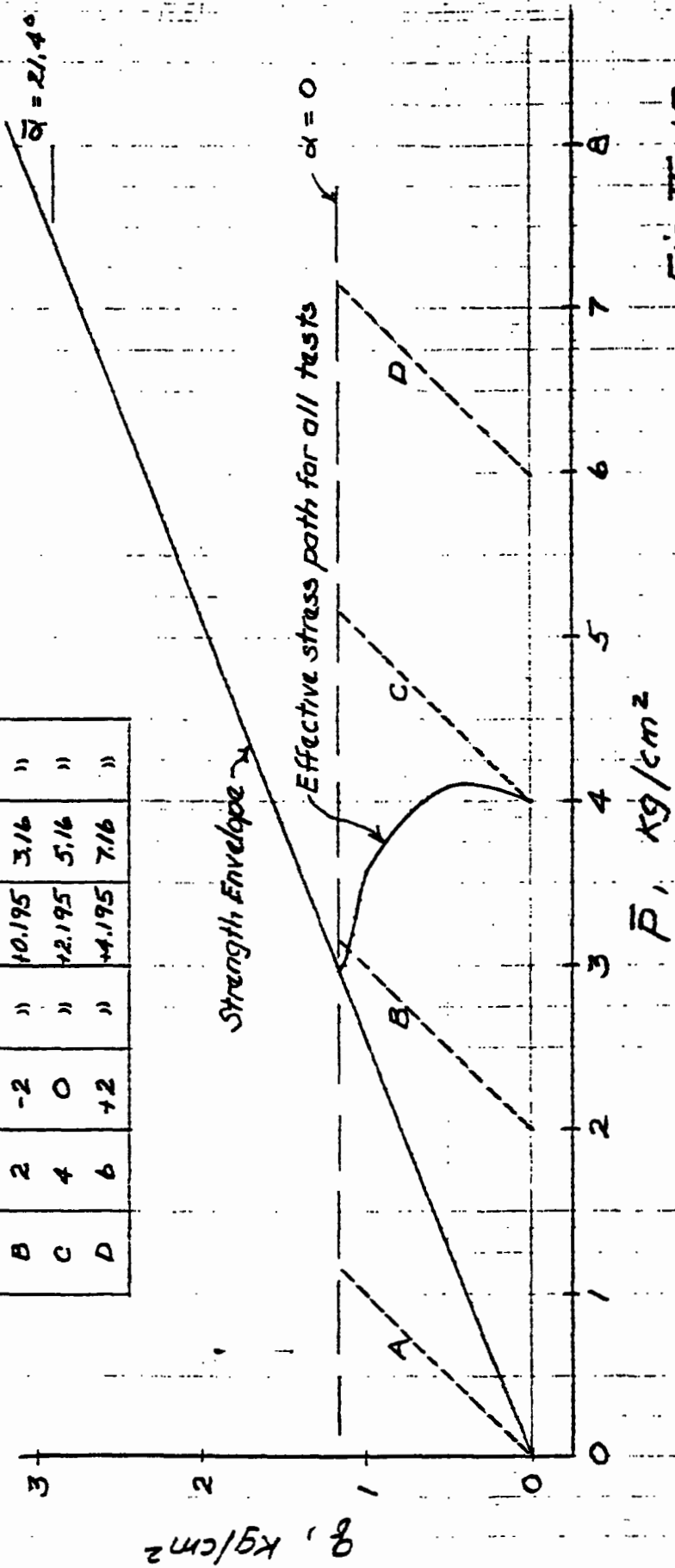


Fig II-15

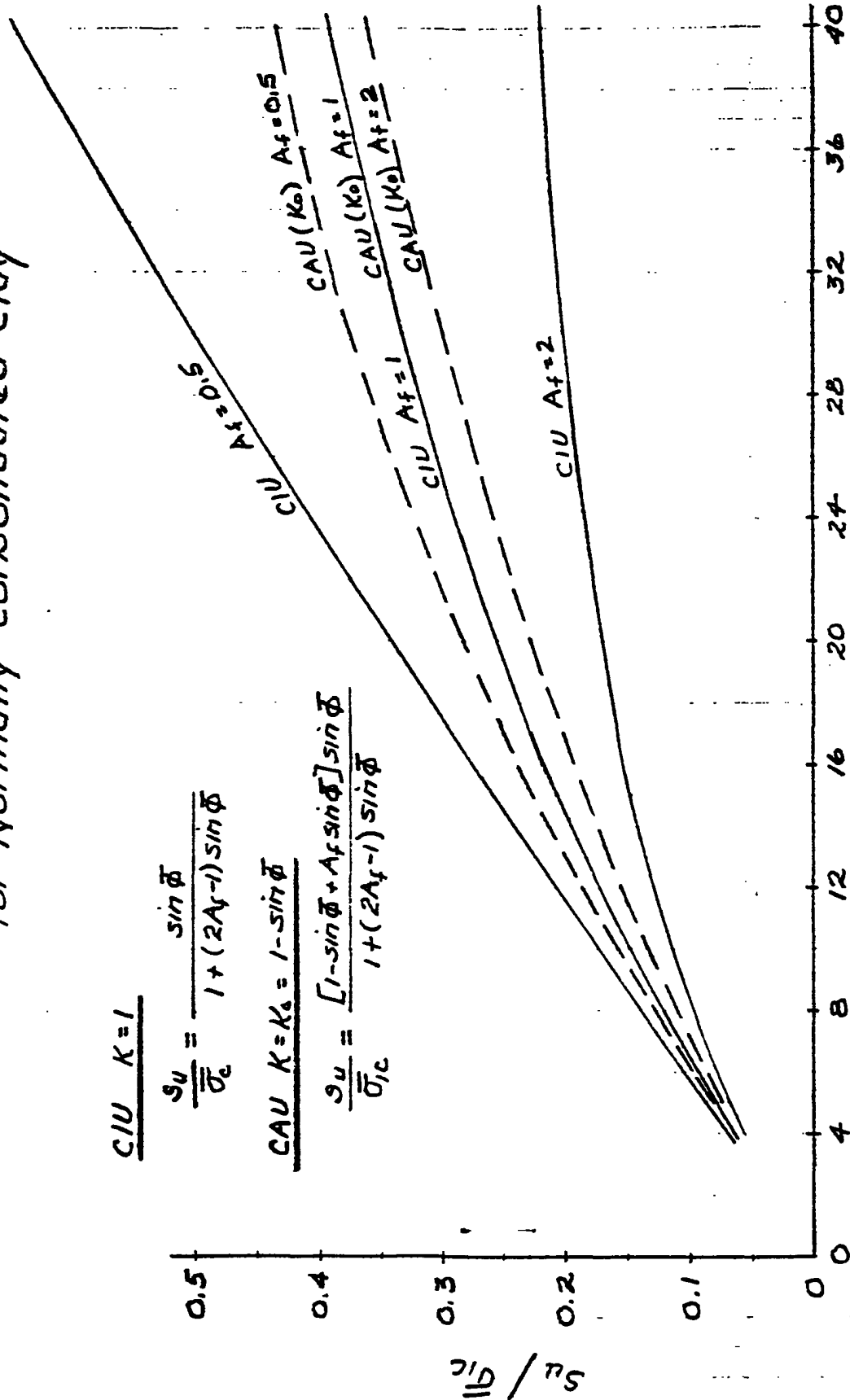
**Ratio of Undrained Strength to Consolidation Pressure
as a Function of Friction Angle and A_f Parameter
for Normally Consolidated Clay**

CIU $K=1$

$$\frac{S_u}{\sigma_c} = \frac{\sin \phi}{1 + (2A_f - 1) \sin \phi}$$

CAU $K=K_0 = 1 - \sin \phi$

$$\frac{S_u}{\sigma_c} = \frac{[1 - \sin \phi + A_f \sin \phi] \sin \phi}{1 + (2A_f - 1) \sin \phi}$$



Friction Angle, ϕ , °

FIG II-16

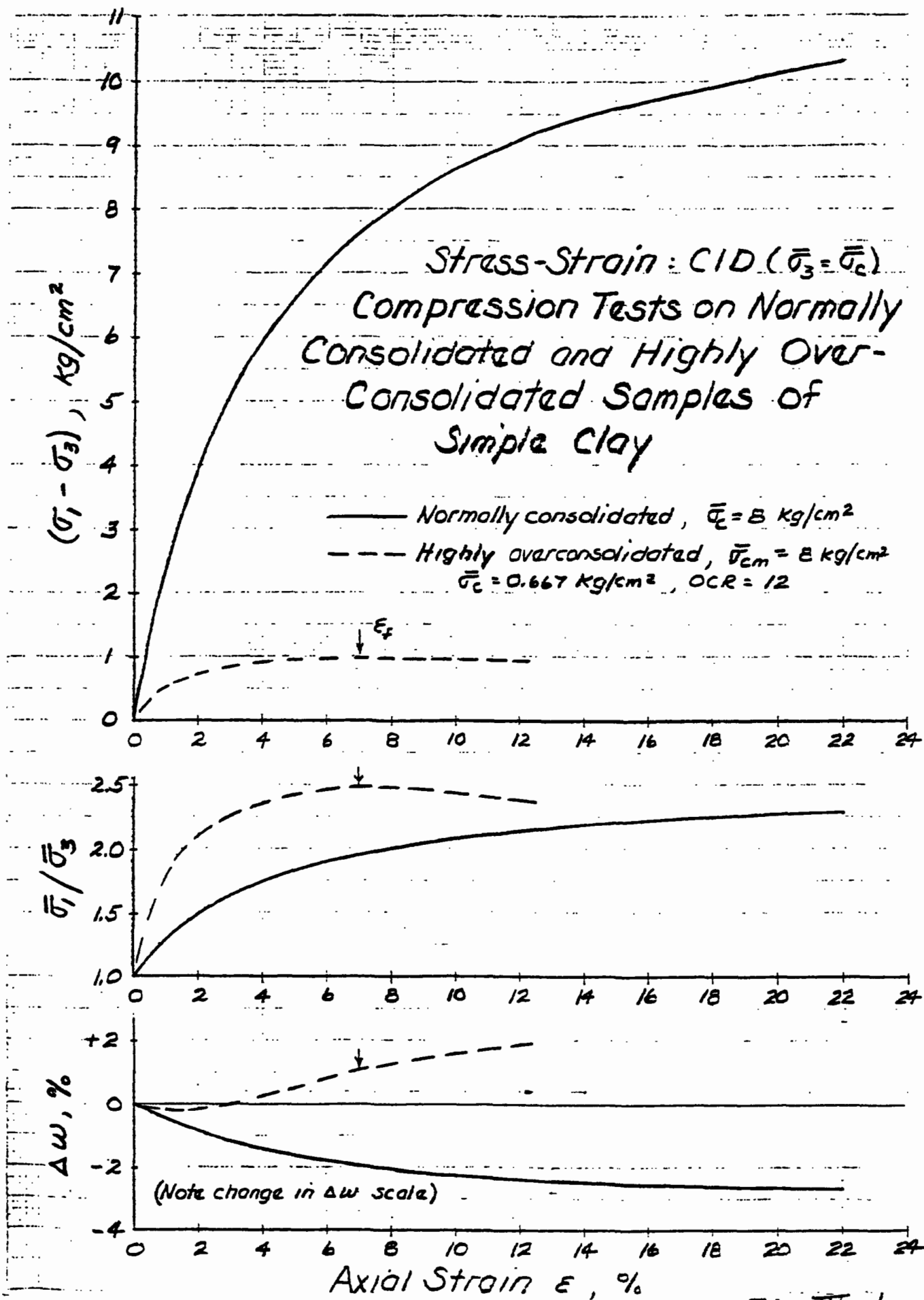


Fig III-1

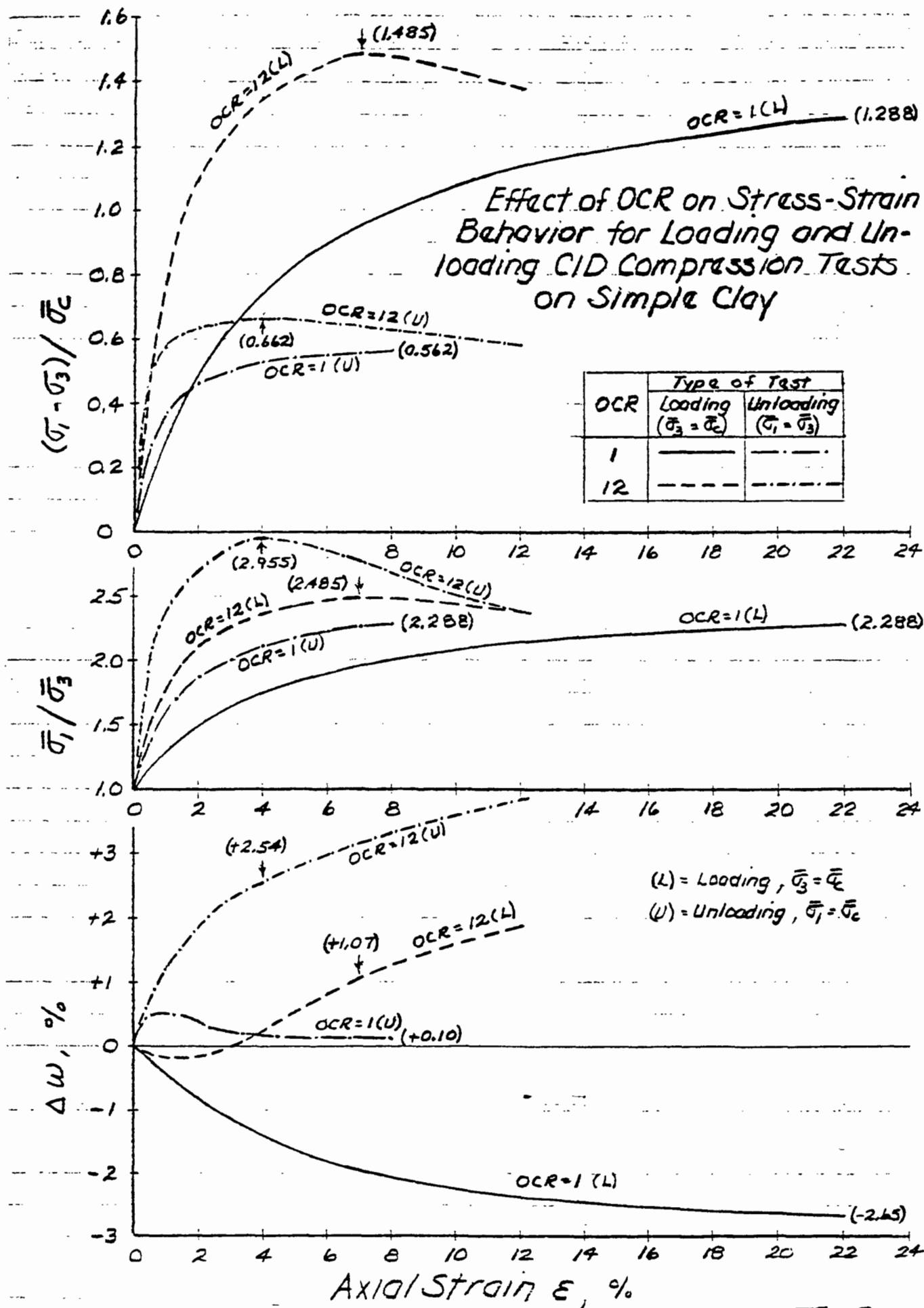


Fig. III - 2

Hyperbolic Stress-Strain Relationships for Loading and Unloading CID Compression Tests on Normally Consolidated and Highly Overconsolidated Samples of Simple Clay

Note: Only values for $\epsilon \leq \epsilon_f$ are plotted.

(L) = Loading, $\bar{\sigma}_3 = \bar{\sigma}_c$
 (U) = Unloading, $\bar{\sigma}_1 = \bar{\sigma}_c$

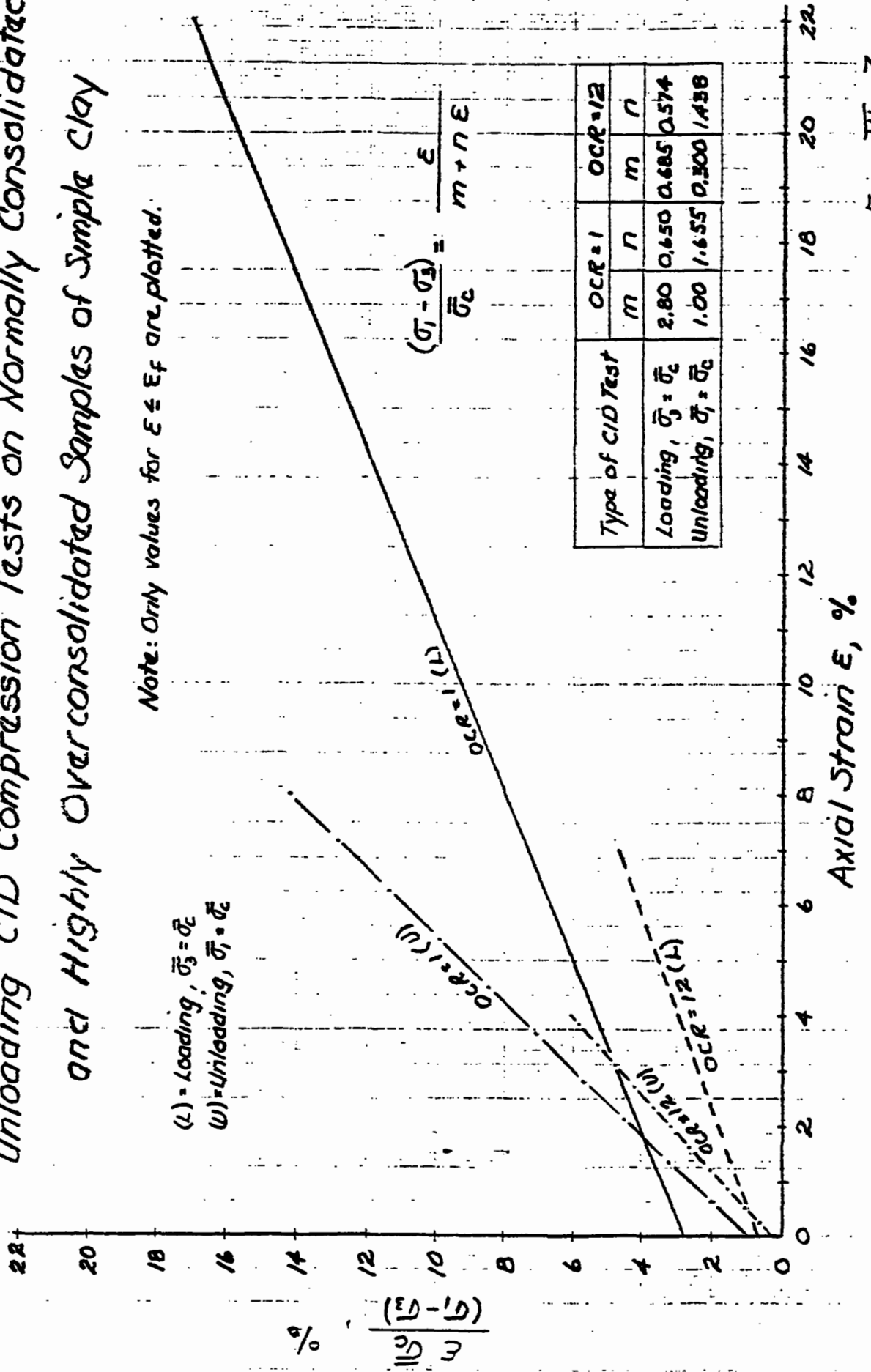


Fig. III-3

Effective Stress Paths for Loading and Unloading CID

Compression Tests on Overconsolidated Simple

Clay with a Maximum Past Pressure of 8 kg/cm²

Overconsolidated

$$q_f = \bar{\sigma} + \bar{P}_f \tan \bar{\alpha}$$

$$\bar{\alpha} = \bar{c} \cos \bar{\phi}$$

$$\tan \bar{\alpha} = \sin \bar{\phi}$$

For $\bar{\sigma}_{cm} = 8 \text{ kg/cm}^2$

$$\bar{\alpha} = 0.05 \text{ kg/cm}^2, \bar{\alpha} = 20.95^\circ$$

$$q_f = 0.05 + 0.383 \bar{P}_f$$

$$q_f = 0.3915 \bar{P}_f$$

Normally consolidated and overconsolidated strength envelopes intersect here $\bar{\alpha} = 21.7^\circ$ (N.C.)

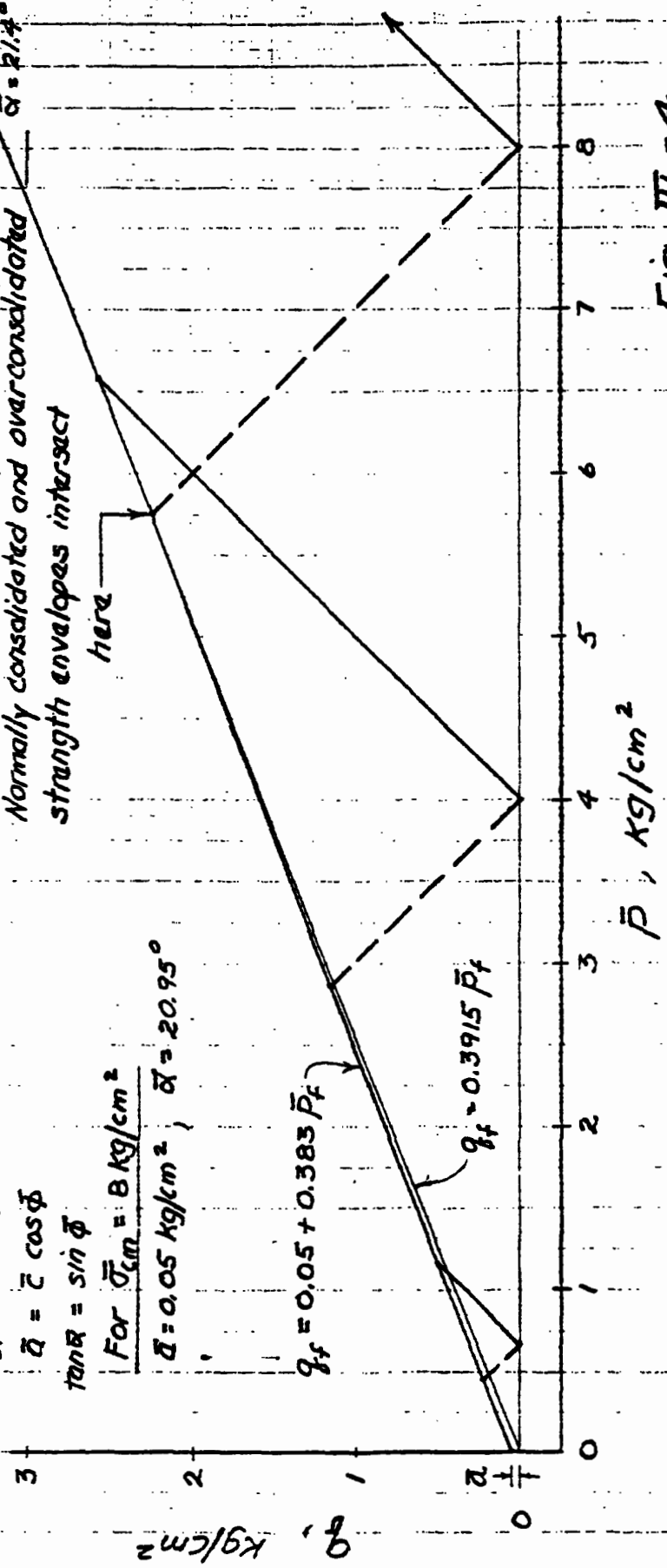
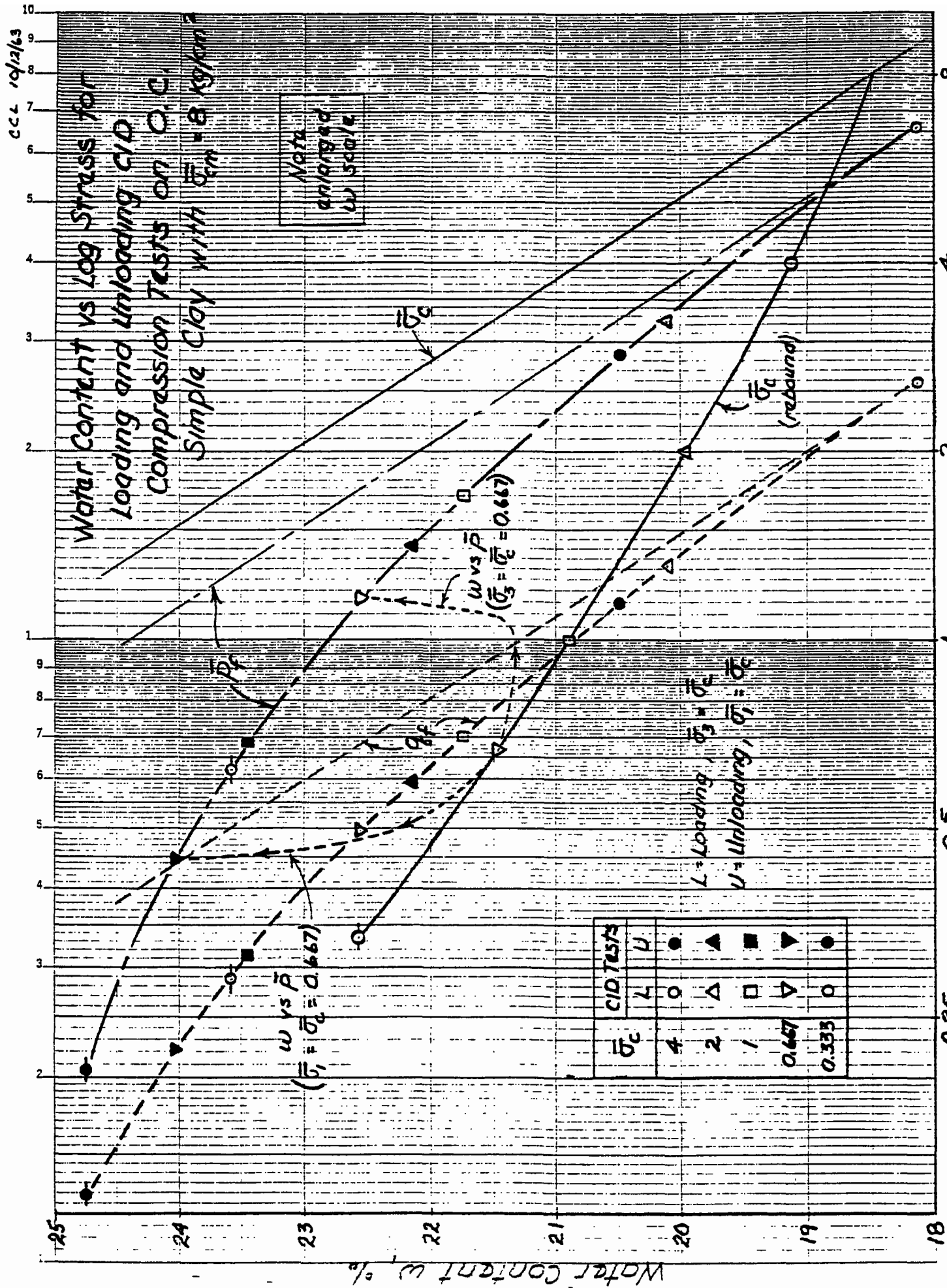


Fig. III - 4



Stress-Strain: CIU Compression Tests on Normally Consolidated and Highly Overconsolidated Samples of Simple Clay

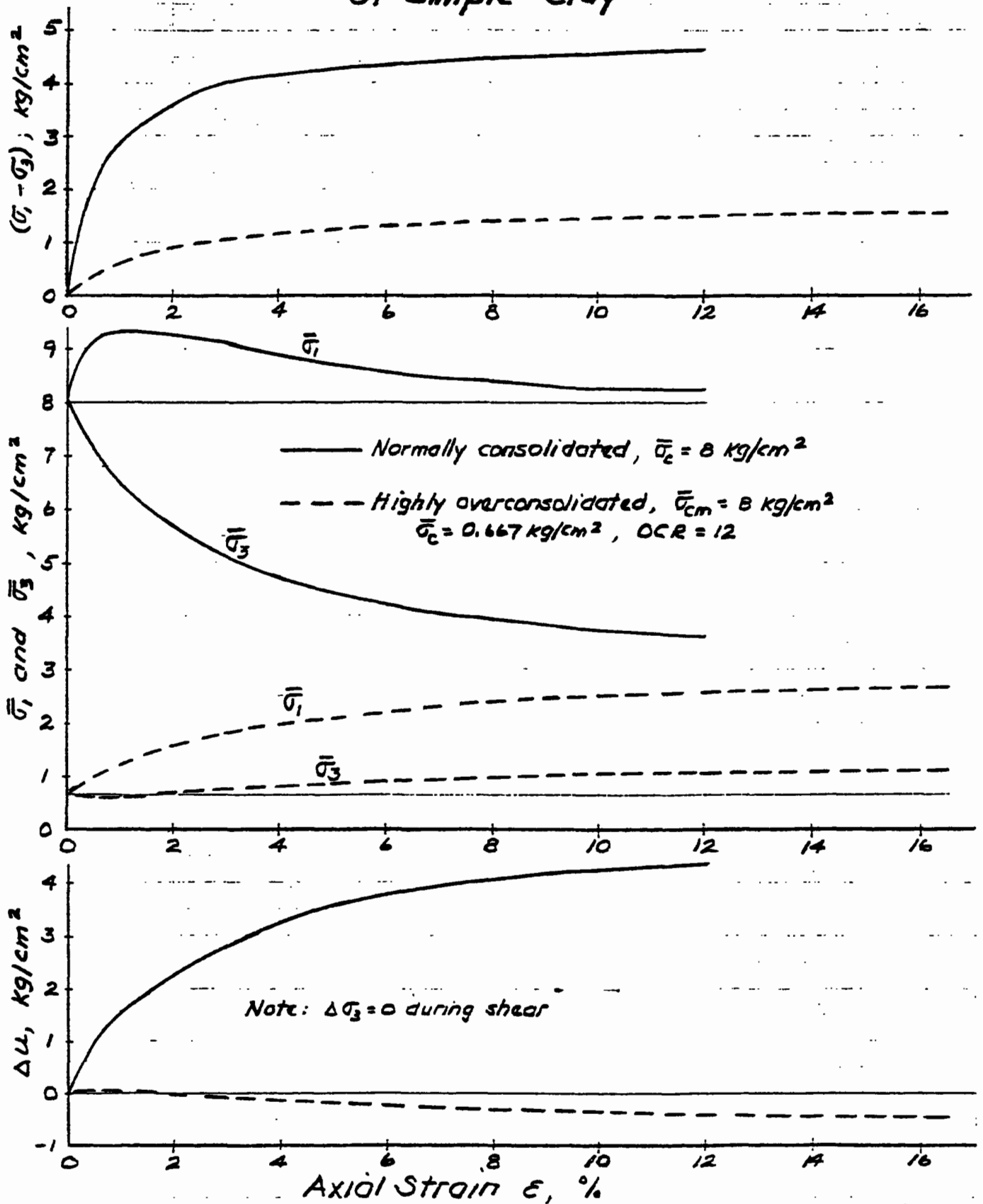


Fig. III - 6

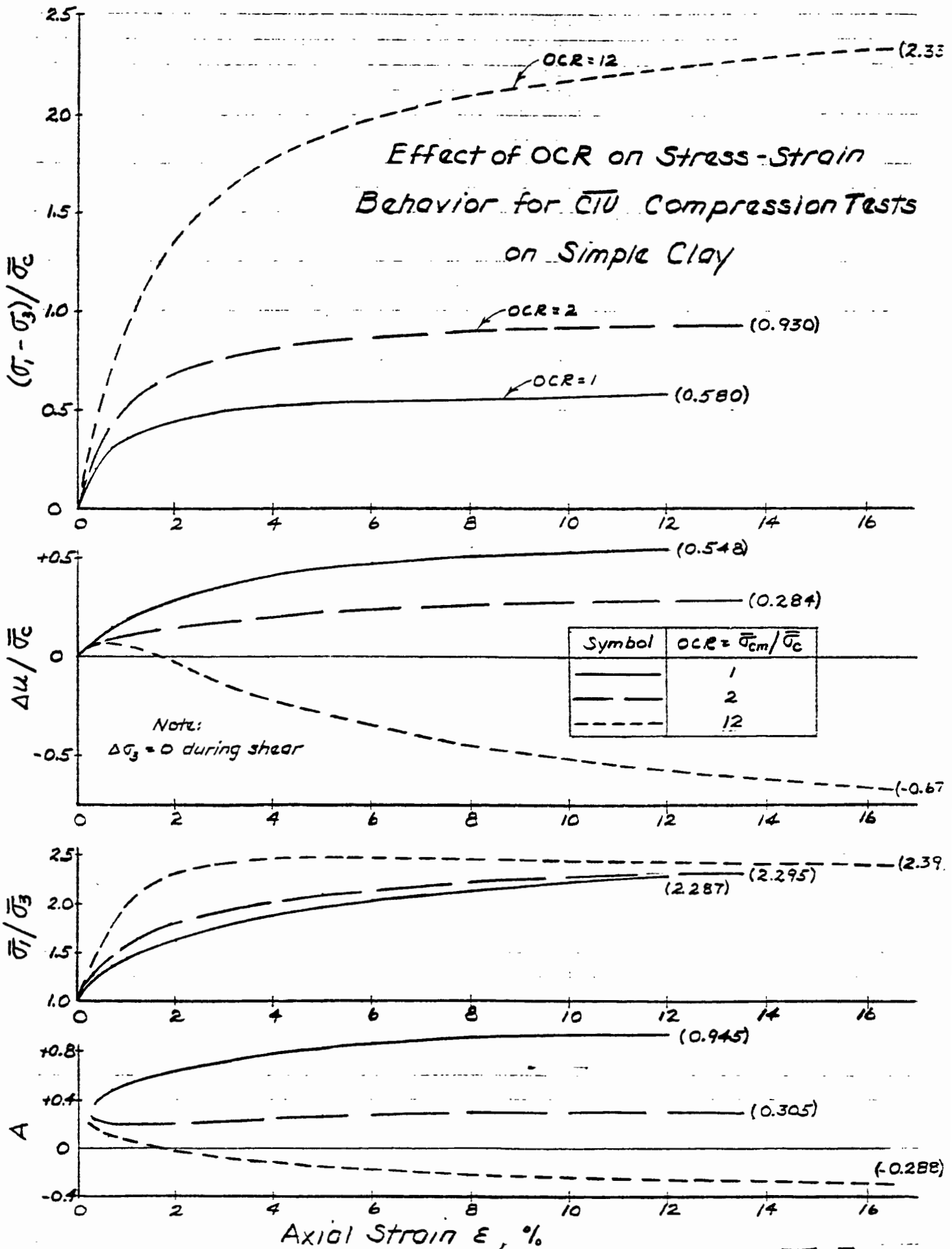


Fig III-7

Effect of OCR on Hyperbolic Stress - Strain Relationship for CTU Compression Tests on Simple Clay

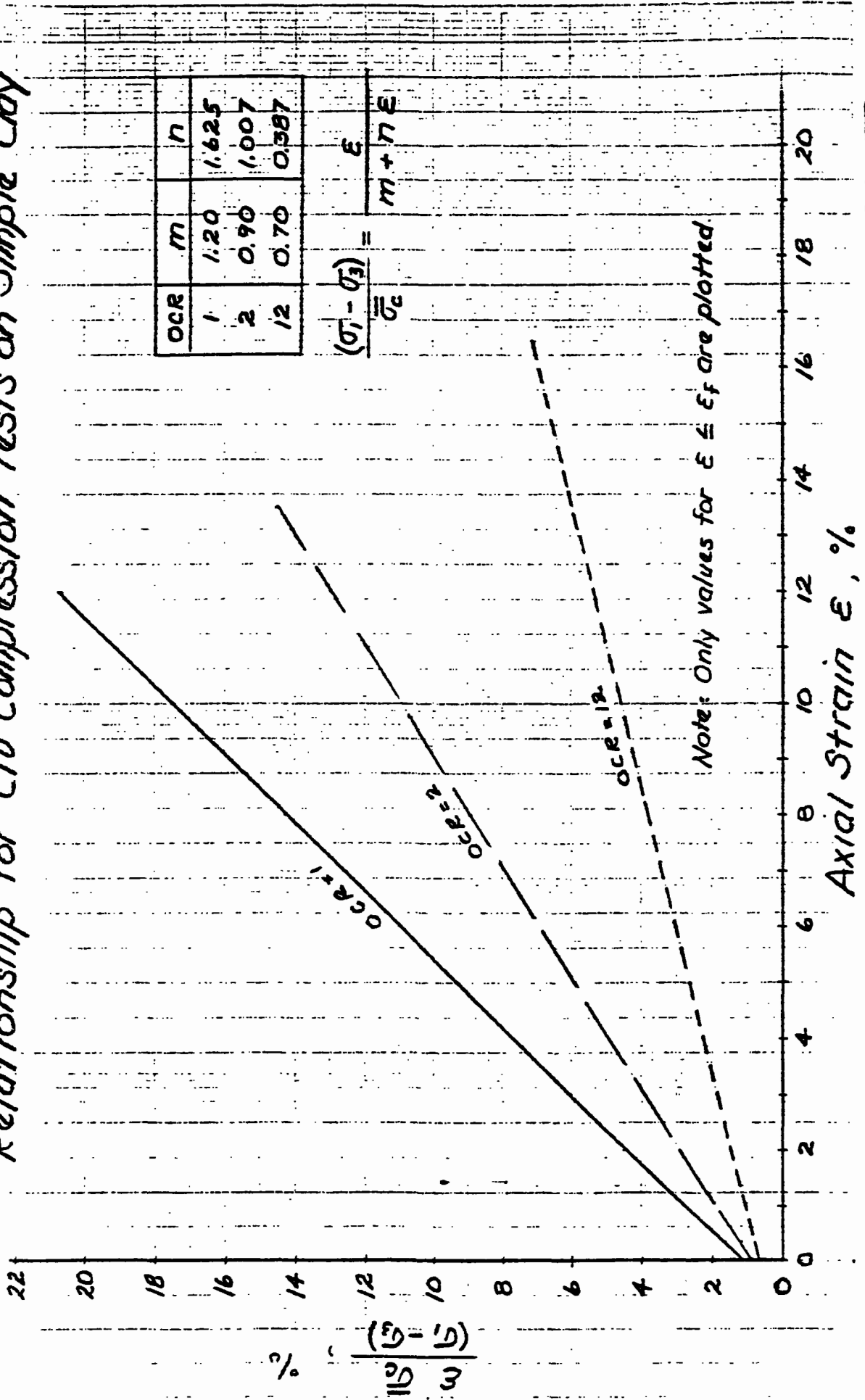


Fig. III - 8

Effective Stress Paths for CTU Compression Tests on Overconsolidated Simple Clay with a Maximum Past Pressure of 8 kg/cm²

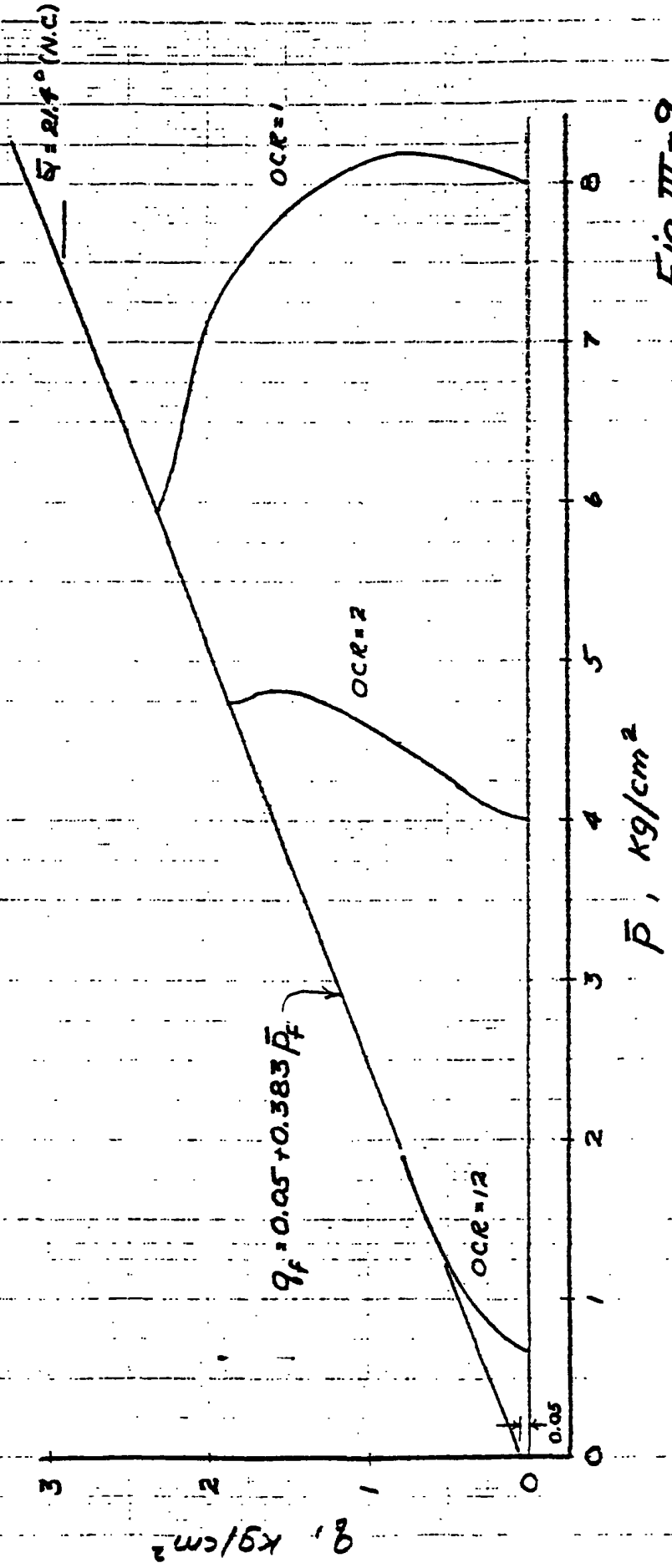


Fig III-9

Rendulic Plot Showing K_0 Consolidation and $\bar{C}IU$ Stress Paths for Over-Consolidated Simple Clay

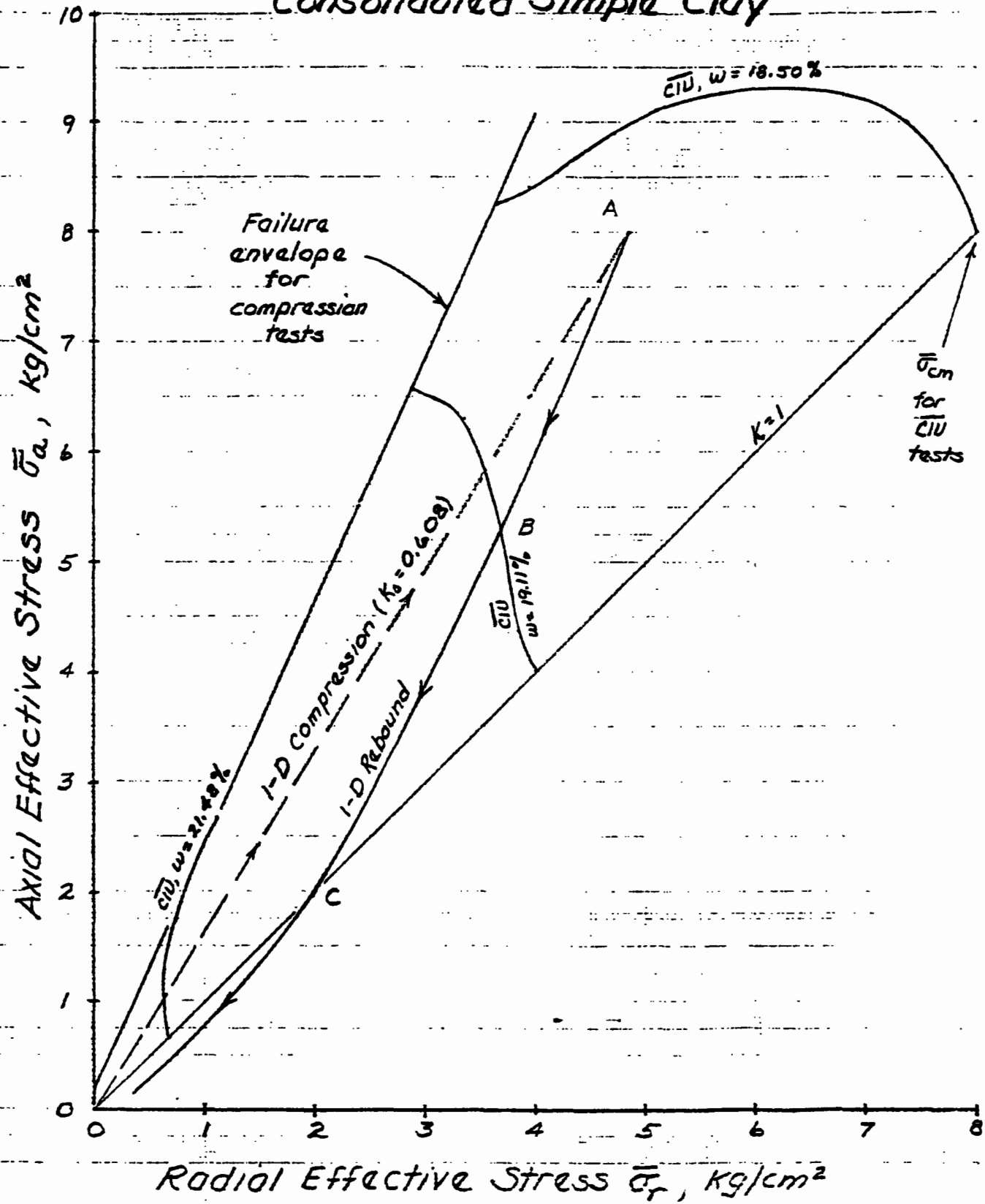


Fig III - 10

OCL 10/17/63

Comparison of Isotropic and K_0 Consolidation and Rebound Curves for Simple Clay

OCR	K_0	Δw %
1	0.608	0
1.20	0.645	0.02
1.52	0.698	0.11
2	0.769	0.30
3	0.900	0.60
4	1.000	0.97
6	1.129	1.43
8	1.220	1.79
12	1.348	2.32
24	1.650	3.29

Water Content w , %

Consolidation Pressure $\bar{\sigma}_c$, kg/cm^2

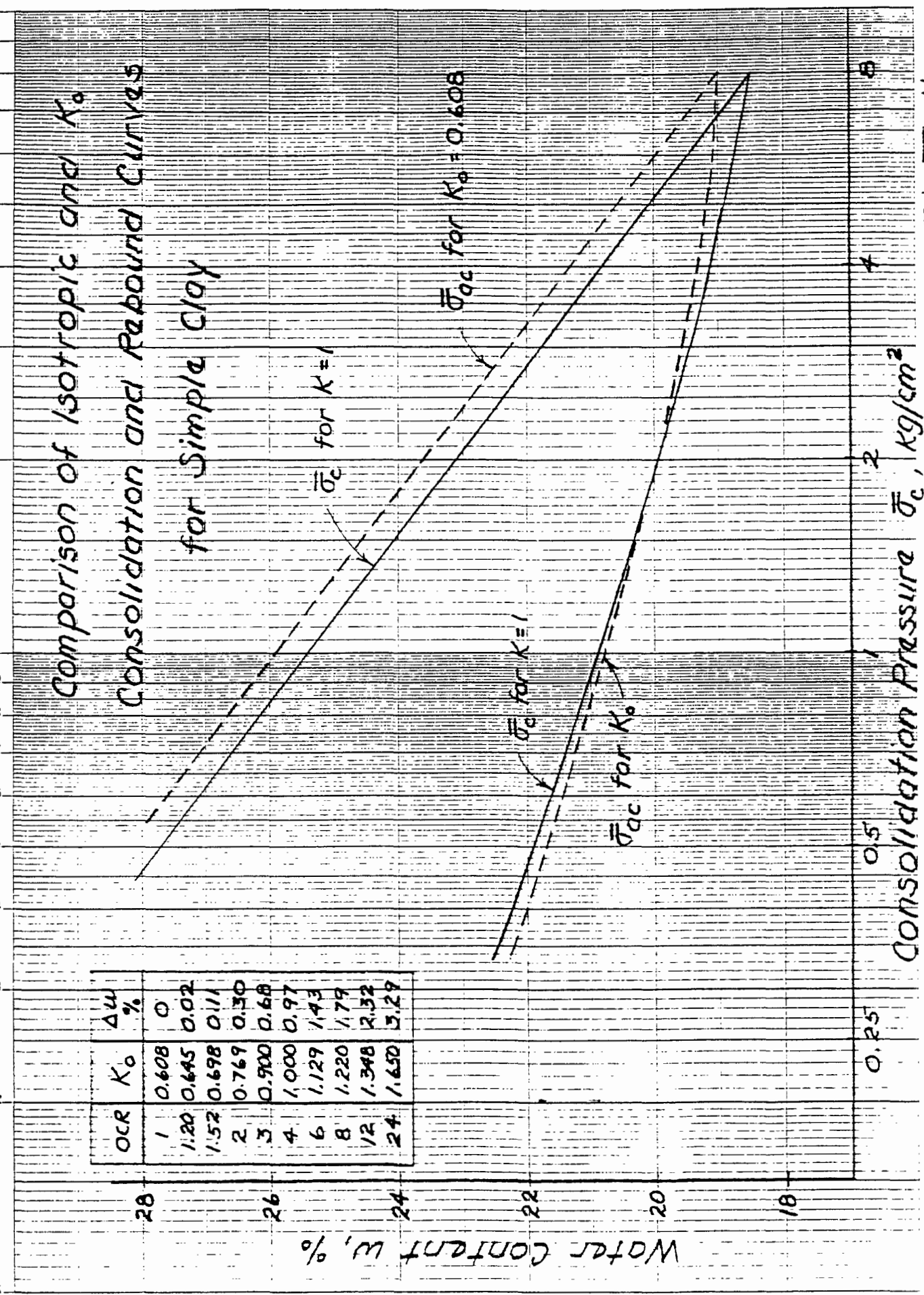


FIG III -11

Strength Data from CIU Compression Tests on Normally Consolidated and Overconsolidated Simple Clay

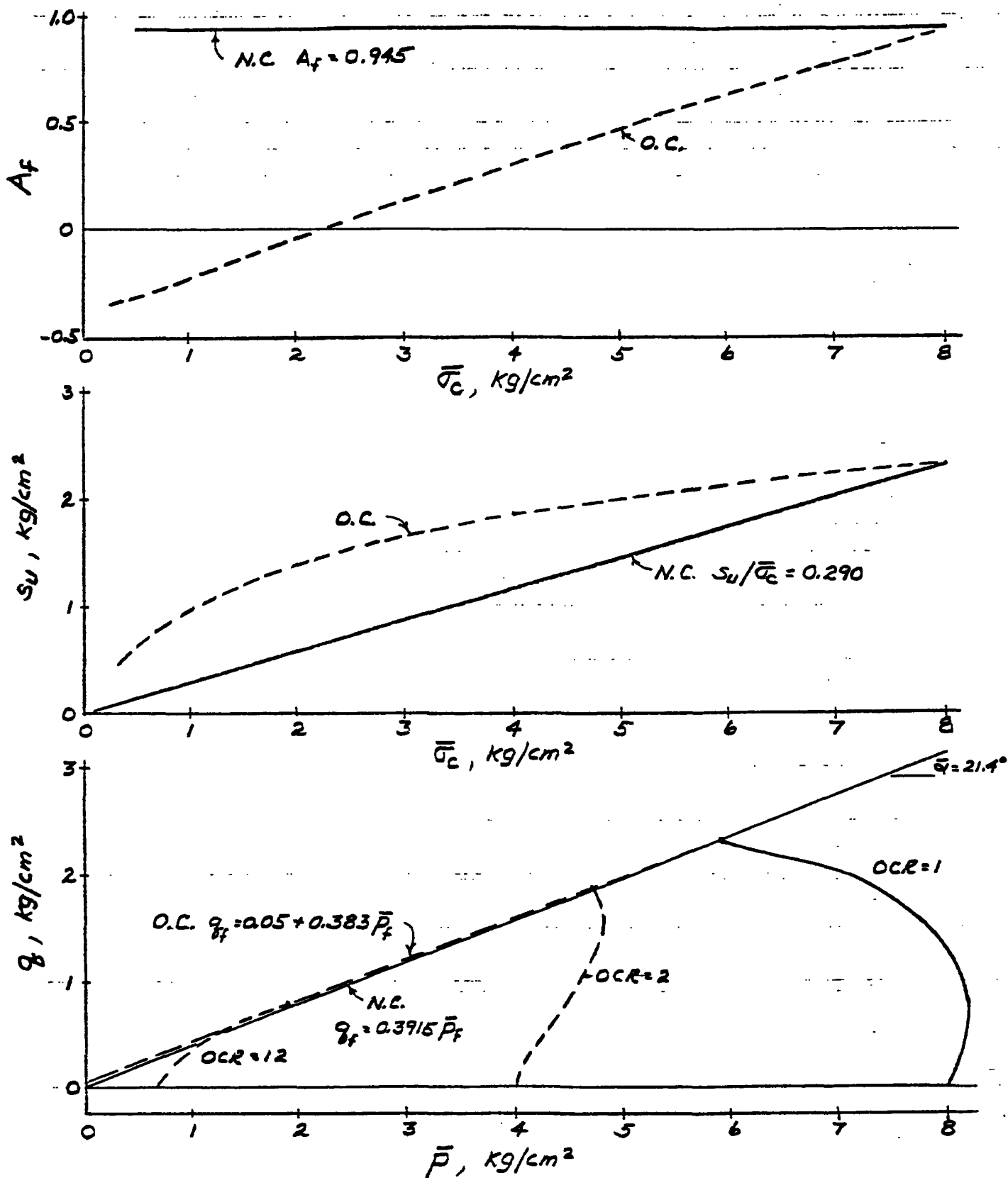
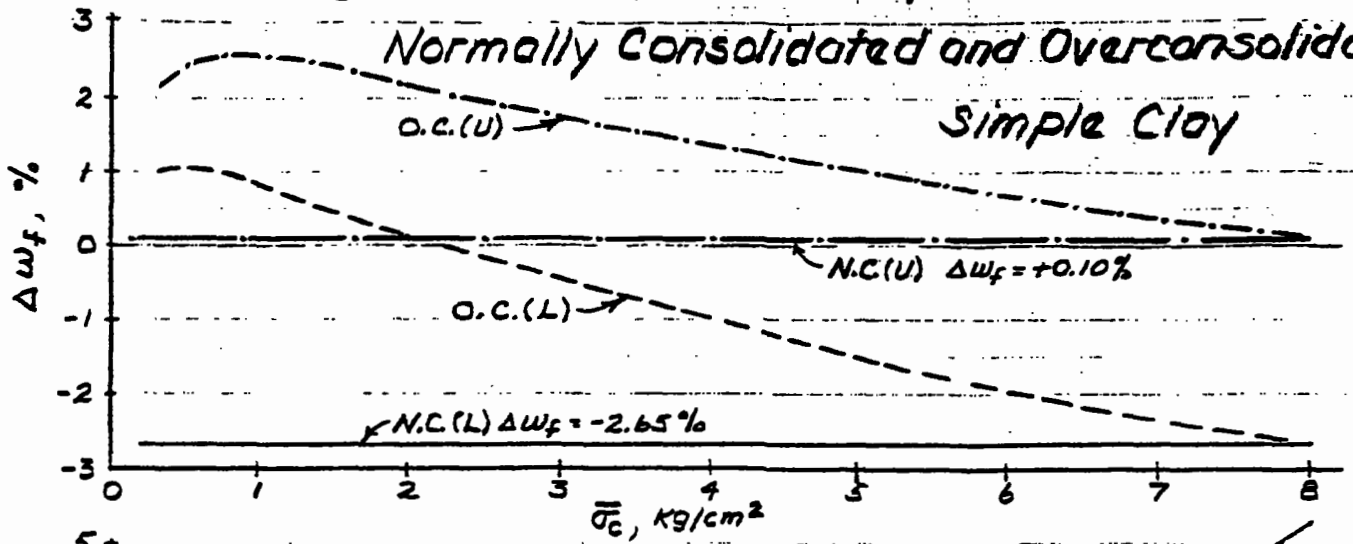


Fig. III-12

Strength Data from CID Compression Tests on Normally Consolidated and Overconsolidated Simple Clay



Type of CID Test	N.C.	O.C.
$\frac{L}{\bar{\sigma}_3 = \bar{\sigma}_c}$	—	- - -
$\frac{U}{\bar{\sigma}_1 = \bar{\sigma}_c}$	- - -	- . - .

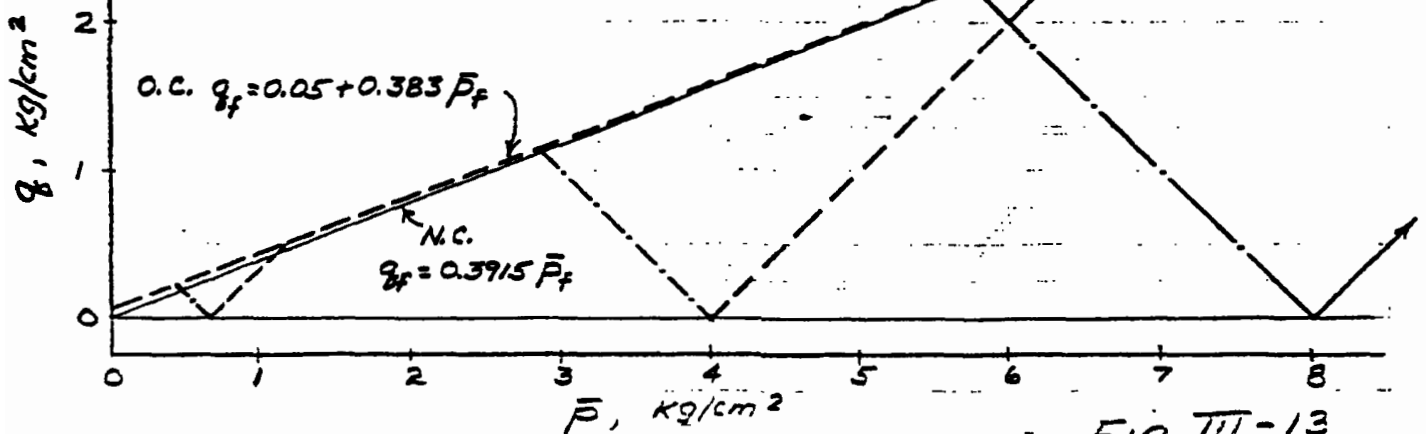
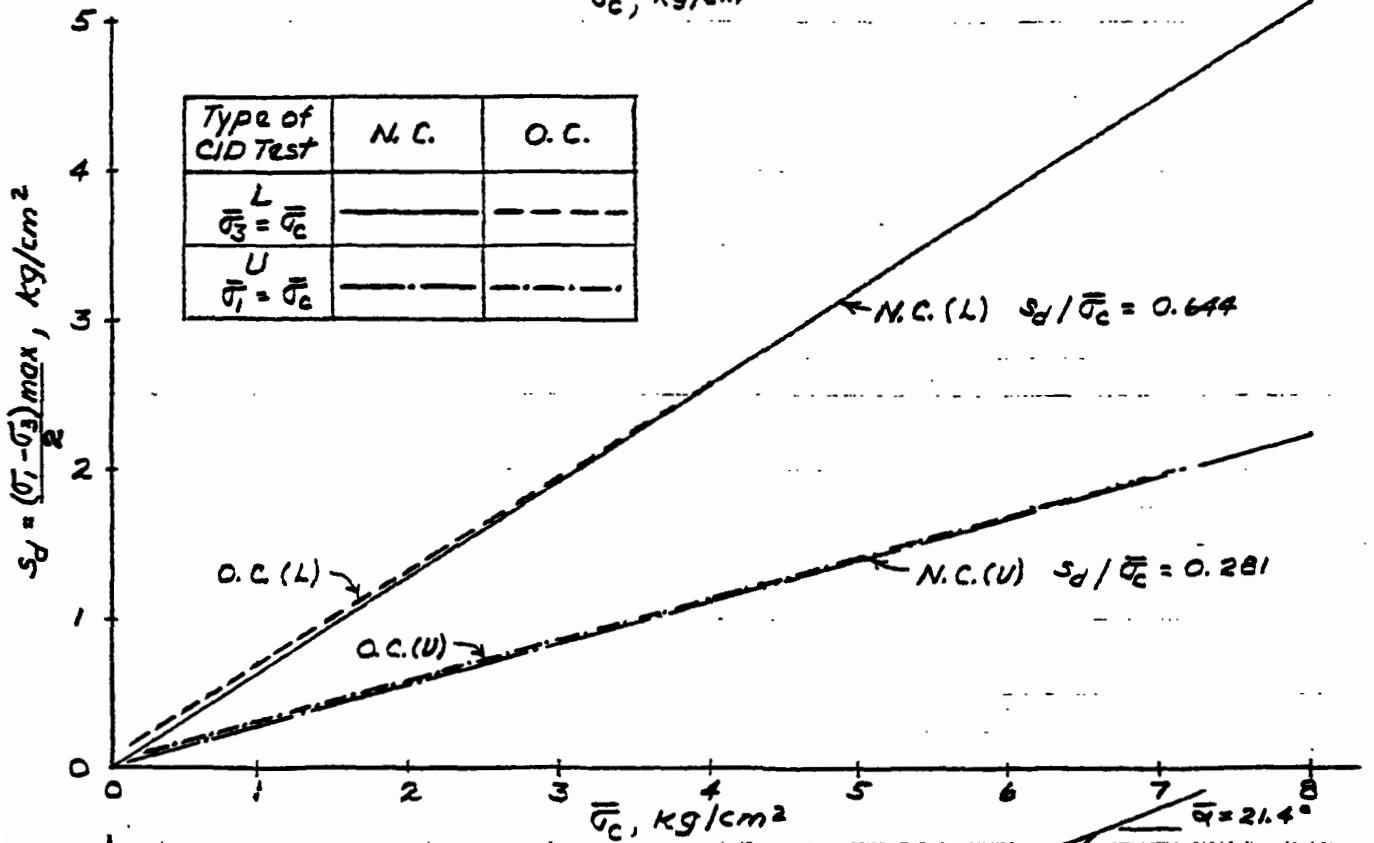


Fig. III-13

Hyperbolic Stress-Strain Relationships for $\bar{C}T\bar{U}$ and CID Compression Tests on N.C. and O.C. Simple Clay

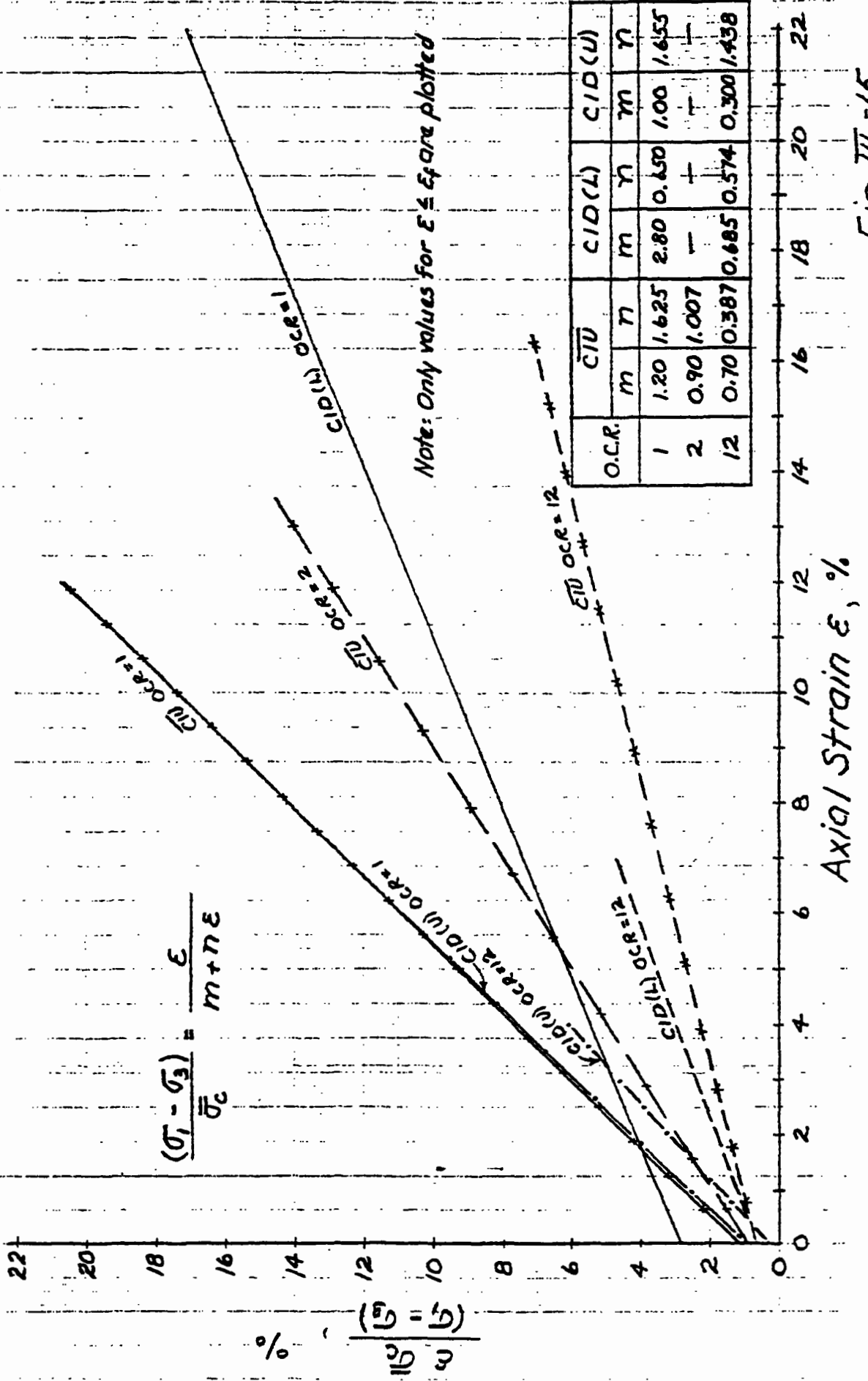


Fig III-15

Stress Difference vs Pore Pressure and
Volume Change for CIU and CID Compression
Tests on N.C. and O.C. Simple Clay

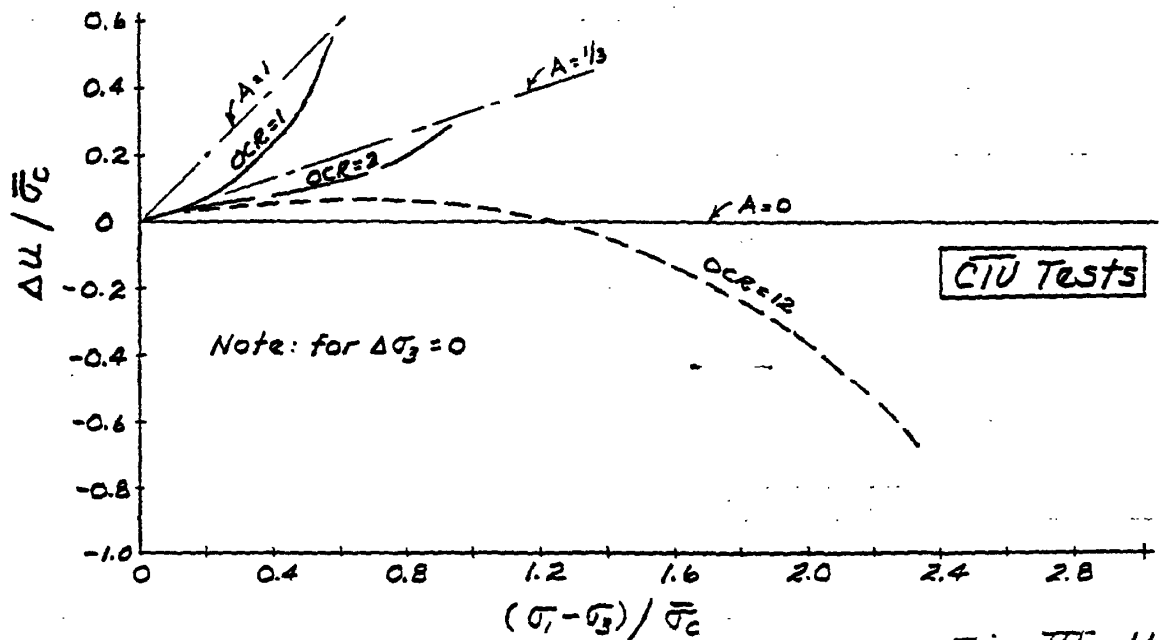
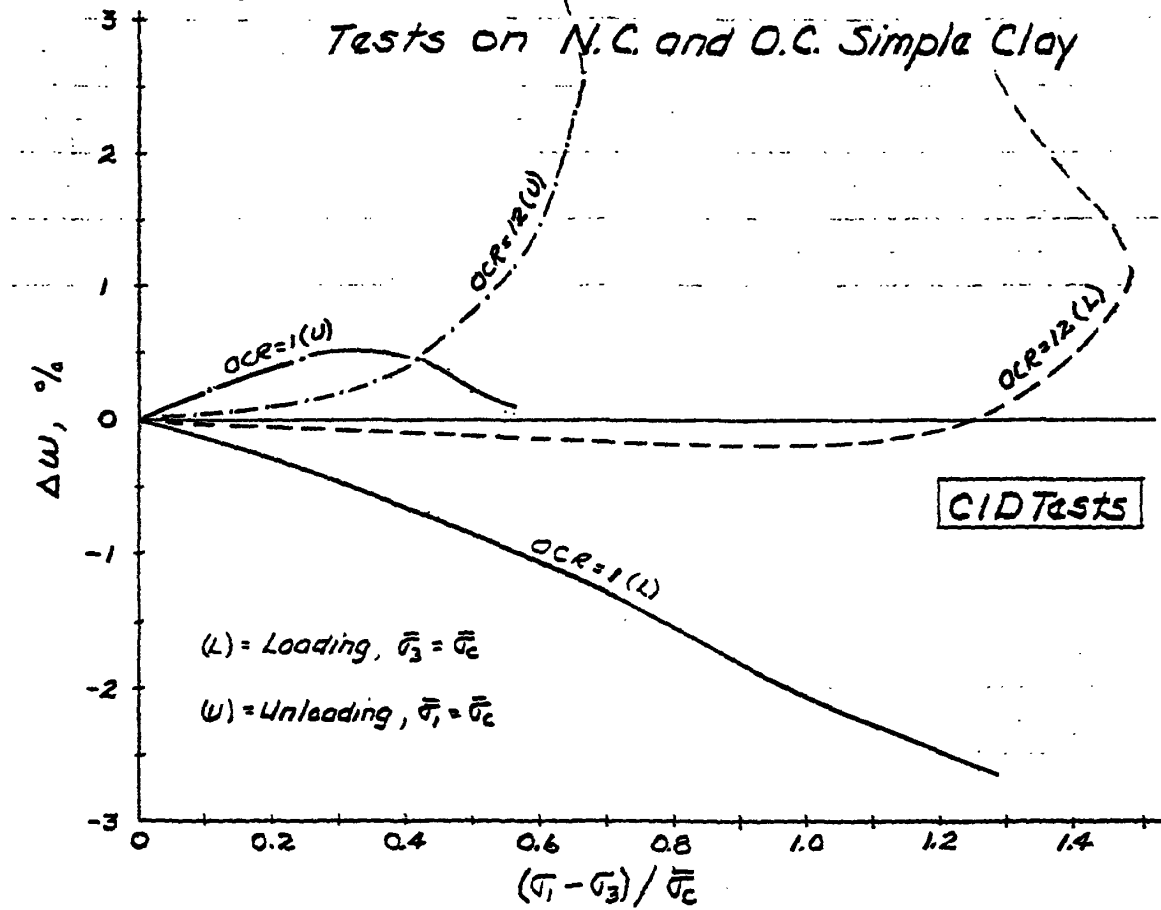
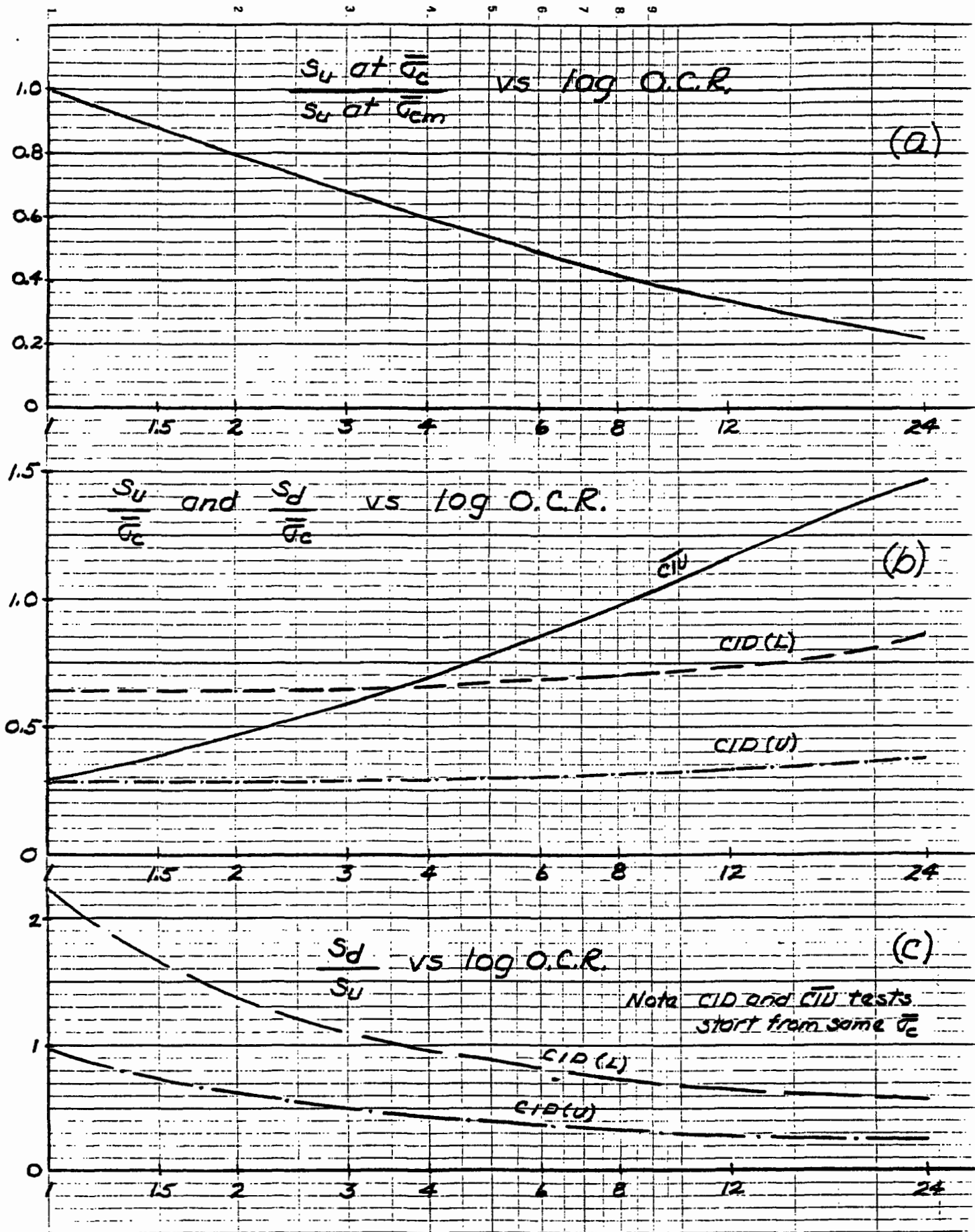
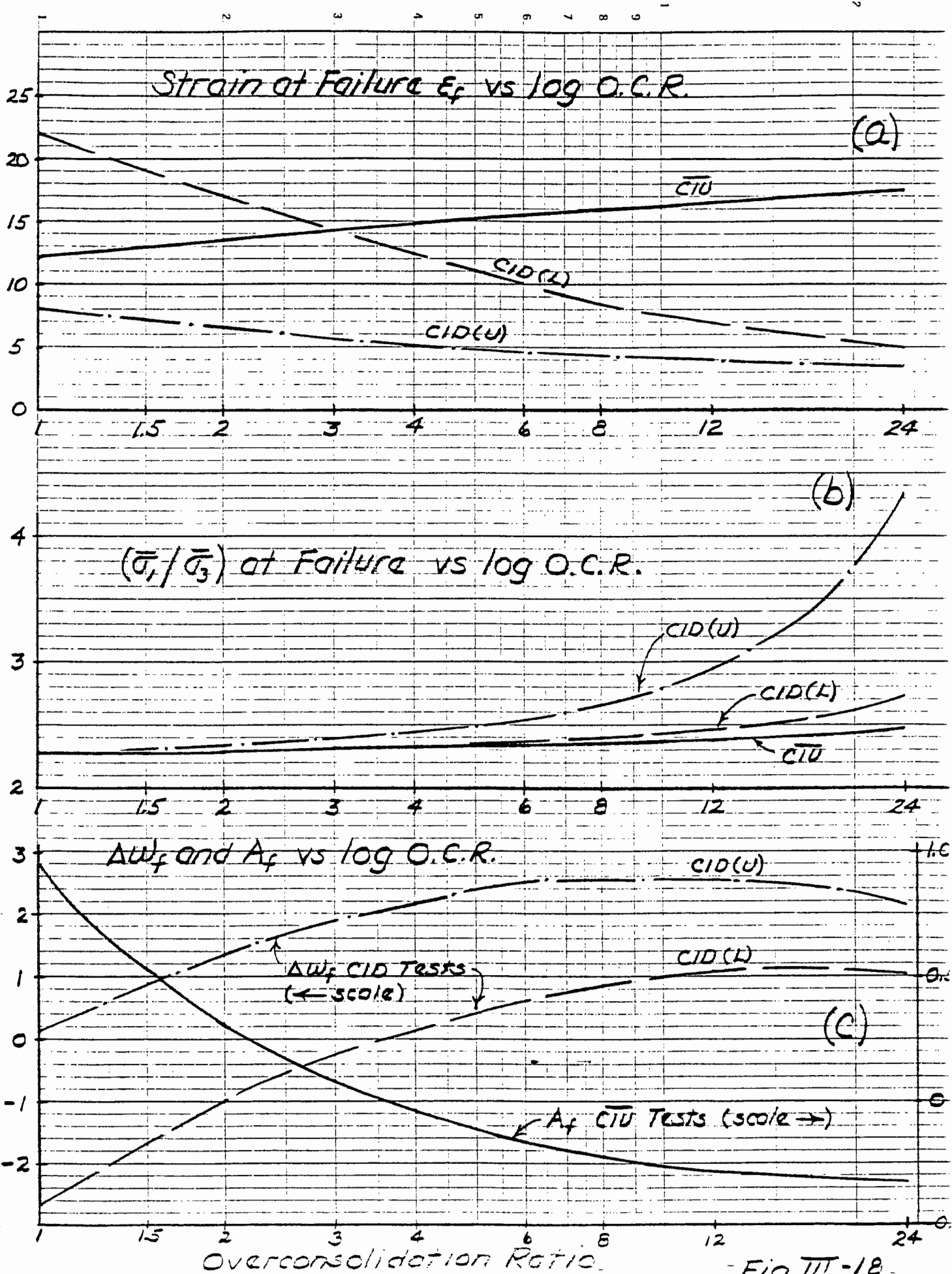


FIG. III-16



Overconsolidation Ratio

Fig. III-17



Overconsolidation Ratio

Fig III-18

Hvorslev Parameters (Drained Direct Shear Tests)

N.C. = normally consolidated
o.c. = overconsolidated

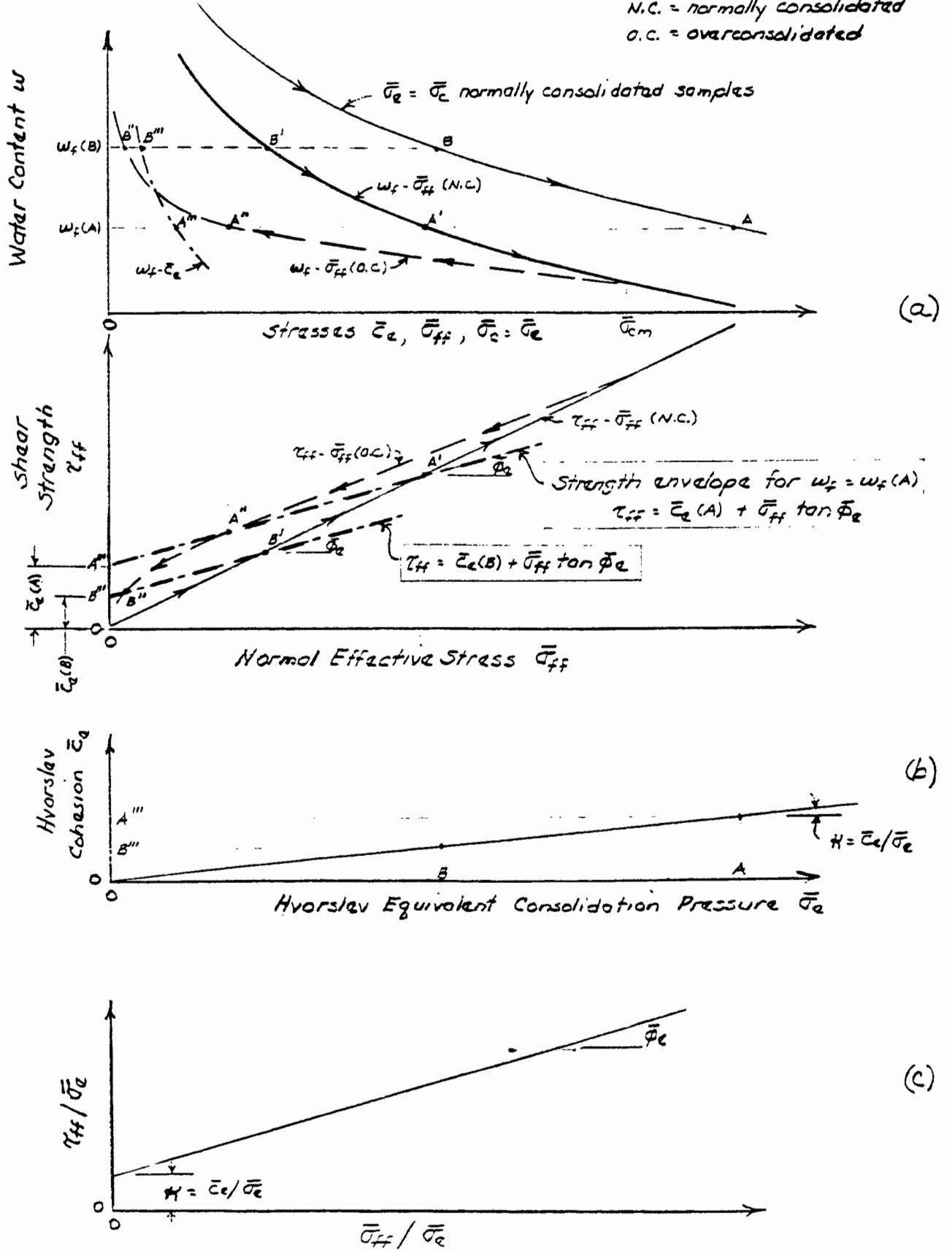


Fig. IV - 1

Hvorslev Parameters from Triaxial Compression Tests on Simple Clay

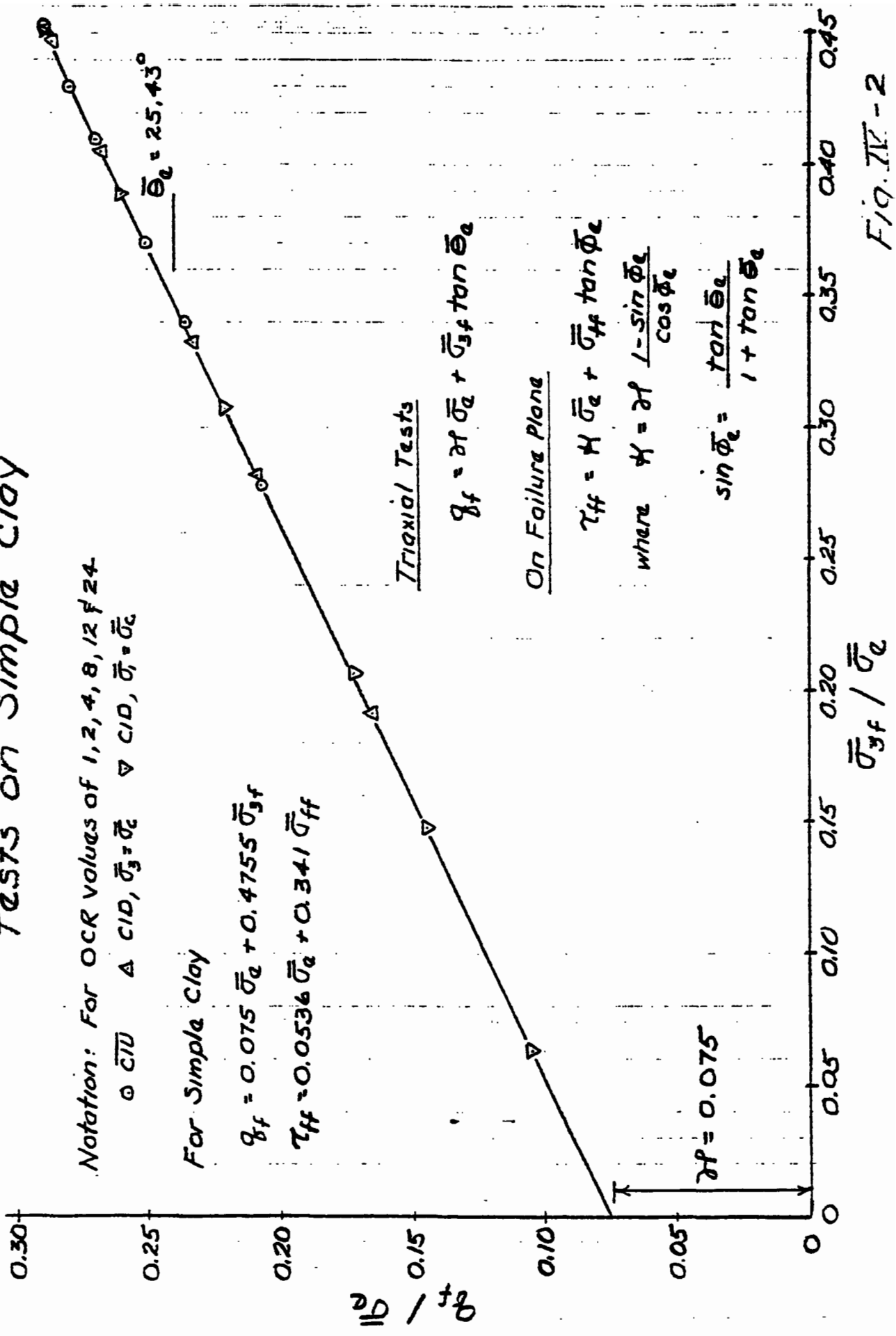
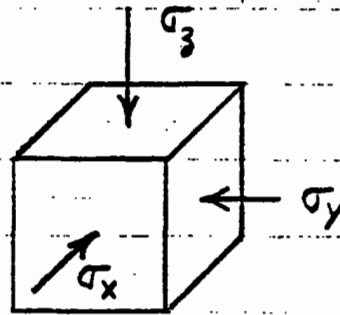


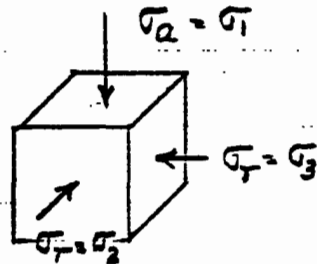
Fig. 11-2

Types of Stress Systems

a) Cube with the 3 principal stresses

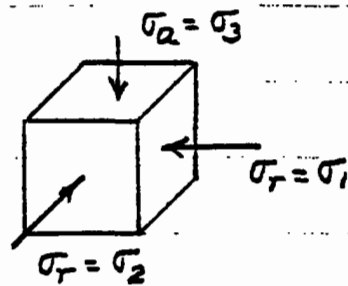


b) Triaxial compression ($\sigma_2 = \sigma_3$)



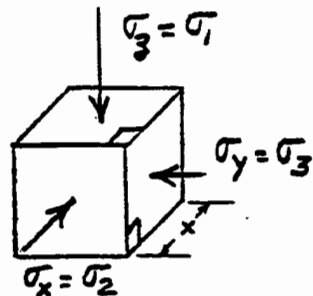
$$\sigma_2 = \sigma_3 = \sigma_1 > \sigma_x = \sigma_y = \sigma_z = \sigma_2 = \sigma_3$$

c) Triaxial extension ($\sigma_2 = \sigma_1$)



$$\sigma_x = \sigma_y = \sigma_z = \sigma_1 = \sigma_2 > \sigma_2 = \sigma_3 = \sigma_3$$

d) Plane strain ($\sigma_1 > \sigma_2 > \sigma_3$)



$$\sigma_3 = \sigma_1 > \sigma_x = \sigma_2 > \sigma_y = \sigma_3$$

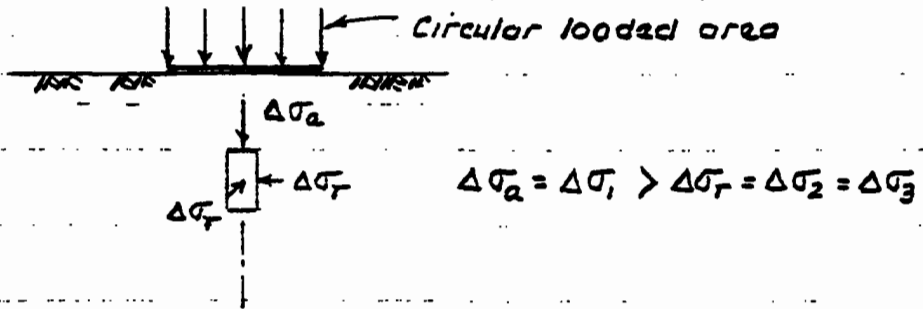
All strains are in the y-z plane so that the dimension x and the indicated right angles remain unchanged.

Fig. V-1

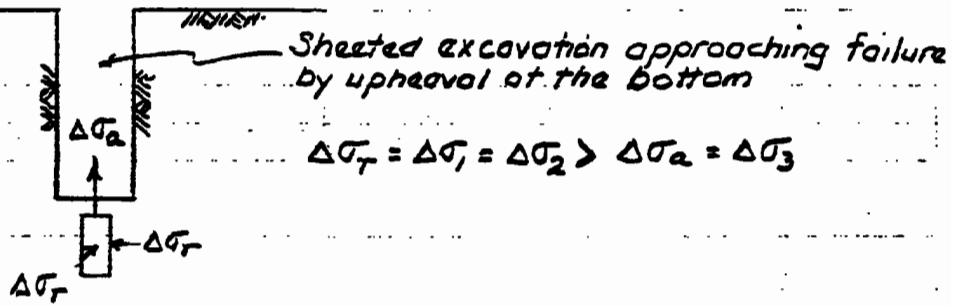
Stress Systems in the Field

(Assuming isotropic initial stresses)

a) Triaxial Compression: ϕ of a circular footing



b) Triaxial Extension: ϕ of a circular excavation



c) Plane Strain: (sections perpendicular to long axis)

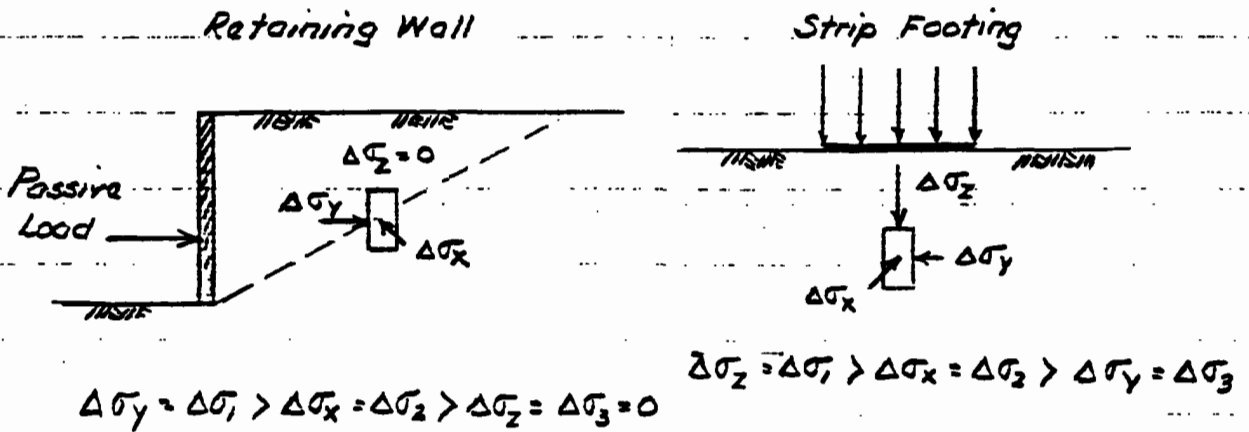


Fig. V-2

Stress-Strain: CTU Compression and Extension Tests on Normally Consolidated Simple Clay

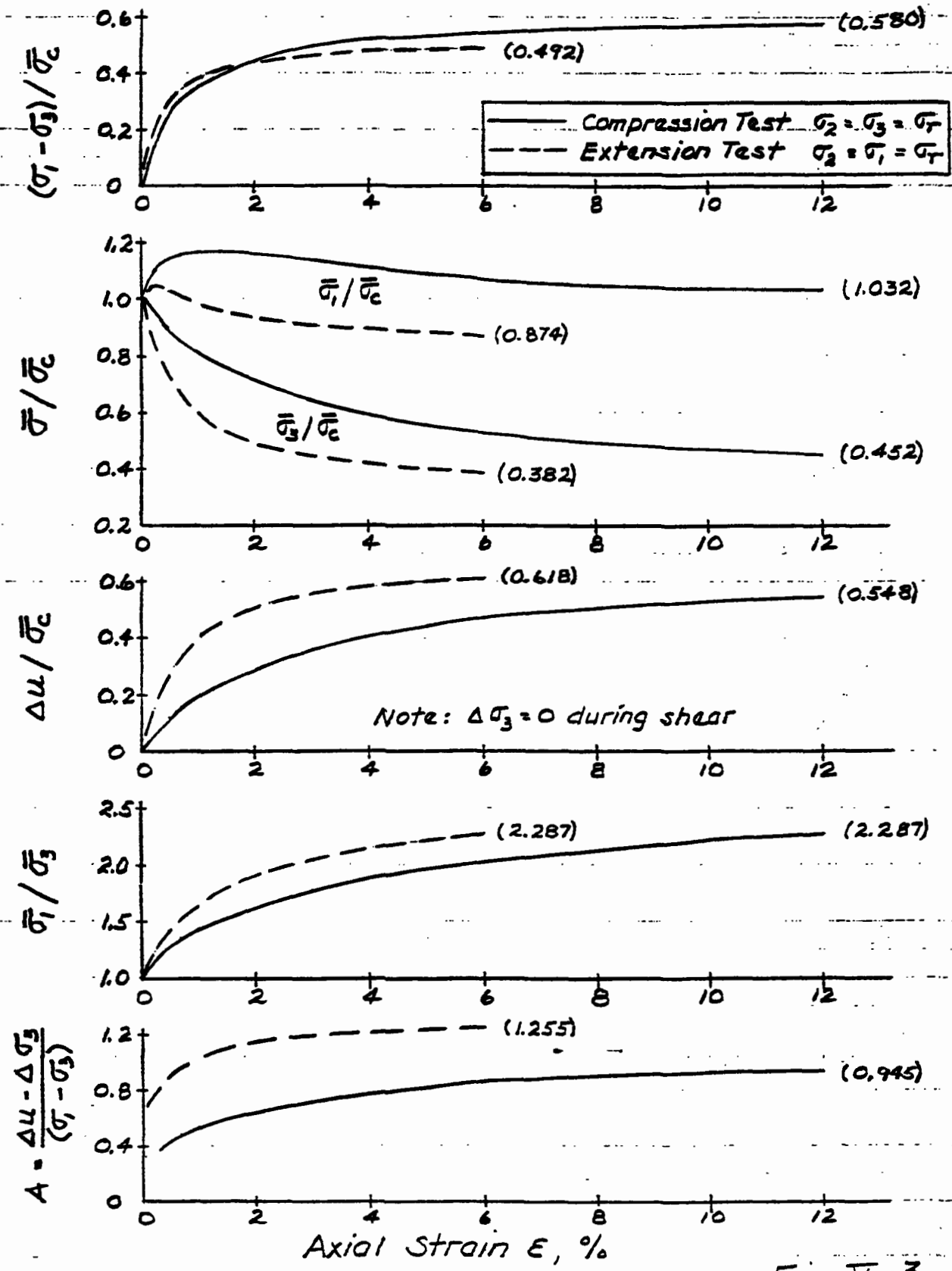


Fig. V-3

CCL 11/10/63

Stress Difference vs A Parameter for \bar{C}_U Compression and Extension Tests on Normally Consolidated Simple Clay

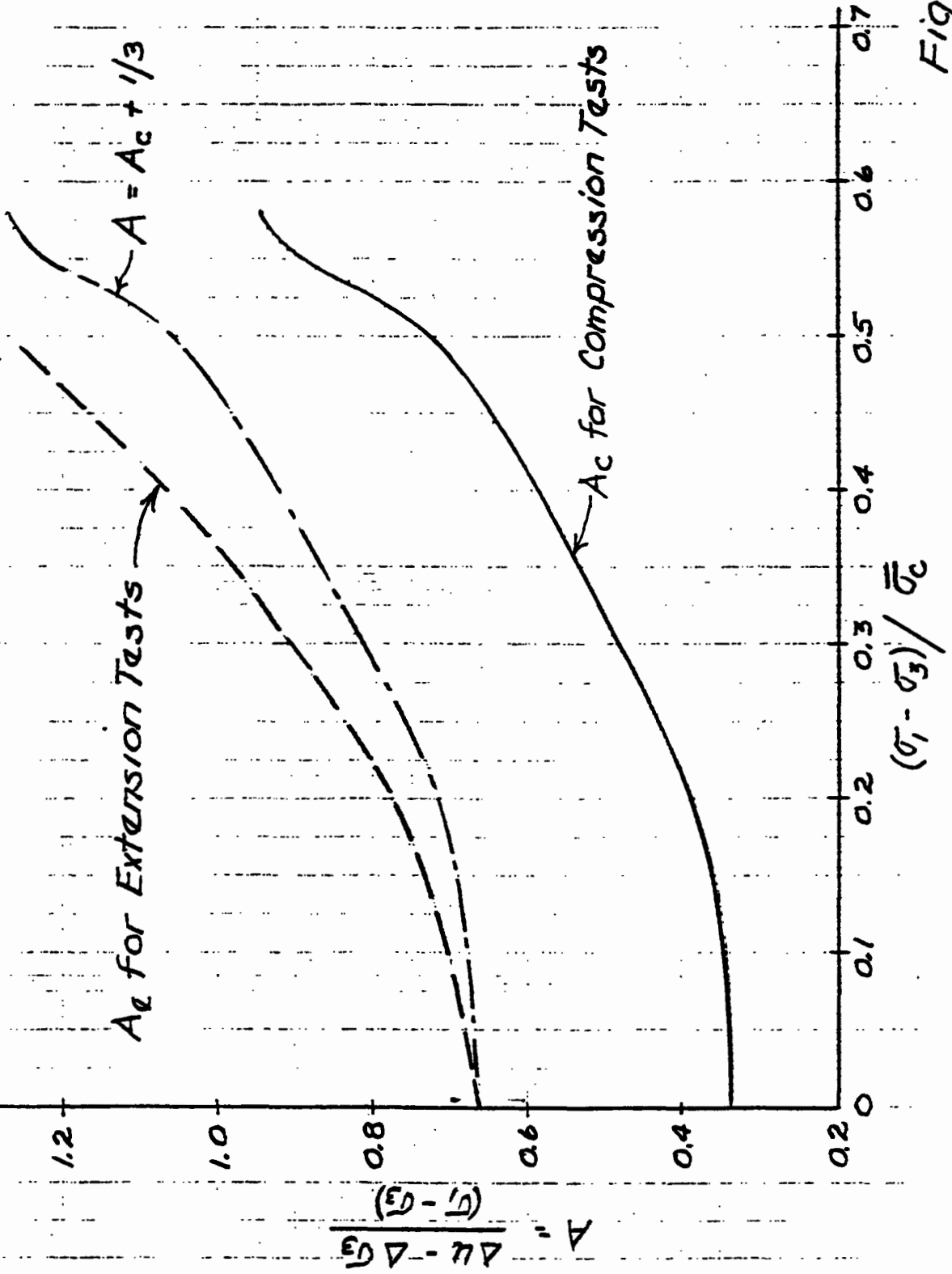


Fig. V-4

CEL 11/10/63

Effective Stress Paths for $\bar{C}\bar{T}\bar{U}$ Compression and Extension Tests on Normally Consolidated Simple Clay

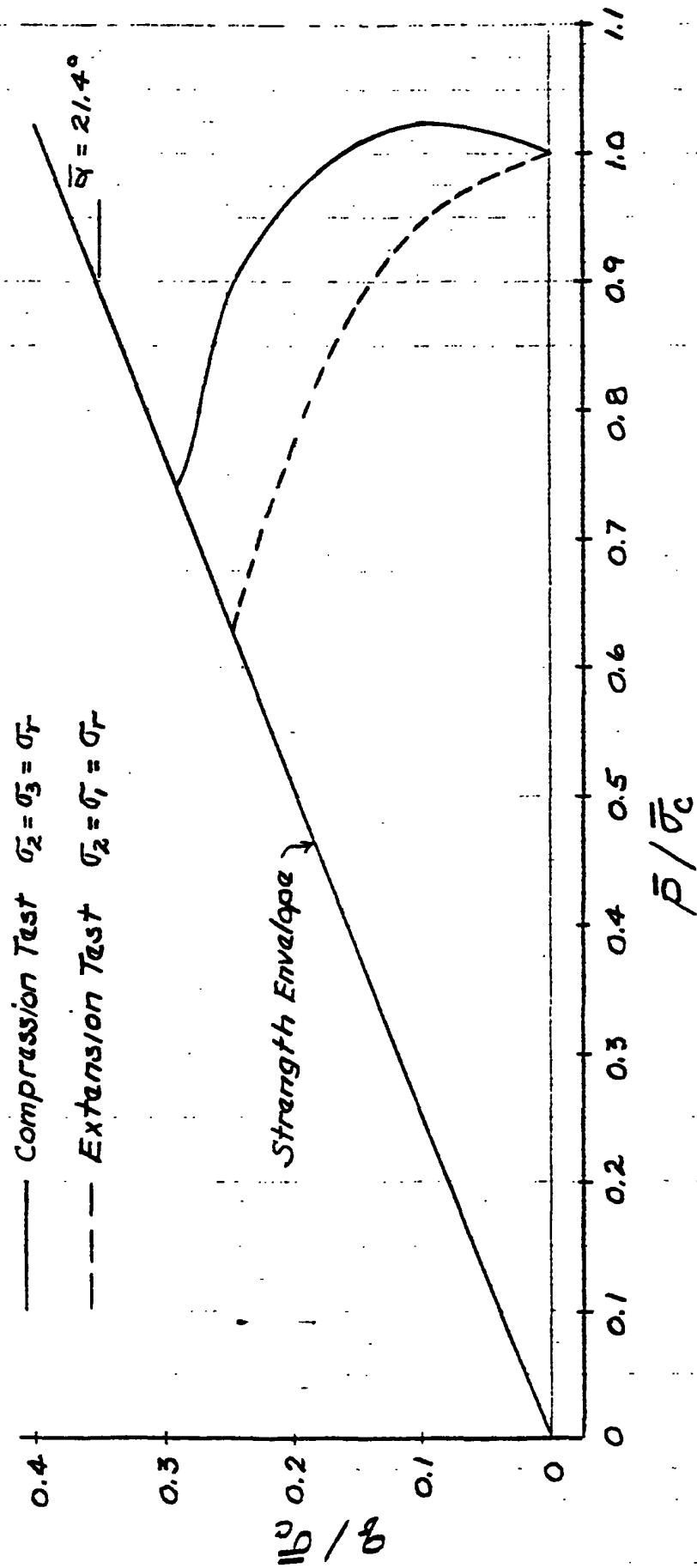


Fig. IV - 5

Rendulic Plot Showing Effective Stress Paths for $\bar{\sigma}_T$ Compression and Extension Tests on Normally Consolidated Simple Clay

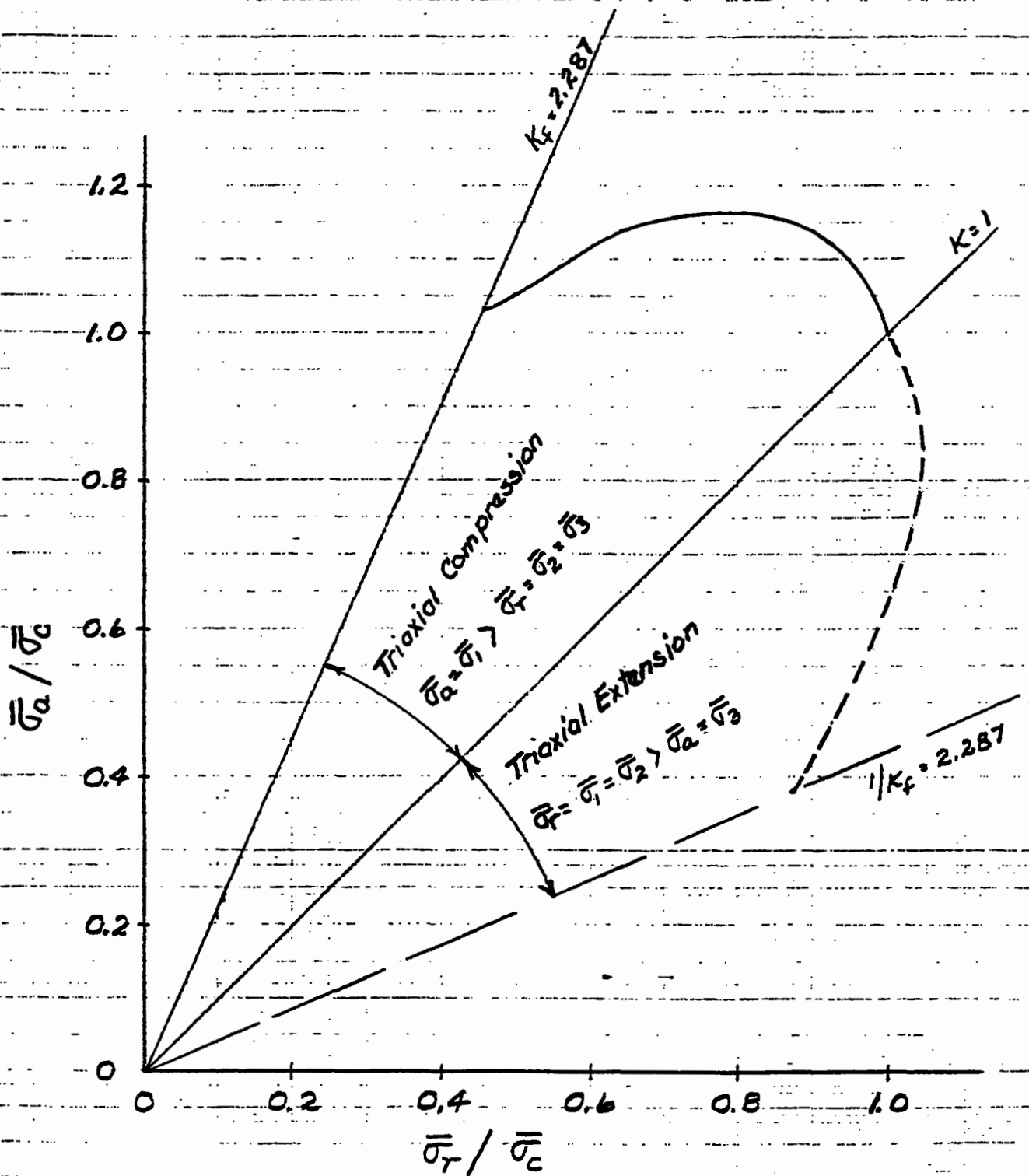


Fig. V - 6

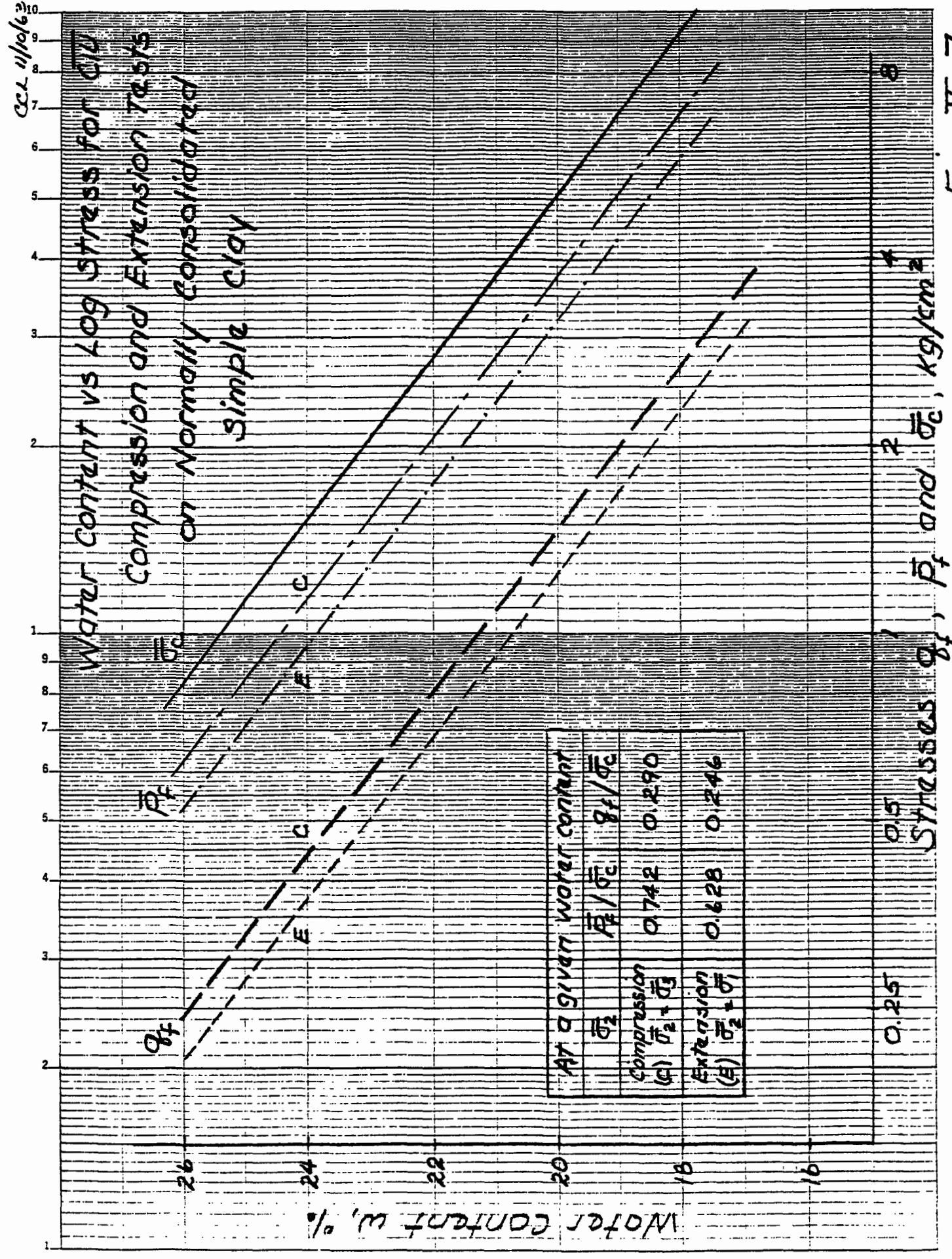


Fig. V-7